Vysoké učení technické v Brně
Fakulta strojního inženýrství
Ústav konstruování

Brno University of Technology
Faculty of Mechanical Engineering
Institute of Machine And Industrial Design

THE BIOCHEMICAL PROCESS OF LUBRICANT FILM FORMATION INSIDE HIP JOINT REPLACEMENT

Risha Rufaqua, MSc, MBA.
Autor práce
Author

doc. Ing. Martin Vrbka, Ph.D.
Vedoucí práce
Supervisor

Disertační práce
Dissertation Thesis

Brno 2021

ABSTRACT

The dissertation thesis deals with the lubricant film formation chemistry on hip implant material surfaces with synovial fluid components. Biochemical and tribological properties of synovial fluid after joint replacement are focused, precisely on the chemical composition of the formed lubricating film and chemical structural changes of the associated constituents under mechanical loading. Nevertheless, the synovial fluid components' chemical structural changes after the joint replacement are rarely addressed and require further attention. Including metal and ceramics, various combination implant materials were applied within the lubricants of synovial fluid constituents separately and different model synovial fluids to reveal the biochemical reactions and frictional coefficients for understanding the possible lubrication mechanism. Raman Spectroscopic technique is manifested as the most appropriate method to explain the biochemical behaviour of synovial fluid and chemisorption on the surface of the implant material. The method is depicted presenting two different studies focusing on the chemical structure of the synovial fluid film on the implant surface and frictional coefficient measurement of the contact pair within the artificial hip joint. This latest methodological precedent also facilitates to evaluate the chemical structural change of the synovial fluid due to the tribological activity in the hip prosthesis. The thesis expounds original results concerning biotribology to increase the depth of knowledge on joint replacement procedure and to enhance the longevity of the orthopaedic implantations.

KEYWORDS

Bio-tribology, synovial fluid, film formation, Raman spectroscopy, tribo-chemistry

BIBLIOGRAPHICAL REFERENCE

Rufaqua, R. *The Biochemical Process of Lubricant Film Formation Inside Hip Joint Replacement.* Brno, 2021, 130 p. PhD Thesis. Brno University of Technology, Faculty of Mechanical Engineering, Institute of Machine and Industrial Design.
Supervisor: doc. Ing. Martin Vrbka, Ph.D.

ACKNOWLEDGEMENT

STATEMENT

I hereby declare that I have written the PhD Thesis, *The Biochemical Process Of Lubricant Film Formation Inside Hip Joint Replacement,* on my own, according to advices from my supervisor doc. Ing. Martin Vrbka, Ph.D., and using the sources listed in references.

…………………………

Risha Rufaqua

CONTENT

1   INTRODUCTION

Millions of people in the whole world are invaded by bone and joint degenerative and inflammatory problems. Half of all chronic diseases occurred in population over 50 years of age in developed countries are caused due to bone diseases [1]. At the same time, osteoarthritis (OA) is reasoned as a foremost source of pain, disability, and socioeconomic damage worldwide [2]. For the comfortable, active movement of the natural musculoskeletal system, a healthy natural synovial joint is essential [3], which allow movement, consist of multiple tissues and structures, skeletal organs are computed by them [4].

To improve the life quality of millions of these patients, hip joint arthroplasty is known to be proficient surgery, to a significant extent [5]. It is a safe process for medicating severe degenerative, post-traumatic and end-stage diseases of the hip joint [6].

Consequently, through the surgeries, orthopaedic biomaterials are implanted within the human body as components of devices. These elements are designed to execute specific biological functions by altering and deflecting different tissues, for example, bone, cartilage or ligaments and tendons, also pursuing bone repairment in case required [1]. Essential service-life of the implants is requisite to repeal its failure. The major reason for the failure of total hip arthroplasty is considered aseptic loosening accompanied by osteolysis, which caused instability and infection [6, 7].

The structure of the protein molecules adsorption on the implant surface is evident. This phenomenon exhibits a certain impact of the kinematic conditions on manipulating the frictional behaviour of the contact couple. Denaturation of absorbed proteins is also proved. The total protein concentration and adsorbed film thickness noticeably affect friction. Eventually, the native structure of adsorbed molecules retainment suggests the impact of the type of the protein and its concentration on the frictional behaviour [8]. It is also found that hip implant materials under reciprocating sliding conditions, the wear depends on the protein content of synovial fluid (SF) [9].

On the contrary, improved lubrication conditions are exposed by adding phospholipids to the solution when γ-globulin used as a base component of a fluid. A combined consequence of hyaluronic acid (HA) and phospholipids caused more accrued lubricant film in case of using complex fluid [10].

Whereas, inside the contact of hip replacements, lubrication mechanisms and film formation depend on the composition of SF. Eventually, the SF composition is affecting the tribological performance of the contact couple, thus impairing the service-life of the implant [11].

It is also shown that thicker film is formed by metal heads compared to the ceramic heads during articulation [12]. In the case of alumina ceramic, the adsorbed film was thicker than zirconia toughened alumina ceramic or metal implants while applying model SF [11]. The selection of the appropriate type and prosthesis design is essential for the long-term outcome of THA [5].
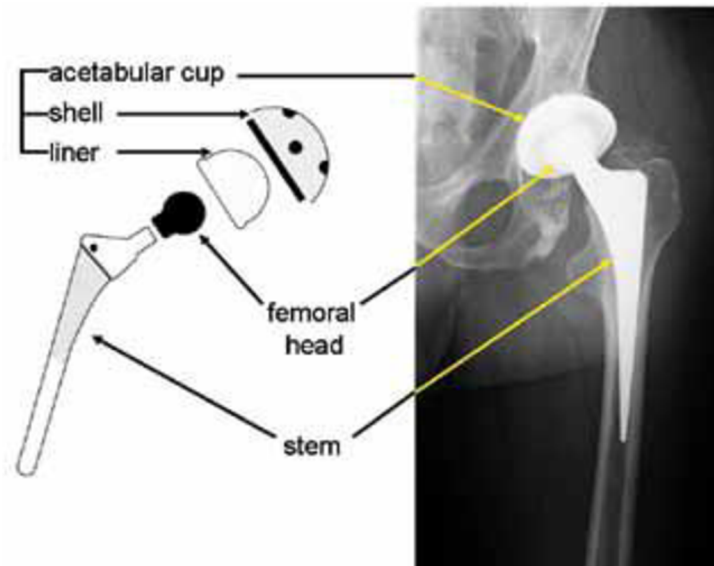
Figure 1.1. Modular hip prosthesis design consisting of the femoral stem, femoral head, and acetabular cup composed of an outer shell and an inner liner. Shell and stem have to ensure good bone integration with the iliac bone of the pelvis and the femur, respectively. The femoral head and the liner provide the articulating surfaces. Their materials are selected for low friction and wear [5].

Therefore, it is revealed that in the case of affecting friction, implant material is the fundamental parameter. Usually, friction is two times increased by the implementation of metal pair compare to ceramic. In the case of hard-on-hard pairs addition of protein to the lubricant exposed a positive result on friction. In contrast adding protein to the hard-on-soft pairs shows barely any responses [13].

To understand the actual correlation between biochemical and mechanical processes of lubrication film formation within the hip joint replacement metal, ultra-high molecular weight polyethylene (UHMWP) and ceramic, all these types of materials should be considered and compared. Human synovial fluid (HSF) found considerably different from all undiluted calf sera, while HSF contains an average total protein concentration of 34 g/L [14]. Also, to acquire in vivo conditions, the impact of proteins lubricants, including phospholipids and HA, friction and wear should be studied [9].

Model fluids of different synovial conditions could be the appropriate selection to elaborate on the present situation of joint replacement with implants of different materials. Raman Spectroscopy could be a suitable technique to explain the function of the fluids and the implant material performance.

2 STATE OF THE ART

In the synovial joint, this highly proficient water-based tribological system is optimized to provide low friction and wear protection at both low pressures and high pressures or loads and also sliding velocities over the whole lifetime [15]. Synovial joints act as bearings for mobility in the skeletal system and SF is responsible for the lubrication of these bearings through various mechanisms [16].

The molecules contributing to joint lubrication are engaged, mainly supporting as an effective surface lubricant reducing the friction and excluding wear damage to the rubbing or shearing surfaces [15]. Therefore the friction and wear properties and chemical behaviour of the joints are governed by key components of HSF, which are proteins such as serum albumin and γ-globulin, phospholipids, and HA [17, 18].

If there is a lack of proper SF lubricating system or any disruption of the chemical environment within the synovial joint, erosion of articulating cartilage surfaces may introduce due to arthritis. In damaged joint SF due to chemical-changes-induced secondary structure modification of the proteins, normal electrostatic interactions are not workable [19, 20]. Variation in SF composition was revealed for typical joint, patients without replacement of joint, patients with primary arthroplasties and patients with revisions of total hip and knee arthroplasties [17]. In particular proteins, HA and phospholipids concentrations differed widely in patients undergoing the joint replacement [21, 22]. The lubricant film thickness within hip prostheses is postulated due to the influence of particular proteins [23].

2.1 Biochemical properties of SF

The SF has a complex biochemical structure, including proteins, phospholipids, HA, cholesterol and glycoproteins, comprises a complex mixture of large and surface-active molecules [24]. However, there is a room for understanding of the proteome composition of healthy SF and cellular origins of its components [25].

The SF functions within the joint as its biological lubrication and acts as a biochemical pool for nutrients and regulatory cytokines outpour. A single mechanism does not describe the tribological performance of cartilage. Instead, multiple activities of lubrication take place mutually. While lubrication is optimum, normal loads, shear stresses, and rates change are observed at articulating cartilage surfaces, generating low-friction and low-wear properties [15].

The main role of articular cartilage is to conduct a smooth, lubricated surface in favour of articulation and to support the load's transmission with a low frictional coefficient. Joint motion and load are significant to sustain normal articular cartilage structure and activity [26]. Within the synovial space, SF is deposited and segregated by the semi-permeable synovial lining. The chemical regulation is probably driven by lubricant concentration, those excreted by chondrocytes and synoviocytes [19]. SF plays the role of transportation of the boundary lubricant to its site of adsorption [21].
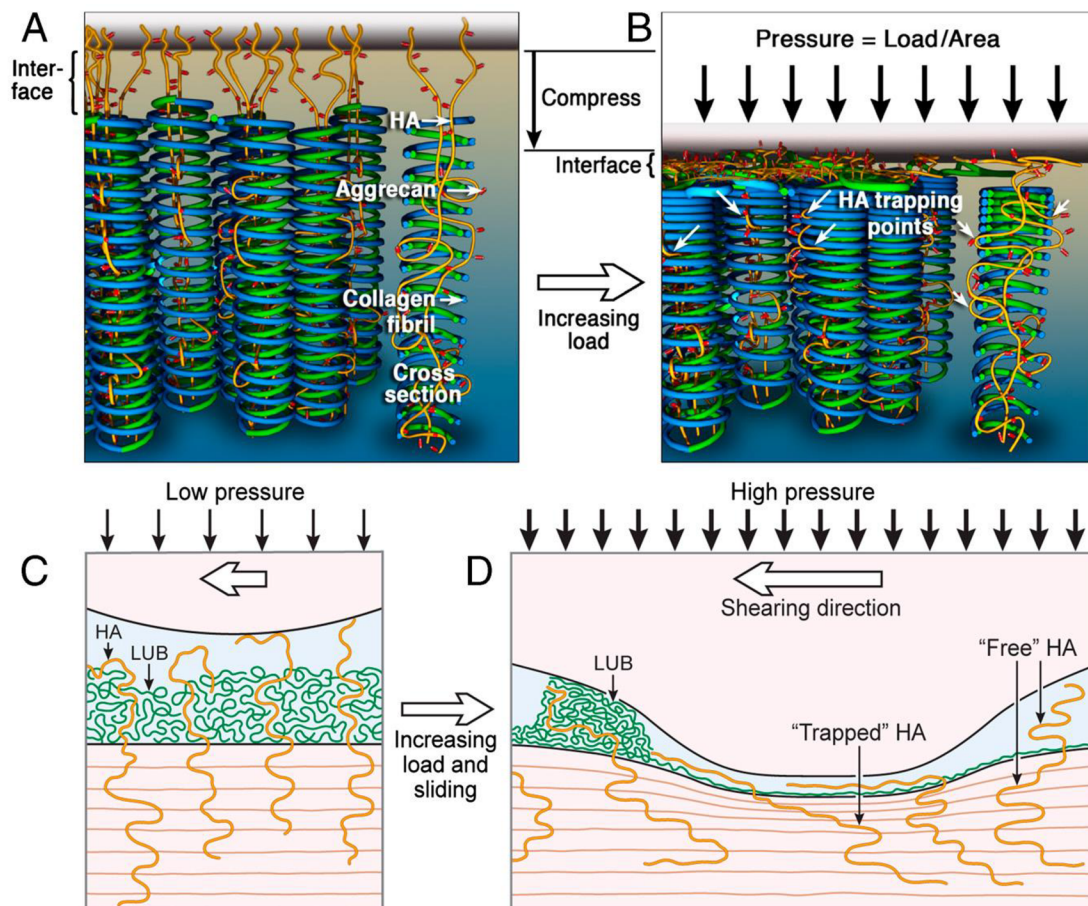
Figure 2.1. Schematic illustration of the HA "mechanical trapping" mechanism [15].

During the first era of bio-tribology research, Dowson and Walker et al. [27], had explained that the cartilage surfaces are obstructed from contacting each other primarily due to the formation of trapped pools of lubricant. As a result of compression and concentration of the fluid between the cartilage surfaces, an acid-protein complex has formed as a protective gel. The combination of trapped pool and fluid concentration is described as "boosted lubrication". Furthermore, the total arrangement of the system is contributed by Proteoglycan 4 (PRG4), HA, and surface-active phospholipids (SAPL).

The proteins are emanated from synovium, cartilage, ligament and meniscus; nevertheless, the structure of the proteins and their functions are featured to phospholipids directly. While HA acts more as a potential boundary lubricant for cartilage and shows a small amount of lubrication activity [15, 19, 27,28].

Blewis et al. [19] described a model where SF is stated as an ultra-filtrate of plasma, which has the capability of filtration through the synovial membrane. Chondrocytes in articular cartilage and synoviocytes in synovium secrete lubricants into SF.
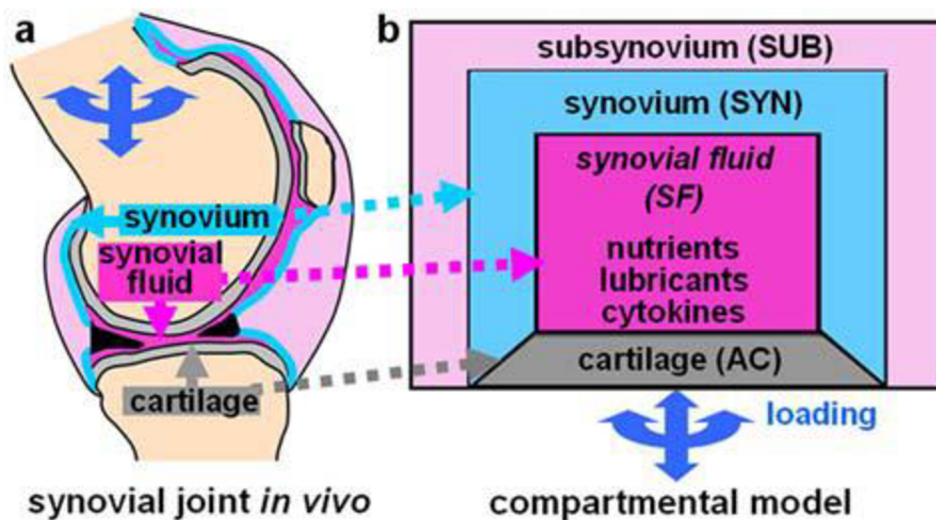
Figure 2.2. (a) Synovial joints composed of cartilage, synovium, and SF; (b) communicating compartments are present in SF, while lubricant secretion is regulated by chemical and mechanical factors [19].

Albumin and γ-globulin, both protein molecules are found abundant naturally in SF. Albumin contains α-helix structure in a huge amount; on the other hand, γ-globulin in constructed with the β-sheet structure mostly. The change of lubricants attributes to the protein boundary film. For instance, the lubricant supports lower friction when it contains albumin than the lubricant consisting only γ-globulin [29].

Albumin is the most extensive protein of SF, which shows affinity to hydrophobic surfaces such as OH-terminated surfaces. By altering the pH value, adherence of albumin to artificial surfaces may be regulated. Albumin plays an important role in lubrication of articular surfaces and interaction with other components. At the same time, γ-globulin's action is towards boundary lubrication. γ-globulin plays the role of pH-independent boundary lubricant at low speeds. At higher speed, boundary lubrication by γ-globulin depends on pH, which helps the formation of hydrodynamic or mixed lubrication [30].

13

HA is an essential element of SF, forms a cross-linked network by complexing with the glycoprotein lubricin (LUB). The solutions are slippery to the touch. This network contributes wear prevention mechanism of joints and is chemically accountable for boundary lubrication [15, 21]. Lubricin is produced by a long, heavily glycosylated, mucinous domain, separating two somatomedin domains at the N-terminus and a haemopexin region at the C-terminus. A small amount of lubricin is present in SF but indulges in a considerable amount in the boundary lubrication and lubrication properties, transporting, anchoring of phospholipids to the cartilage surface and the friction coefficient of the various ground of articular cartilage. Moreover, lubricin provides significant support to chondroprotective properties of articular cartilage; this behaviour is further enhanced by interaction with HA via dissipation of shear-induced energy. Therefore, effective biolubrication is contributed by lubricin in the presence of other major constituents in SF [21, 30].

One of the main components of SF is phospholipids, phosphatidylcholine is extremely surface-active due to huge amount of saturation of joint phospholipids. Another element abundant in SF is the SAPL. These small molecules function as binders of amino acid groups [21]. In the synovial joint environment, occurring chemical change due to injury and disease were predicted to modify lubricant concentration [19].

Another study covers the analysis of differences of the compositions and the constituents of SF extracted from respectively patients of primary arthroplasties and revision arthroplasties and without joint replacement and healthy SF. The average concentrations of different components of the joint fluid in the four distinct groups are summarized in Fig. 2.3.

Galandáková et al. [17] concluded that lubricant film is predominantly formed because of proteins. Therefore, albumin and γ-globulin readily adsorbed on artificial materials, whereby have an influence on the frictional properties of the lubricating surface. The γ-globulin concentration found remarkably higher and the concentration of phospholipids observed significantly lower with revision of joint replacement patients and with patients without joint replacements. HA and viscosity of different groups were observed unchanged.

Therefore, biological and chemical features of the synovial joint environment plays a vital role in the longevity of the implant and the likelihood of failure [24].
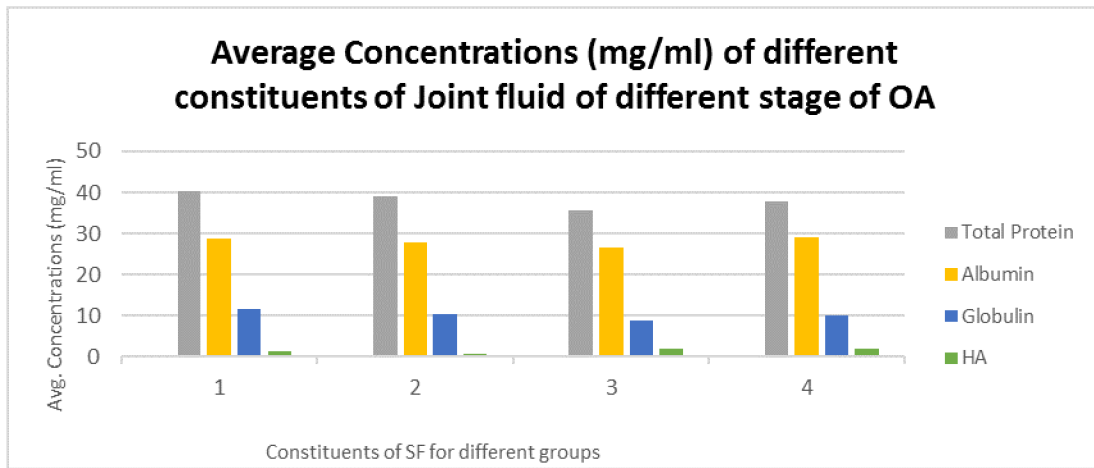
Figure 2.3. The average concentrations of the constituents of the joint fluid from the different stages of OA. Average total concentration of protein found 40.3-35.5 mg/ml, average concentration of albumin 29.1-26.7 mg/ml, average concentration of γ-globulin 11.5-8.7 mg/ml and HA 0.8-2.0 mg/ml for different groups of patients as described above [4].

2.2   Lubricant film formation and thickness analysis

The diseased and periprosthetic SF alters the concentration of proteins and other components and also contains decreased effective viscosity, increased protein content and increased pH. [17, 24, 31].

The film lubrication may influence the bulk properties of the SF as proposed by Mazzuccoa et al. [22]. Some relations occur between the composition of the joint fluid and the tribology of joint replacement prostheses. Proteins, HA and phospholipids contents of joint fluid samples obtained from patients undergoing TKA (total knee arthroplasty) and revision TKA discloses that despite normal total protein content, the individual protein concentrations deviated in the diseased joints from that in healthy joints. In the case of the implant wear and failure of joint replacement, patient SF chemistry has a significant role [24].

To determine the lubrication processes inside the artificial joints, optical methods have been extensively employed to investigate film formation in situ [11]. Film thickness was measured by optical interferometry as a function of time by Vrbka et al. [32]. From this study, it is suggested that kinematic condition and conformity of the contact surface has a fundamental effect on protein film formation while wettability has no effect on protein film formation. Due to protein aggregation, the film formed within the ball on disc configuration. On the contrary ball on lens configuration hydrodynamic effect leads to film formation.

The lubricant film formation is attributed to the meaning of particular proteins. It is comprehended that the thickness of the film is formed predominantly due to the presence of albumin, specifically under pure rolling and positive sliding conditions. Hence under negative sliding, the film thickness is strongly dependent on time and sliding distance. At higher speeds, the film is mainly caused by γ-globulin. γ -globulin forms a very thin protein layer on the base material, while the albumin adsorbs onto the layer and therefore, increases the total film thickness. Thus, in most cases, albumin contributes to increasing the total film thickness [23].
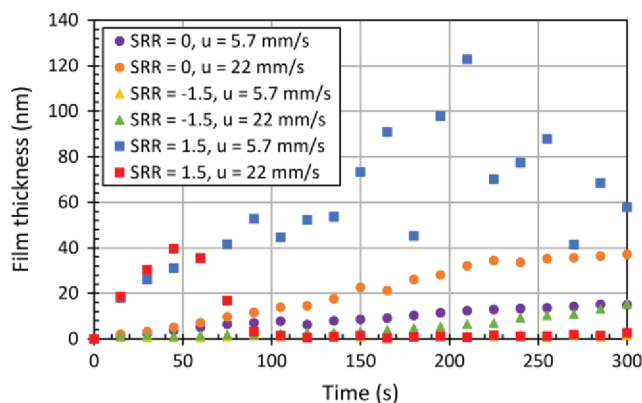
Figure 2.4. Comparison of film thickness measurements by thin film colorimetric interferometry for various operating conditions [23].

It is stated that the film formation within protein solutions is subjected to both on the protein content and pH of the solution [33, 34]. While comparing the film thickness during and after rolling tests, it is displayed that the deposited films formed by bovine γ-globulin (BGG) were quite firmly bound. Also, mixed proteins showed the same result. On the other hand, bovine serum albumin (BSA) films were only weakly bound. In the case of BSA and BGG deposited layers, the BGG films formation were much thicker. Under the condition of mixed proteins, the competence of BGG to form thick layers was decreased. Therefore, the process of film formation is influenced by the interaction between the proteins [33, 34].

Large irregular deposits of films are formed in solutions at physiological pH. Under static condition or the rolling conditions, solution pH controls both the protein adsorption kinetics and the formation of tribofilms. At the lower pH, the adsorbed protein layers are in the early stages rigid and relaxed, over time to form viscoelastic layers, the rate of adsorption enhanced with time. At higher pH, even in the first instance, adsorbed films are found to be substantial viscoelastic [34].

Nevertheless, no significant changes to protein adsorption were exposed to the solutions tested in different buffer chemistry. In comparison, the rate of protein adsorption and the viscoelastic properties of the adsorbed layer are similar for all buffer chemistry. In rolling contact buffers with pH 7.4 or lower, a formation of thicker protein films was found than under static conditions [34].
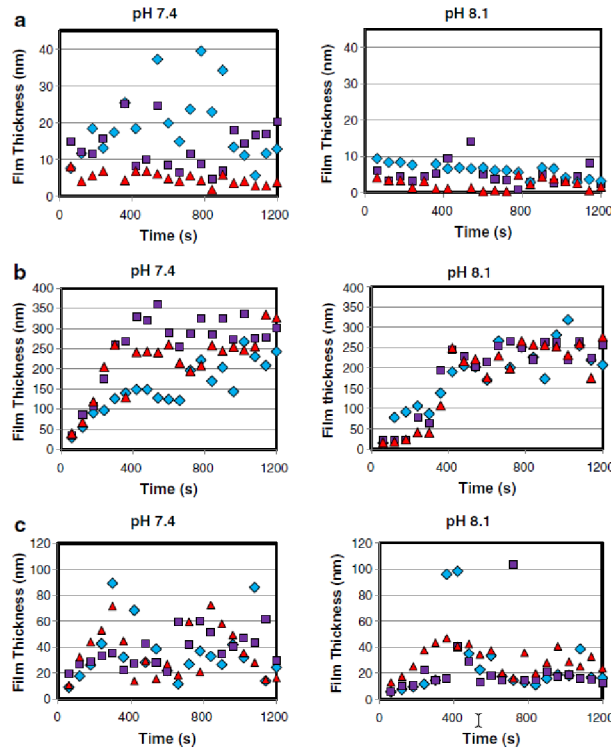
Figure 2.5. Film thickness results for three tests (different symbols) for (a) BSA (b) BGG and (c) mixed protein solutions in a rolling contact (10 mm/s) at pH 7.4 and 8.1 [33].

Film formation mechanisms were determined by imitating an adsorbed surface film and a high viscosity gel by an inlet reservoir of viscous material produced from high concentration protein fluids. Film thickness and wear measurements were concluded for various model SF solutions of different pH according to diseased or post-operative SF solutions. Film formation signifies by two distinct mechanisms: boundary lubrication mechanism and high viscosity gel mechanism. As explained by the boundary lubrication mechanism, with the formation of a thin, discontinuously deposited films, the proteins adsorb at the Cr-Co-Mo surface. These films occur to survive rubbing. In contrast, an inlet reservoir of viscous material is formed by fluids with high-concentration protein that is entrained into the contact forming a separating film; the agglomerated protein forms organic deposits on the surface of implants [24]. These deposits appear viscous in the fluid environment and could be easily dispelled by surface scratches. After removing from the fluid, dried formation of highly-adherent, solid films are observed. Wear mechanism is designated through the tribo-corrosion process, with higher pH, wear increases [24].

The wear scar width pH 7.4 < pH 8.5   pH 7.4 < pH 8.0 _ BCS25 < pH 8.5

By using the various composition of SF, lubricant film formation on metal and ceramic femoral heads were analyzed [11]. From the analysis practically, it is proved that the film formation is affected by the composition of SF and lubrication performance of the contact couple, using hard-on-hard hip replacement pair. In the case of metal head adsorbed film thickness increases, not influenced by the fluid composition, although higher concentration of HA and phospholipids causes the reduction of the film thickness. Thicker film absorption was found for alumina ceramic and thus, strong protein agglomeration was exhibited compared to zirconia toughened alumina ceramic or metal exposed. Although the correlation between the level of load and film thickness is not clarified, it is stated that enhanced load may influence the adsorbed layer. It is proven here that the interaction of all the components of SF is required to take into consideration. At the same time, simple solutions may not provide the actual lubrication mechanism inside the replaced joint [11].
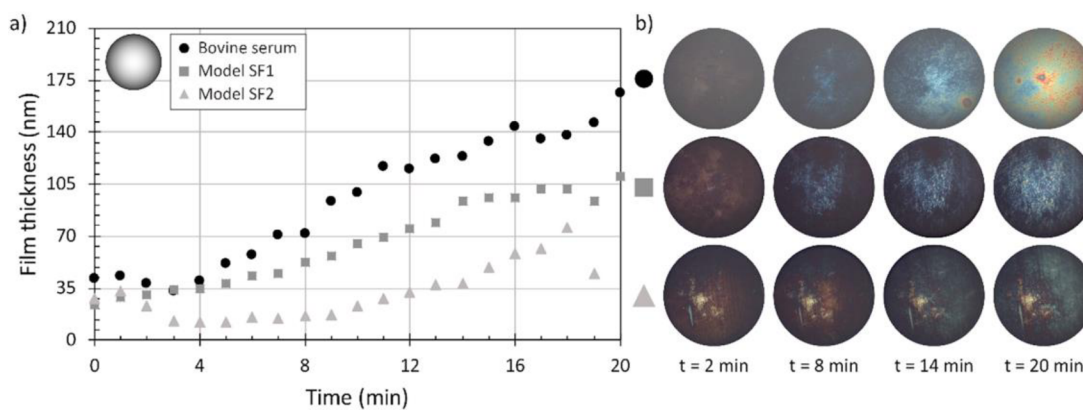
Figure 2.6. a) Static test - film thickness of the adsorbed film as a function of time for 36 mm metal head and various model fluids. b) Chromatic interferograms taken during the experiment; from the top: BS, model SF1, model SF2 [11].

Electrochemical oxidation was used to determine the composition, thickness and structure of the oxide layer formed on the Cobalt chromium molybdenum (Co-Cr-Mo) alloy. The observation was carried out at various passivation potentials in simulated physiological solution. Noticeable variation was displayed in the oxide layer found depending on the applied passivation potential. Presumably, the analysis of the structure of the SF film could be done in a similar way [35].

18

Another study of electrochemical techniques was focused on the interfacial conduct of BSA on Co-Cr-Mo surface to understand the mechanism of protein adsorption at different surface conditions with consideration of different passivation times. At open circuit potential (OCP), adsorption kinetic was interacted by surface passivation with lower passivation time smaller than 1 hour. In contrast, the kinetic mechanisms of adsorption were without a remarkable change at higher passivation times. On the Co-Cr-Mo surface lowering the amount of adsorbed BSA observed with the passivation time. Therefore, the impact of the BSA addition at the applied passive potential is conditional to the passivation time [36].

While explored with the integration of gravimetric analysis and electrochemical measurements of tribo-corrosion behaviour, the surface interactions with organic species were observed for Co-Cr-Mo and stainless steel. The elements of bovine serum (BS) found to have a huge influence on the corrosion behaviour of both materials, playing an active role in the mechanism of increased ion release and passive film breakdown in static situations. In contrast, tribological condition introduced biofilm, which is forming a lubricating film that is effective in reducing friction. An extremely complex nanostructured layer formed by high carbon Co-Cr-Mo reactions at the surface in the contact area, which consist of biofilm as well as wear debris, and reaction products. The nature of passive film formation is also changed by this process. This film is protective in nature by reducing material loss. Including proteins, the organic species were also influencing to boost corrosion-related destruction on the material surface [37].

Using BS as lubricant a tribological experiment was conducted with diamond-like carbon (DLC)-coated and a micro dimpled steel ball against a Cr-coated glass disk at 37°C temperature. The lubrication behaviours of the contact area were observed by optical interferometry and a torque sensor was utilized to measure the simultaneous friction coefficients [38].

The lubricating film formation was insignificant for scuffing-free sliding of DLC/glass when coefficient friction was low. In contrast, the dimples retained lubrication with minimizing wear of the glass disk without reducing friction coefficient [38].

On a DLC film surface was considered by applying the method of quartz crystal microbalance, including dissipation (QCM-D) and antigen-antibody reactions. In this experiment, adsorption and competitive adsorption behaviour of BSA, human γ-globulin (HGG), and HA molecules were observed. BSA monolayer found to be formed on the DLC film surface with side-on orientation. In contrast, an HGG monolayer explained to be formed on the DLC film surface with end-on orientation by using pure solutions of BSA and HGG, respectively [39].
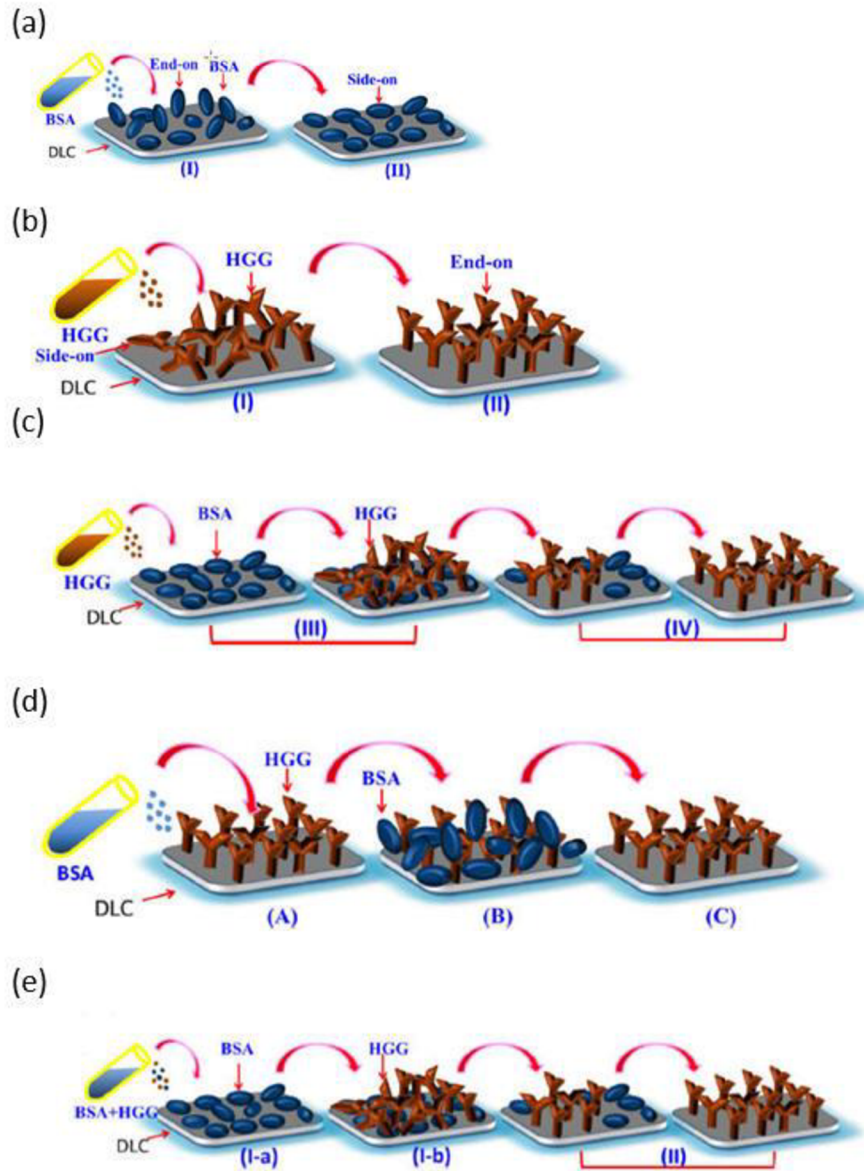
Figure 2.7. (a) Adsorption of BSA on DLC surface, configuration changing process of BSA molecules. (b) Adsorption of HGG on DLC surface, configuration changing process of HGG molecules. (c) The sequential adsorption in BSA→HGG procedure on DLC surface, conformation changing process in BSA → HGG sequential adsorption. (d) The sequential adsorption in HGG → BSA procedure on DLC surface, conformation changing process in HGG → BSA sequential adsorption. (e)The simultaneous adsorption from binary mixture solution of BSA (20 mg/mL) and HGG (6 mg/mL) on DLC surface [39].

HA molecules were barely adsorbed to form film onto the surface of DLC film as well as HGG or BSA biomolecular layer. In case of using mixed lubrication of BSA, HGG, and HA, HGG molecule was observed as the prime component that formed the lubricating film on DLC film sliding against Al2O3. From the competitive adsorption determined that HGG molecules are capable of displacing BSA molecules. Simultaneously, HGG was the major adsorbed molecule on the DLC film surface when using a mixture of BSA, HGG, and HA [39].

2.3   Joint implants SF correlation with tribological properties

Artificial hips and knees, as well as artificial discs exhibited wear mechanisms, long-term results along with the incidence of late complications due to procedure needs more clear understanding [40]. While it is described within the joint implant, mainly the presence of the proteins in SF induces the corrosion-enhanced wear occurs. More precisely, the occurrence of the proteins propagates wear component. Most likely, adsorption of proteins in the particle entrainment also increase the rolling efficiency of the abrasives. Within a tribological contact of a knee or a hip, the Co-Cr-Mo implanted into the human body (pH 7.4) is namely susceptible to corrosion. As a result of initial corrosion of Co-Cr-Mo alloy. Co2+ and Cr2+ ions in acidic conditions and Co-O and Cr-O species at neutral pH are produced. Therefore, the wear-corrosion behaviour of the cast Co-Cr-Mo alloy can be removed noticeably with a minor change in test solution chemistry. [41, 42].

A series of Co-Cr-Mo alloy sample was undergone with various sequences treatments, including solution heat treatment, hot isostatic pressing and sintering to consider thermal effects. The volume fraction of carbide present was evaluated by metallographic analysis. It is observed that the level of carbide, as well as the morphology, differs significantly among the samples depending on the thermal condition. According to this research result, the development of a low wear rate system is influenced by microstructure and specifically the volume fraction, size and allocation of carbides. In comparison with single or multiple heat-treated materials, as-cast materials have enhanced abrasive wear resistance [43].

The relationship between the coefficient of friction of protein constituents of lubricating fluid and pH value, along with viscosity, were explained by Kitano et al. [31]. The alteration of protein content may influence the pH and viscosity dependency. Without reliance on the tribological properties at low speed, the presence of albumin, the lubricant promotes pH dependence and viscosity. In contrast, γ-globulin contributes with pH and viscosity independence at low speed, alternatively pH and viscosity dependence in the lubrication of UHMWPE against stainless steel at high speed. Finally, the effect of SF components and pH variation in the periprosthetic fluid can lead to change lubrication, which may result to understand the complications in total joint replacement.

HA with albumin has a huge effect on the coefficient of friction at a low range of angular velocity, including the variation in pH without depending on viscosity. Again, HA with γ-globulin affected the coefficient of friction with the variation in pH with viscosity dependence at high angular velocity. Moreover, dipalmitoylphosphatidylcholine (DPPC) as of Lα-DPPC showed a small effect on the coefficient of friction at low angular velocity [31].
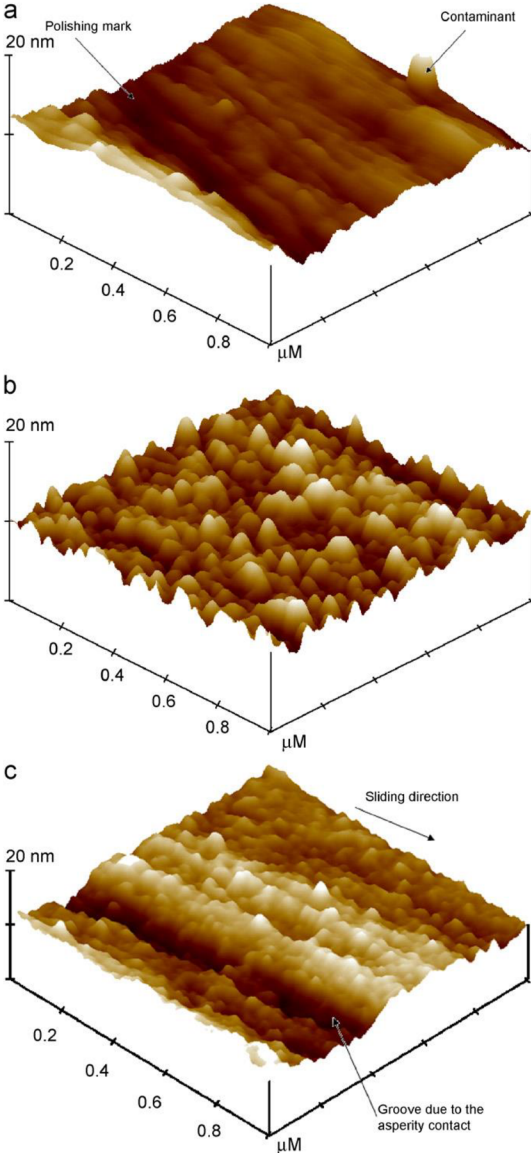
Figure 2.8. AFM study of the Co-Cr-Mo surface (a) as polished, (b) after immersion in 25% BS for 30 min at 37°C and (c) after Sc test in 25% BS at 37°C [41]

The research revealed frictional consequences on porcine cartilage and lubrication mechanism of enzymatic digestion of HA. Using surface force apparatus with friction device attachment, the normal and frictional force was measured under various loading conditions with a friction device. HA and LUB complex as HA-LUB, trapped at the interface to form a cross-linked network, which plays a role of boundary lubricant and prevent wear mechanism [15].
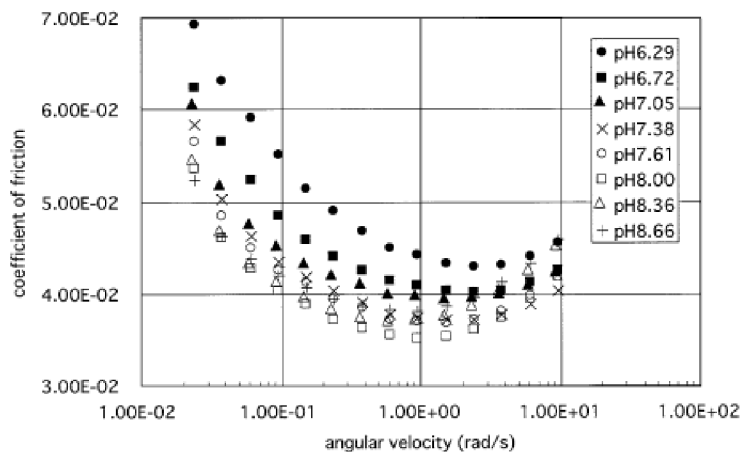
Figure 2.9. The coefficient of friction versus angular velocity curves. The variation in pH had a large effect on the coefficient of friction in the low ranges of angular velocity [31].

Whilst covering the area of adsorption and frictional property of BSA in rubbing condition of UHMWPE and Co-Cr-Mo alloy, the electrochemical method was used to investigate in-situ, real-time information on adsorption and desorption of proteins. The onset of desorption at first rubbing was exhibited, with the gradual decline of desorption. phosphate buffer solution (PBS) without protein has low friction. Whereas for protein, higher concentration showed higher coefficient friction. As absorbed BSA films prevent direct contacts and the increase in potential for BSA solution expressed the amount of desorption under shear stress. Thus, it is disclosed that BSA film is reconstructed during rubbing on Co-Cr-Mo alloy surface, under rubbing condition by shear force. The absorbed film formed become strong and stable and optimally adapted structure for shear force by receiving shear force [44].
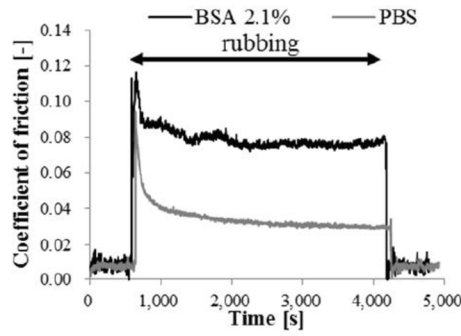
Figure 2.10. The effect of friction transition under OCP condition [44].

While focusing on concentration levels dependency of BSA and γ-globulin, influence on the lubricating ability and the frictional coefficients of Co-Cr-Mo hip prostheses has been revealed. Atomic force microscopy (AFM) was used to measure applied normal force and surface roughness to analyze microscopic frictional measurements. Friction coefficients of the Co-Cr-Mo femoral head with boundary lubricants were calculated afterwards. It has been stated that the maximum level of BSA and the optimal concentration of γ-globulin leads to effective boundary lubrication. Thus, the concentration of BSA and also γ-globulin control the friction of Co-Cr-Mo head. These optimal concentrations of BSA and γ-globulin can be utilized to increase the lubricating ability of Co-Cr-Mo hip prostheses by altering the surface roughness and coating materials of the bearing surface [45]. Boundary lubrication ability was determined for retrieved Co-Cr-Mo head within HA and phospholipids along with microscale frictional coefficients. Concentration-dependent behaviour of HA and DPPC revealed. The optimal concentration that ranges to maximize frictional behaviour is similar to the concentration of HA and DPPC of human SF [18].
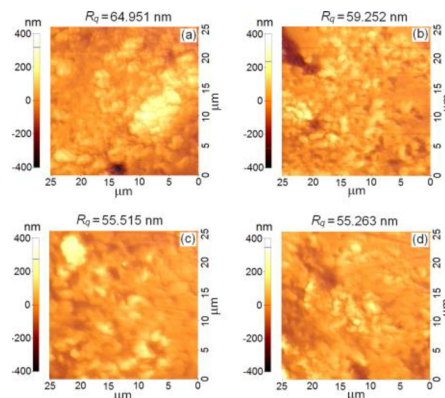
Figure 2.11. *Typical AFM images (2D) with a colour scale in nm range of surface roughness (Rq) for the retrieved Co-Cr femoral head surface, taken over the scanned area of 25 lm_25 lm with a resolution of 256_265 pixels using sharp silicon tips, showing similar Rq values in different lubricants: (a) PBS, (b) HA 3.5 mg/ml, (c) PG, and (d) DPPC 0.2 mg/ml* [18].

Interfacial rheology and bulk rheology of model SF were also focused parameters, which are effect by the proteins and HA for respectively various shear rates, strains and frequencies. During interfacial rheology measurement, the applied frequencies and strains were set to match those of bulk experiments. In the case of bulk rheology, measurement solutions were featured in both steady and oscillatory shear within a considerable range of applied rates, strains and frequencies. In a volume aggregation of proteins or interaction between the HA and BSA changed in geometry were not affect measured viscosity. A significant interfacial viscosity was observed in interfacial steady shear tests. BSA solutions showed remarkable interfacial elasticity in oscillatory interfacial shear tests. In the steady and oscillatory condition of model SF composed of HA, BSA and γ-globulin interfacial rheology occurred due to protein adsorption at the interface are rejected. On the contrary, bulk rheology was controlled wholly by HA of model SF in difference of shear rate, strains and frequencies [16].

Both at physiologic and pathophysiologic concentrations, constituents of SF contribute to the boundary lubrication of the apposing articular cartilage surface. The contribution found individually and also in combination with the constituents of SF. Normal SF acts as an operative boundary lubricant at the articular cartilage–cartilage interface. The important role of HA in the boundary lubrication of resisted articular cartilage surfaces reported precisely in case of boundary mode of lubrication was prevailing. HA in combination with PRG4 lowering friction at the cartilage–cartilage interface. The reason is probably molecular interactions is helping a molecular distribution of shear at the articular surfaces. The lubrication mechanisms correlated with pressurized fluid, inside cartilage and between its surfaces, probably impact considerably due to lower friction and decreased wear articulation contained by synovial joints. Relative to other standing modes of lubrication mechanisms, the features of boundary lubrication in vivo remain to be fully manifested [46].

2.4   Spectropic analysis of synovial joint

The actual reasons for OA are supposed to be classified into two prime areas. The first one is the alteration of mechanical loading, which causes the total joint replacement of patients due to the stiffer structure. Another principal point could be explained as a variation of the chemical composition of the bone matrix and the SF. It could be assumed that the secondary structures of SF proteins and tropocollagen are oppressed in OA [4, 17, 20].

The basic doctrine of protein structure is that the amino acid sequence identifies the structure of the protein. The belief regarding the proteins fold is to attain the lowest energy structure that may be achieved for a certain sequence.

To uncover the three-dimensional structures of proteins, spectroscopic methods, including Raman, are especially useful for measurements over a range of temperatures. Small volumes of protein solution can be used to analyze by Infrared (IR) and Raman spectroscopy. The frequencies of amide bands are evaluated to define the distribution of secondary structures in proteins [47].

Esmonde-white et al. [20] investigated differences between biochemical compositions of healthy joint SF and SF of OA patients. The evaluation was enrolled for patients with clinical evidence of chronic pain and patients scheduled for elective surgical treatment. To assess symptomatic knee, pre-operative conventional postero-antero radiographs of the patients were reviewed. Drop deposition/Raman Spectroscopy protocol (DDRS) was utilized as an evaluation tool to distinguish between OA patients' SF and healthy joint SF. Light microscope was used for coarse separation from the dried drop. From DDRS, the dried drop contains two distinct regions, a glassy appearance of outer edge and center with fern shaped crystalline deposits and also some radial cracks along the edges. Primarily protein Raman bands are visible from spectra of drop edges. The remarkable differences between no damage and damage groups are ratios 1080 cm^{-1}/1001 cm^{-1} and amide I band intensity ratios, respectively sorted by K/L score. This ratio increases in the damage group, that characterized the chemical environment of the protein backbone is changing with OA damage. Disorder in protein secondary structure provides further evidence of altered electrostatic interactions.
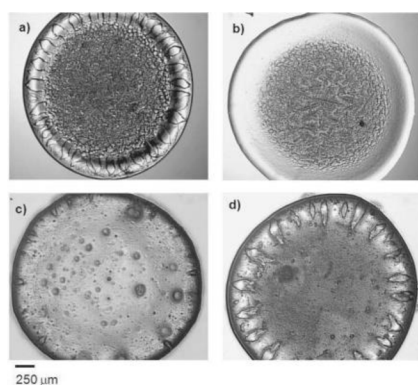
Figure 2.12. Microscope images of human SF dried drops at low magnification show a heterogeneous deposit [20].
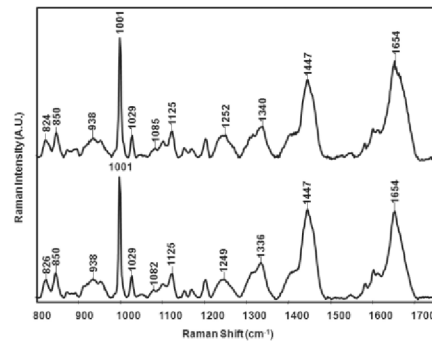
Figure 2.13. Raman spectra collected from SF drop edges contains bands that convey chemical and structural information [20].

Thus, DDRS method can be used as an appropriate detector of SF of OA patients; namely, the Raman band describes protein secondary structure. Raman data clarified that disorder within regular electrostatic interactions of SF occurs due to OA [20].

Raman-scattering spectroscopy method was also used to observe SF from the joint cavity during the surgery. The composition of SF expressed that with the development of degenerative-dystrophic process within the SF of the affected joint, there is the huge increment of the structure of components of HA (C-O, C-C) and Amide III [48].

By using Raman spectroscopic technique, differences of molecular structures between tibial plateaus of respectively healthy joints and joints with total replacements due to OA were compared. Also, comparison of medial and adjacent compartments of subchondral bones was observed as different load baring sites. While determining the density, it was found that the OA tibial plateaus have significantly higher density across compared to the non-OA samples of the subchondral bone. Whereas comparing the tibial compartments, the medial subchondral bone had a significantly higher structural density than the lateral subchondral bone. Principal components analysis from Raman spectral signature revealed a large separation of spectra between the non-OA and OA specimens. Although, between the medial and lateral compartments within each cohort, there was no difference observed. There was a huge remarkable difference observed between the profiles of the non-OA and OA specimens. Specifically, tibial plateaus of medial and lateral for both bone matrix significant chemical structural changes appear due to OA. At the same time, spectral differences were not found between medial and lateral compartment of the subchondral bone matrix [4].

Therefore Kerns et al. [4] ensured that the subchondral bone matrix also differed in its chemical structure due to OA. Both above intimations of chemical structural alteration were observed by means of Raman spectroscopy. However, the structural changes of each of the components separately and combinedly are required to be disseminated to understand these chemical changes thoroughly. The sought-for information of the tribo-film chemical composition on implant should be addressed, including simultaneous discretion of mechanical properties and control of temperature, pressure and frictional force.

Confiding on the change of molecule's bond polarizability, the optical method of Raman spectroscopy provides information through inelastic probing of its vibrations. It is extremely sensitive to intramolecular conditions; nevertheless, the cross-section of Raman scattering is low. One of the most important factors is the presence of water as one of the elements of the biological materials, does not disrupt the biomolecular fingerprint obtained by Raman spectroscopy [28].

Through the Raman spectrum, there are various remarkable qualitative and quantitative indicators to demonstrate peptide conformation. The hydrogen bond supports secondary structural motifs of peptides extensively [49].

For instance, α-helix or β-sheet structures imprints are well identifiable on the Raman spectrum. The stand of Amide I band (exploring with the C=O stretching, contributions from C-N stretching and N-H deformation) for the α-helical peptide structure is 1645-1660 cm-1. On the other hand, the position for β-sheet peptide structure the band is remarked at 1665-1680 cm-1. While Amide III band (explaining the vibrational coupling between adjacent C-H and N-H deformation) is found at 1265-1300 cm-1 for α-helix, however, β-sheet peptide structure shifts the band to 1230-1240 cm-1. Thus, the variation of a peptide conformation, as a result of chemical reactions or denaturation, can even be the consequence of loss of biological activity of proteins, can be easily observed by using Raman spectroscopy [49].
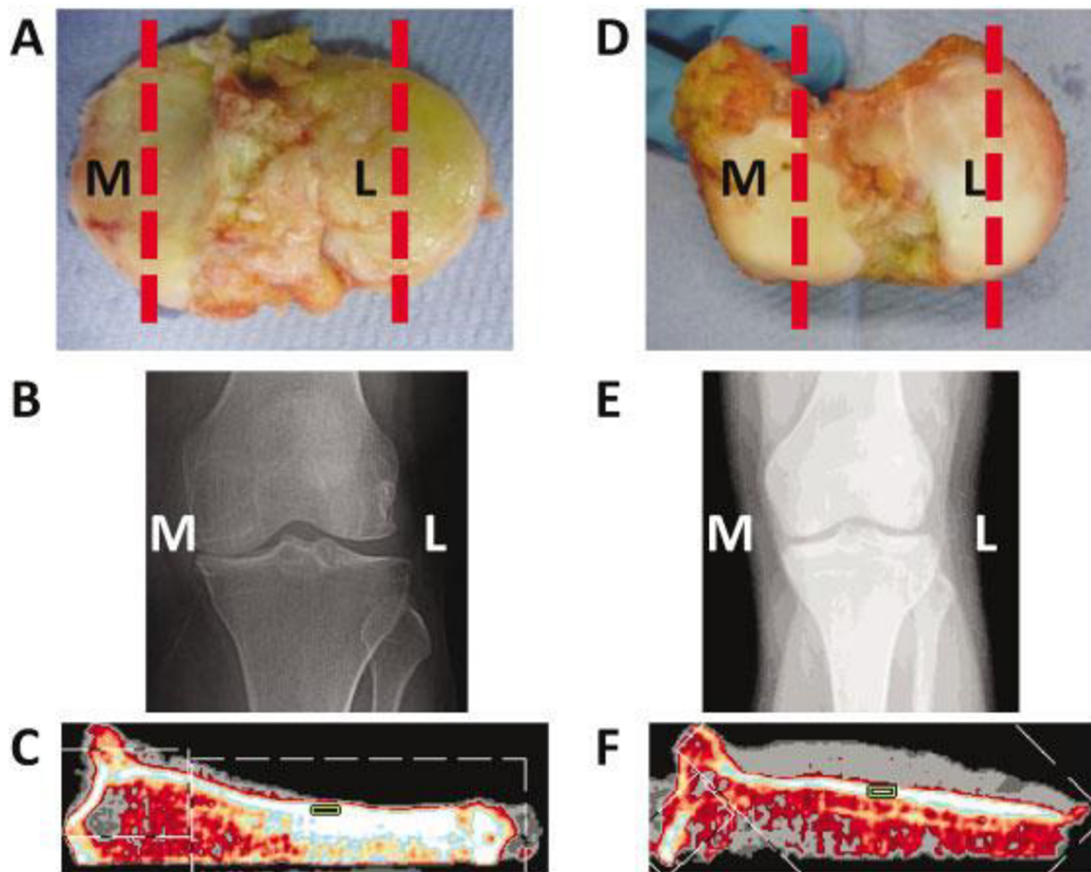
Figure 2.14. Assessment of the tibial plateau from a patient with OA compared to that from a non-OA control. Postoperative photographs (A and D) and preoperative radiographs (B and E) of the medial (M) and lateral (L) tibial plateaus from a representative patient with OA (A and B) and a non-OA control (D and E) are shown. The medial tibial plateau (C) and lateral tibial plateau (F) from a patient with OA were assessed by peripheral quantitative computed tomography (pQCT). In the pQCT images, the region of interest is demarcated as a green box. The red broken lines in A and D indicate the plane from which the pQCT measurements were obtained [4].

Raman and IR spectroscopy were utilized in the study of Depciuch et al. [28] to assess the balance between phospholipids and proteins in blood serum, notifying a remarkable decrease in the amount of phospholipids and proteins due to depression. The importance of phospholipid-protein balance has also been described here. It is explained that the structure of the proteins and their functions are directly influenced by phospholipids. As a result, the reducing levels of phospholipids would causes the introduction of affective disorders occurrence. Also, it is concluded here that the spectroscopic method yields quick measurement results for the analysis of biological material. Thus spectroscopy is demonstrated as a successful diagnostic tools to indicate the changes in the blood serum of humans and other disorders.

The utilization of one of the plasmonic-enhanced Raman modalities is proved to study the variation of the protein study in more detail. Precisely, the drastic development of surface-enhanced Raman scattering (SERS)-based biosensors justify the applications of chemical analysis, nanostructure characterization as well as for biomedical sectors [50]. SERS is a very efficient technique to determine the high increase of Raman signal after protein binding to the metallic nanoparticle(s) [50-52]. However, Laruinaz et al. [53] utilized SERS study for protein-nanoparticle interaction, bio-conjugated silver nanoparticles. Finally, it is substantially ascertained that Raman spectroscopy could be a very successful operative analytical tool due to its high sensitivity, high selectivity, and fluorescence-quenching properties [50, 53].

2.5   Joint implant material analysis by spectroscopic method

The research area of synovial joint replacement has been expanded with the imposition of spectroscopic technique. Several studies are proclaimed with evaluation by spectroscopic method on the ground of joint implant materials.

Zhu et al. [54] studied polarized Raman analysis of wear-induced (residual) stress fields on two different long-term alumina ceramic hip femoral retrievals working against polyethylene (PE) liners. There is also an analysis of tensor-resolved residual stress motifs in the three-dimensional space.

Both alumina hip femoral retrievals of the head were slid against PE liners. Raman spectra of these samples were obtained at room temperature while using back-scattered confocal laser microscope to determine the optical morphologies of the samples. The microstructure of the Al2O3 heads surface in the main wear and non-wear zones were analyzed under the laser microscope. It was found a coarse grain structure and extensive grain pullout throughout the head surface. At room temperature, α-Al2O3 possesses a structure belonging to the 3m (D3d) point group and shows seven Raman active bands, including two A1g modes and five Eg modes.On the ceramic surface of the two femoral heads a remarkable difference in the residual stress field stored was found. The evolution of residual stress motifs in space, including exceptionally high shear stresses in one case, were revealed. The micromechanical features linked with the joint performance that occur in real in vivo condition could be uncovered by this development of Raman spectroscopic algorithms [54].
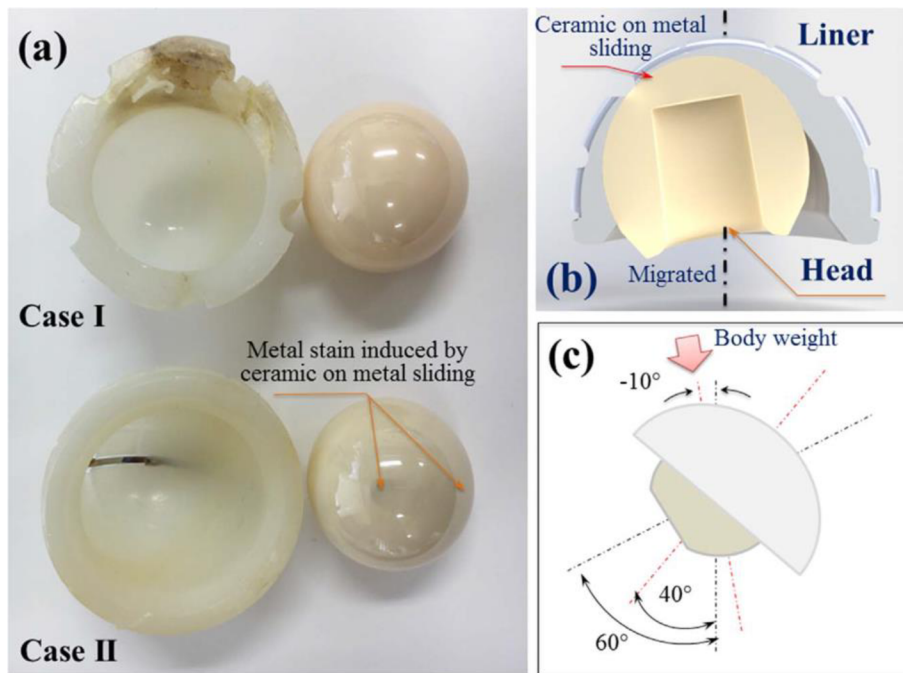
Figure 2.15. (a) Photograph of the two studied Al$_2$O$_3$/PE retrievals; (b) schematic draft of Case II after migration of the femoral head occurred during long-term service; and (c) draft of the altered inclination angles of both head and liner as compared to the original configuration (black dot line) of Case II. [54].

In an orthopaedic, implant UHMWPE debris is produced in a sub-micron-sized within the joint space due to articulation and cyclic loading. To determine the debris, tissue slices or fresh SF were digested with sodium hypochlorite directly on polycarbonate filter. It is explained that plastic particles of the debris were not disrupted during this analysis procedure. While micro-Raman spectroscopy was utilized to verify the integrity of retrieved PE particles and electron microscopy was used to characterize the size and shape of PE particles [55].

Three-dimensional Raman algorithms have been developed nowadays for local mapping of oxidation. It is possible by this means to obtain microscopic spatial resolution of plastic strain, as well as the ability to resolve molecular orientation patterns. In vitro and in vivo tribological responses of UHMWPE bearings for artificial hip and knee joints were measured to reveal the microscopic nature of surface degradation within the human body. From the Raman analyses, a complex scenario of physical chemistry appears, which focuses on the significance of molecular-scale phenomena than unadorned microstructural change. [56].

Ten retrieved and four new mildly cross-linked UHMWPE acetabular liners were analyzed in terms of surface deviation, oxidative degradation and changes in material properties [57]. Techniques used for the measurements of these experiments were, respectively micro-computed tomography (micro-CT) scan, 3D laser scanning microscopy, Raman spectroscopy and nanoindentation. To characterize the microstructures of the UHMWPE liners in terms of variation in the orthorhombic crystalline phase fraction and oxidation indices, the utilized equipment was confocal Raman microscope (inVia™, Renishaw) and instrumented nanoindenter was used to measure the hardness and modulus of elasticity. It is observed that the mapped surface deviation spectra across the acetabular liners have positive values indicates material inflation and negative values indicates penetration (wear/creep) on the retrieved liners. Interestingly, most of the wear/creep areas were eccentric, but a few were centric.
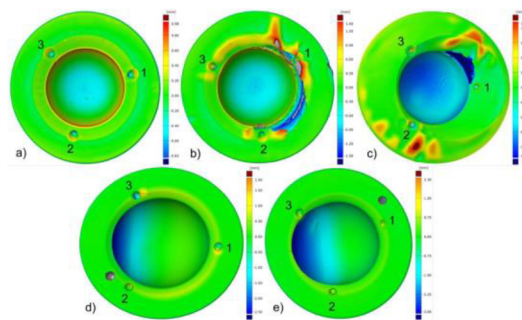
Figure 2.16. *Mapped surface deviation (mm): (a) sample 1, (b) sample 2, (c) sample 3, (d) sample 4 and (e) sample 5. Positive values refer to material inflation and negative values refer to material wear* [57].

Samples with centric wear area had higher surface roughness compared to the samples with eccentric wear area. But in case of few samples had eccentric wear but exhibited on the rougher surface followed by failure mechanisms.
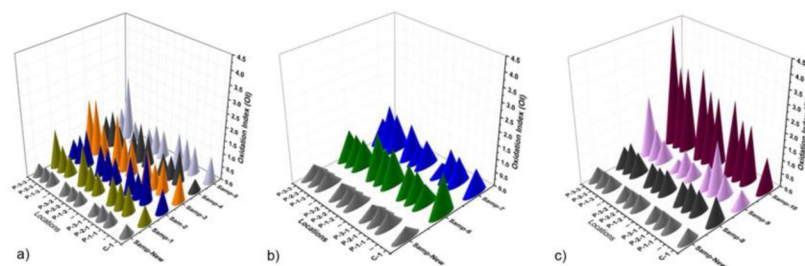
Figure 2.17. Oxidation index for the retrieved samples: (a) group 1, (b) group 2, and (c) group 3 [57].

The oxidation indices were measured and found that all retrieved samples have higher oxidation indices at the contacting sidewall and the rim regions compared to that of a new sample. Chemical degradation was identified in the retrieved prosthesis through the oxidation indices. One of the most denominating factors was the eccentrically worn track for higher penetration rate. Also, material inflations were found in few samples rim areas and contact areas. Ultimately hardening and stiffening were observed in these analyzed prostheses [57].

Taddei et al. utilized Micro-Raman spectroscopy to analyze the wear degradation of the UHMWPE, Highly cross-linked polyethylene (XLPE) and vitamin E-added XLPE acetabular cups for total hip arthroplasty on a molecular scale. However, it is stated that the wear mechanisms of each type of cups were different. An improved wear behavior appeared for the vitamin E-added XLPE cups for the long-term and more rigorous testing environments. It is revealed that in the presence of third-body particles, the cups experienced the lowest rise in wear rate and more substantial structural modifications were observed. The lowest mass loss was integrated with the XLPE cup, including the exceptionally modified articular surface. Therefore, the morphological attributes of these total hip arthroplasty cups, along with gravimetric wear rates, could have significant information regarding the wear degradation characterization [58].

Micro InfraRed Reflection Absorption Spectroscopy (Micro-IRRAS) was used by Stevenson et al. [59] to reveal wear scar on the disc, surface deposits in and around the rubbed region of a Co-Cr-Mo ball-on-flat test setup. 25% bovine calf serum (25BCS) and human SF were used as the lubricants of the arrangement. The HSF samples exhibit increased wear compared to the 25BCS solution mostly. Primarily denatured proteins, including excessive nonnative β-sheet content were observed within the deposits, while with an amyloid-type fibril structure formation is found by ThT (Thioflavin T) fluorescence imaging in this β-sheet aggregates. In a few cases of HSF samples, trans-alkyl chain/carbonyl components were also detected, indicating the presence of lipids in these deposits. Inlet shear stimulates denaturing of proteins and thus the construction of non-native β-sheet accumulations. SF proteins denature in the restricted gap geometry, proximity to the contact zone and are entrained into the contact developing the lubricating film. Surface protection during rubbing seems to be provided by this insoluble, denatured protein films through the primary lubrication mechanism [59].

(a)

(b)
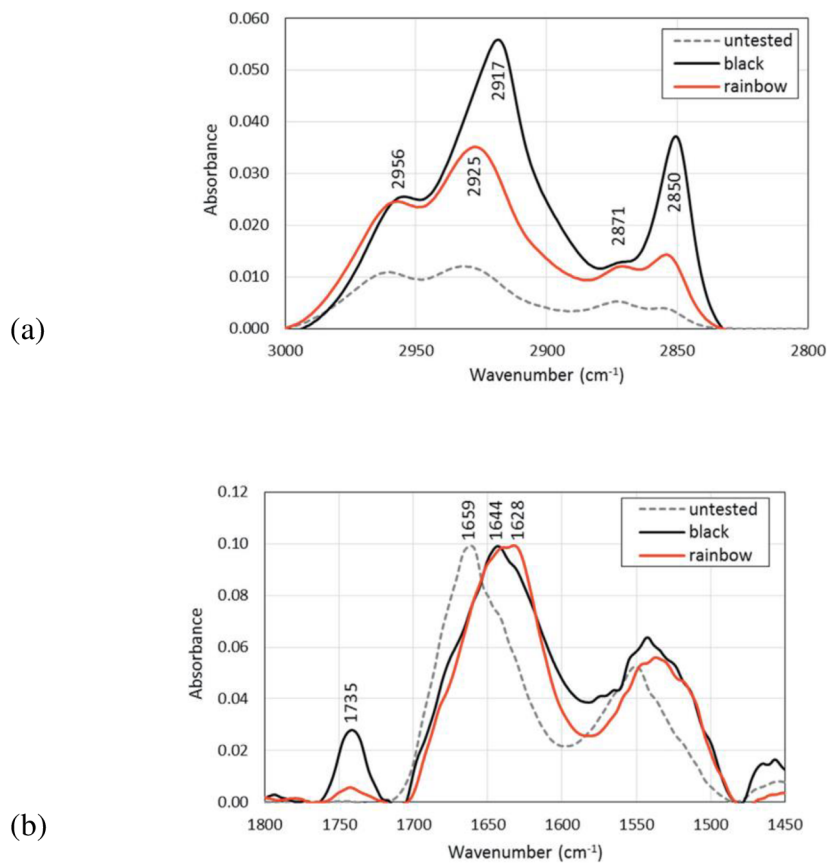
Figure 2.18. Micro-IRRAS analysis of surface films: human HSF041 (a) 3000–2800 cm−1 (b) 1800–1400 cm−1 range [59].

A carbonaceous tribo-films existence in Metal-on-metal (MoM) hip retrievals originated from synovial proteins are also suggested in other studies, reducing corrosion and wear of the articulating surfaces. The treatment potentials generated corrosion of Co-Cr-Mo alloy in the form of pits and/or grain boundary corrosion explained by the mechanistic study. Therefore, mechanical stability of the film, mainly at the subsurface level, is under consideration in this case. However, it is stated that for the film formation release of metal ion release required an optimum level and the certain state of decomposed protein existence is necessary. Thus, this procedure determines the chemical nature of the carbonaceous tribofilms. Raman spectroscopy was utilized in this experiment to comprehend and quantify the carbon the appearance, to indicate the treatment potential that results in increased carbon content film applying potential treatments as well as protein content. Scanning Electron Microscopy (SEM) was used here to reveal film composition and surface homogeneity of the treated surfaces. The metal alloy displays a lighter, but when the film formation occurs, the colour of the carbonaceous film obtained a darker shade [60].

On the other hand, in a protein lubricated metal-on-metal (MoM), sliding contact tribochemical reactions may play a remarkable role on the wear performance. Simultaneously, combined interactions of wear and corrosion seem to act on the surface to add important feature. In a ball-on-flat test configuration, a ceramic ball articulating against low-carbon wrought Co-Cr-Mo alloy pins was lubricated with BS. Wear tests were taken place within a range of contact loads at a single potentiostatic condition. The loss of weight, including variations in surface properties, were observed, indicating that the loading condition influenced wear. Wear enhanced with load, though linear relationship alignment between employed load and measured weight loss was not observed. Scanning electron microscopy and Raman spectroscopy determined that in case of low loading, the absence of tribofilm. On the other hand, in case of higher loading, the tribofilm was present within the contact area [61].

The molecular-level characterization of BIOLOX®delta retrievals was focused on by fluorescence and Raman spectroscopic technique, where the obtained results showed material properties alteration of BIOLOX®delta femoral heads. From six different patients who underwent primary total hip arthroplasty of six retrieved BIOLOX®delta femoral heads were collected and analysed. Also, new BIOLOX®delta femoral head was coupled with a homologous acetabular cup and the bearing was run into a hip joint simulator for 1x105 cycles without lubrication was analysed for comparison [62].
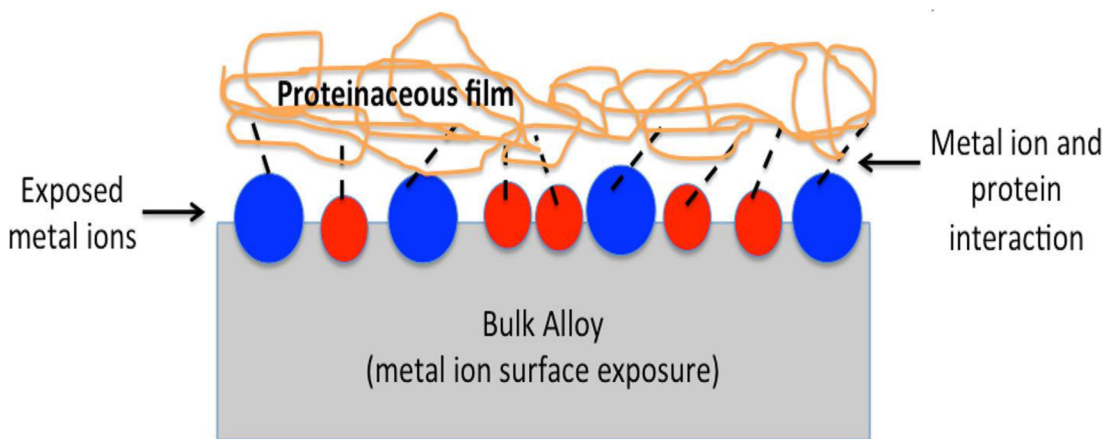
Figure 2.19. Proposed schematic diagram shows the interactions between the metal ions and the surrounding proteinaceous electrolyte. The chemistry and structure of the film are determined by such interaction and chemical bond formed between metal ions and decomposed proteins [60].

A progressive improvement of the material properties occurrence in the period comprised between 1999 and 2009 is proved by fluorescence and Raman. Also, the spectroscopy proved tetragonal-to-monoclinic t zirconia transformation occurrence is due to wear. It was found that the mechanism operating in vivo was found to be the same active in vitro, as that can simulate the effect if in vivo wear [62].

In another study, Raman spectroscopy was applied to measure the tetragonal to monoclinic zirconia phase transformation of eleven Biolox®delta femoral head retrievals altered by metal transfer (MT). The existence of metal transfer may deal with ceramic chemical stability as well as mechanical strength. Raman and photoemission spectroscopy also obtained the residual stress state. From Raman data the mechanism of zirconia phase transformation was evaluated and proved that the growth stage was deficient, and the nucleation stage was not transpiring as freely as it would in unrestricted zirconia. Near the centre of the articulating surface, also in the MT area, Vm (monoclinic volume fraction) zirconia contents were elevated than in the border control area of the retrievals. Stress related to MT seemed a more serious condition in one retrieval that produces zirconia phase transformation. Rest of the sample were favourable to a zirconia phase transformation of almost similar amount to stresses associated with loading in the central area and related to MT. The transformation differs in thicknesses for different samples revealed by Vm depth profiling [63].
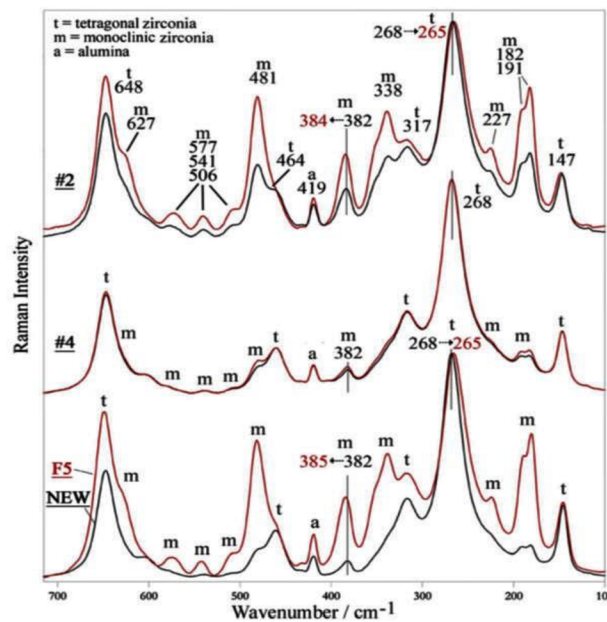
Figure 2.20. Average micro-Raman spectra recorded on some representative BIOLOX®delta femoral heads [62].

Hence from above literature, it could be postulated the to demonstrate the condition of joint replacement and to enhance the longevity of the replaced area, spectroscopy could be used to comprehend the biochemical behaviour of the materials using in joint replacement

36

3   ANALYSIS AND CONCLUSION OF LITERATURE REVIEW

SF is a complex mixture of vast and surface-active molecules [24] that functions as a biological lubricant within the joint [19]. In a typical joint, lubrication is in best possible amount, following normal loads, shear stresses, and rates change within the articulating cartilage surfaces, causing low-friction and low-wear properties during movement [15]. The tensile properties of cartilage depend on the area of articular cartilage, which is in connection with SF and permit it to resist the sheer, tensile, and compressive forces executed by articulation. The degradation of cartilage can be introduced due to the inactivity of the joint. OA and other disease development are the reasons for a drastic change in the metabolism of cartilage [26]. The concentration of the constituents of SF, specifically for the proteins, may differ greatly due to various reasons. Diseased and periprosthetic SF alter its features and changes occur, including decreased effective viscosity, increased protein content and increased pH [24].

Therefore, it could be assumed that due to OA and joint replacement, the mechanochemical environment of synovial joint and SF undergoes alterations. OA is reasoned as complex epidemiology, including the disorder of multifactorial, with genetic, biological, and biomechanical components. While joint replacement is an efficient treatment for the symptomatic end-stage disease, with inadequate functional outcomes can be persisted and the limited lifespan of prostheses is constrained [2]. Tribology describing interacting surfaces in relative motion in collaboration with rheumatologists, orthopaedic surgeons and biochemists cover the research area of the lubrication of joints and to design the articular prostheses [64]. The service life of the implant material is affected by various issues, including aseptic loosening due to an inflammatory reaction against polymer wear debris, which is more common in metal-on-polymer combination [5]. Also, due to the lack of mechanical stimuli on the bone may stimulate its resorption that causes the eventual failure and loosening of the implant [1]. In the case of ultra-pure alumina ceramic, the risk of fracture is revealed, and the poor toughness of alumina develops a serious limit in some cases. [65]. In the case of zirconia-toughened alumina hip implant head tetragonal-to-monoclinic zirconia transformation has been reported due to wear [62].

Consequently, the failure of hip replacement is strongly influenced by particles released from the tribological process of the surfaces during joint articulation. Hence lubrication mechanism has also vigorous effect on the service life of the implant materials [12].

Several studies are concerned with adsorption and desorption of proteins in different kinematic conditions and film thickness in different pH, buffer and various concentration of proteins [23, 24, 32-34, 44, 46]. While wear measurement, frictional coefficients, frictional force, shear force, surface geometry, boundary lubrication, rheology of various constituents are also regarded in connection with proteins and other SF elements to explore the understanding in this area [15, 16, 18, 30, 44-46]. To consider the mechanical and chemical environment of human synovial joint, the viscosity of various modal fluids and wettability of various surface materials were also measured [17, 18, 30, 32, 34] with respect to their duration in time and under varying temperature and pressure [15, 32].

Film formation and film thickness had been analyzed in different types of materials including metal such as stainless steel and Co-Cr-Mo, ceramic, materials containing DLC coating surfaces with extensive lubricants comprising BS, γ-globulin, BSA, HA and different types of model SFs. Optical interferometry and electrochemical method were utilized for various experiments. Thus, the lubrication process and film formation are focused on several studies [11, 23, 24, 32, 35-39]. While the chemical structure of the formed film on different implant materials is needed to be addressed for more exclusive understanding of film formation and lubrication mechanism.

It is explained that the organic deposits of agglomerated-proteins are formed on implant surfaces [24]. The formation of a passive film is assumed by the absorption of organic species of the SFs, which may perhaps modify the surface reactions of the implant materials. The adsorption of the protein over the metallic surfaces has an influence on the biocompatibility of the biomaterials. Due to this formation of the biofilm by protein or amino acids on the surface can occur as a lubricant film reducing friction while reducing mass lost [36].

To expose the protein structure, the sequence of amino acid is required to be expressed. Hence, spectroscopic methods are able to reveal the three-dimensional structures of peptide conformation of proteins. Notably, the hydrogen bonds in between the secondary structural motifs of peptides significantly α-helix or β-sheet structures are detectable by means of the Raman spectrum. Raman spectroscopy measurement may conduct over a range of temperatures. While a tiny amount of solution is required to analyze by Raman spectroscopy. In contrast water does not interrupt the Raman figure print evaluation, though water appears as an essential element in all the biological molecule [28, 47, 49].

Raman spectroscopic technique has been already widely used in the area of biomedical implants in both qualitative and quantitative measurements. Tensor-resolved residual stress motifs of alumina heads in the three-dimensional space were obtained by Raman, concluding with the fact that by the developments of Raman spectroscopic algorithms, the micromechanical features of joint performance is possible to explore. [54]. UHMWPE bearings for artificial hip and knee joints were evaluated with Raman spectroscopy to disclose the microscopic nature of surface degradation by tribological reactions of within human body [56]. While in another study, the variation in the orthorhombic crystalline phase fraction and oxidation indices of the UHMWPE liners were observed by confocal Raman microscope [57].

While assuming a carbonaceous tribofilms presence in Metal-on-metal (MoM) hip retrievals initiated from synovial proteins, Raman spectroscopy was employed to comprehend and quantify the carbon content and the appearance of protein molecules [60].

The molecular-level characterization and measure the tetragonal to monoclinic zirconia phase transformation of Biolox®delta femoral head retrievals distorted by metal transfer were also revealed by Raman spectroscopy [62, 63].

It is visible from the above discussion that the formation of the film is dependent on various parameters, such as pH of the solution and static and rolling conditions, viscosity and concentration of the solution, which are already revealed. Thus, it is high time to detect the occurrence of the chemical change of SF for the proper understanding of the condition of joint replacement and further improvement of the durability of the replaced area. Raman spectroscopy is a unique technique to explain the biochemical behaviour of the materials using in joint replacement. Therefore, chemical analysis, including the study of tribological and biological properties of the SF of joint replacement, will improve the concept of the process.

Due to the different biological components' existence within the SF, the characteristics of formed films are dependent on the variety of SF protein and other constituents. Depending on the chemical composition of these components, the chemical nature of films could also differ. It is considered the combination of the chemical reaction and frictional coefficient within artificial joint replacement may reveal some reality, to uncover more practical results to realize the lubrication chemistry and mechanism of SF within the prosthesis.

4   AIM OF THE THESIS

The aim of the dissertation is to clarify the chemistry of lubricant film formation on hip implant material surfaces while concerning on the compositional variability of the SF lubricants. To achieve this objective an experimental approach is introduced facilitating Raman spectroscopic technique, utilized for the chemical structure analysis of formed lubricant film by SF components, including model fluids of different concentrations. Subsequently, following the method authentication, several different combinations of hip implant materials are explored to uncover extensive analysis of film formation, including the measurement of the friction coefficient of these sets of hip implant materials lubricated by various SF. To accord with the main goal of the thesis, resolution of the following steps were initiated:

- Design the methodology of Raman spectroscopy for the chemical analysis of lubricant film.
- Study the chemical composition of the film formed on the surface of the implant materials.
- Investigate of the chemical structural changes of SF constituents in interaction with implant materials.
- The coefficient of friction calculation for numerous implant pairs along with the lubricants
- Evaluation of the Raman Spectra
- Compare and contrast the Raman data with frictional coefficient data to comprehend the relation.
- Discussion and conclusions of the revealed results.

4.1   Scientific questions

From chemical perspective:

- *Which components of SF are adsorbing chemically on hip implant material surfaces while lubricant film formation within artificial joint replacement?*
- *How is SF changing the chemical structure of its constituents due to artificial hip implant?*

From tribological perspective:

- *How are frictional coefficients differing with this chemical change in the hip joint replacement?*

4.2   Hypothesis

- *On the surface of implant material, protein content is a significant factor for chemical interaction and involving chemisorbed film formation rather than HA and phospholipids.*

- *Metal hip implant materials are more chemically reactive with SF components to form tribo-film on the surface and could act as heterogeneous catalyst to form lubricant film within joint replace. While ceramic implant materials are less chemically reactive to sustain chemisorption process with SF fluid contents.*

- *With the elevation of chemical reaction occurring within a certain arrangement of implant materials and the lubricants, the friction coefficient of friction of the contact pairs is probably increased.*

4.3 Thesis layout

The dissertation thesis is comprised of three papers will be published in peer-reviewed journals (Paper A, B, C). The main goal of the research is chemical analysis, including the tribological and biological properties of the SF after total joint replacement to aid in comprehension of the process. Paper A provides a systematic review of the SF focusing on the biochemical and mechanochemical properties of SF after joint replacement. It exposed the requirement of understanding the chemical composition of the formed lubricating film and structural changes of the associated proteins under mechanical loading. A preliminary study of selected proteins of the SF within a tribological condition of Co-Cr-Mo was pledged here by using Raman spectroscopy.

Consequently, to realize the biochemical reaction during the formation of the lubricant film SF constituents such as albumin, γ-globulin, HA, and model SF at physiological concentrations in the experimental condition are considered as the reactant of this process. Within a pendulum hip simulator, the tribological process were continued, including the measurement of frictional coefficients of the contact pairs. Raman spectroscopic technique was applied to understand the chemical reactions between the SF and implant material. Cobalt-chromium ball on an UHMWPE cup arrangement was employed in Paper B to reveal the reactivity of metal against PE contact pairs. The experiments conducted in the ball-on-cup configuration also consist of two types of commercial ceramic hip implant pairs, namely BIOLOX®forte and BIOLOX®delta in Paper C, to uncover the biochemical responses of SF lubricants in the ceramic interface.

A. Rufaqua R, Vrbka M, Choudhury D, Hemzal D, Křupka I, Hartl M. A systematic review on correlation between biochemical and mechanical processes of lubricant film formation in joint replacement of the last 10 years. Lubrication Science. 2019 ;31(3):85-101.
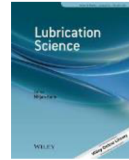
B. Rufaqua R, Vrbka M, Hemzal D, Choudhury D, Rebenda D, Křupka I, Hartl M. Raman analysis of chemisorbed tribo-film for metal-on-polyethylene hip joint prostheses. (Submitted to the Journal Biosurface and Biotribology).

C. Rufaqua R, Vrbka M, Hemzal D, Choudhury D, Rebenda D, Křupka I, Hartl M. Analysis of chemisorbed tribo-film for ceramic-on-ceramic hip joint prostheses by Raman spectroscopy. (Submitted to the Journal of Functional Biomaterials).

5   MATERIALS AND METHODS

5.1   Experimental devices

In this present research, mainly two types of experimental devices have been applied. To realize the chemical reaction in artificial hip implant and coefficient of friction measurement of the ball-on-cup contact pair, a customized hip joint simulator was used to investigate various contact pairs. This novel methodology has been tooled with the help Raman spectroscopic technique, where Renishaw inVia Raman spectrometer was employed to reveal the spectroscopic information.

5.1.1   Pendulum hip simulator

The Pendulum hip simulator is explained as an unprecedented and unique bio-tribological instrumentation that replicates 'flexion and extension' of artificial hip joints condition, alongside their real geometry, body temperature and load. It is also suitable for measuring a real-time velocity profile, average friction coefficients and a viscous effect (an indicator of lubrication film formation).
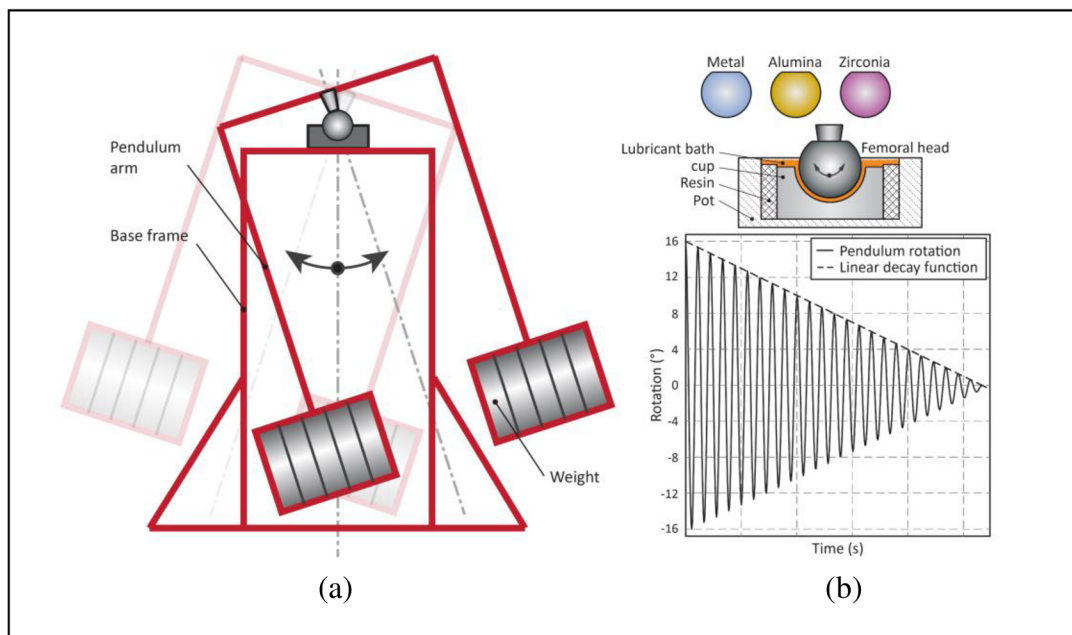

Figure 5.1. (a) A schematic illustration of the pendulum hip joint simulator. (b) Overview of the tested femoral components, detail of the contact couple, and representative linear decay signal [67].

Vrbka et al. [66] conducted his experiment with this mechanism to visualize lubricating films between artificial head and cup concerning real geometry and Necas et al. [12] also utilize the same to understand the effect of diameter, clearance and material of in situ observation of lubricant film formation.

Choudhury et al. [68] used this simulator to understand a significant friction coefficient reduction to the 'dimpled a-C:H/ceramic' prosthesis compared to a 'Metal(Co-Cr)/ ceramic' prosthesis. As a result, it is indicated that the simulator can be utilized as an advanced bio-tribometer. Based on the principles of the pendulum hip joint simulator was used as a test device for film thickness measurement by an optical imaging system.

The simulator is composed of a base frame with the acetabular cup and the swinging pendulum with the femoral head. Electromagnetic motors are employed to drive the pendulum allowing a continuous motion in the flexion-extension plane [12].

The coefficient of Friction for several contact pairs were determined within the pendulum hip joint simulator. The acetabular cup is installed by resin in a stainless-steel pot. This set up is mounted to the base frame. The swinging arm using a cone is connected to the head. When the experiment starts, the pendulum arm is deflected to the primary position and then released. Between the ball and the cup, the impulsive swinging is then damped due to friction. Instant deflection of the pendulum is recorded via an angular velocity sensor. Consequently, the processed signal is enclosing to obtain the friction coefficient. A linear model of damping is utilized for evaluation [67].

It is supposed that this kind of instrument set up could be helpful for determining the chemical reaction within SF after artificial joint replacement along with the frictional coefficient of each contact pair.

5.1.2 Raman spectrometer

In recent years different analytical methods with certain limitations are operated for material identification. Among laser spectroscopic methods, Raman spectroscopy is one of the most valuable methods, which enable correlating the chemical details of molecular structure for material identification [69].

The entire technique is named after one of its discoverers, the Indian scientist Sir Chandrasekhara Venkata Raman was awarded a Nobel Prize in physics in 1930 for the discovery of the Raman effect and the scattering of light. The fundamental principle of Raman method is recognized nearly one hundred years ago, and widespread potentialities are finally able due to technical advancement and unique engineering solution of this technique nowadays [69].
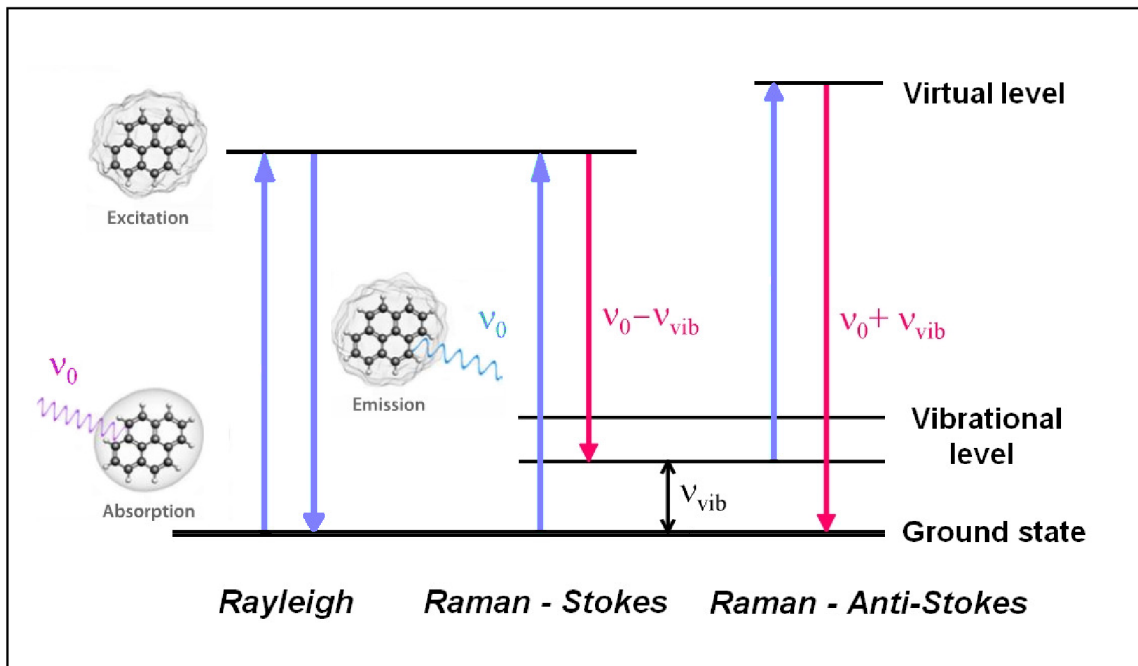
Figure 5.2. Energy level diagram of Rayleigh and Raman scattering [69].

Rayleigh scattering

An inelastic scattering effect originates Raman spectroscopy, which is a monochromatic excitation radiation source. In case of elastic scattering, which named Rayleigh scattering, the molecule is excited to a virtual state and then re-emit a photon at the same frequency as in incident light and relaxes to the initial vibrational state. No absorption of energy from the incident radiation happens by the molecule in this case.

Raman scattering

While inelastic scattering occurs for only a very small fraction of molecules, which may address as Raman scattering. In this condition, the excited molecule relaxes to a separate vibrational level, other than the original state. The energy of an inelastically scattered photon is different from that of the incident radiation.

In Raman spectrum the incident and scattered radiation appear with the energy difference. This difference is the frequency shift between the scattered light v' and the excitation frequency v, are related by the following equation of vibrational energy:

$$hv = hv' + \Delta E_{vibration}$$

Anti-Stokes lines

In the case of Raman, the final vibrational state may be either higher or lower in energy than the initial state of the molecule. If the final vibrational state is lower in energy than the preliminary one, Raman bands are named anti-Stokes lines.

Stokes lines

While the final state exhibits higher energy than the initial state, these Raman bands are called Stokes lines [70].
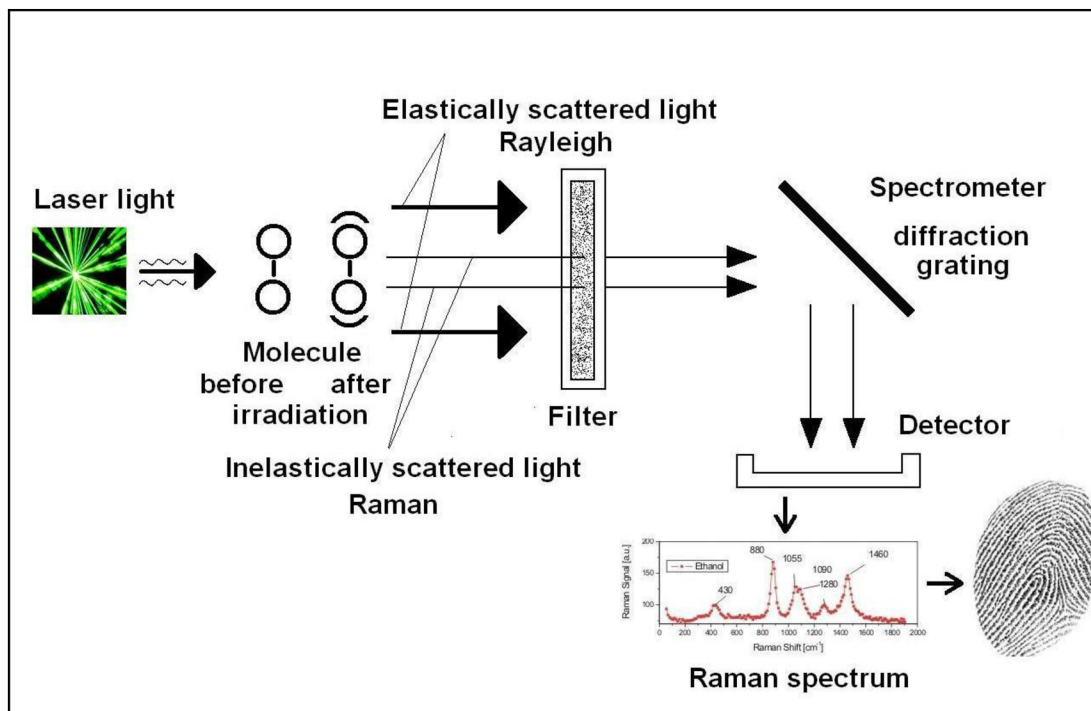
Figure 5.3. The sample is irradiated with laser, molecule vibrates, filter eliminates intense Rayleigh scattering, the grating disperses the light onto a detector to generate a spectrum, which gives the information about molecule bonding and provides a chemical fingerprint utilizable for identification. [69].

Therefore using RENISHAW in Via Raman spectrometer, spectra were obtained for different SF contents before and after tribological experiments within the simulator. Also, the surfaces of the balls were observed to detect if the chemical properties are changing with the tribological process.

5.2 Test sample and experimental conditions

5.2.1 Ball-on-cup configuration

Ball-on-cup configuration proves to be an ideal arrangement for lubricating film formation within the hip joint simulator. To investigate the lubrication processes within artificial joints considering the ceramic femoral heads were focusing on the role of particular proteins, by Necas et al. [11]. The experiments were conducted in a ball-on-cup configuration, where the contact couple was the ball made from ceramic and the acetabular cup from glass. The measurements were conducted using colorimetric interferometry and fluorescent microscopy under pure rolling, partial negative and partial positive sliding.

While clarifying the lubrication processes considering within artificial joints, this experiment was conducted in a ball-on-cup configuration. The first contact couple were the ball made from Co-Cr-Mo and the acetabular cup from glass and PE. Thus, for this experiment to explain the effect of tribology, metal hip prosthesis head of Co-Cr-Mo ball (28mm) from Zimmer were used as per ISO 5832-12, which contains metal as cobalt-chromium casting alloy. The cup was used made from PE from Smith and Nephew 28mm. In contrast, a tailor-made acetabular cup from optical glass (BK7) was also used in the initial stage of the experiment.
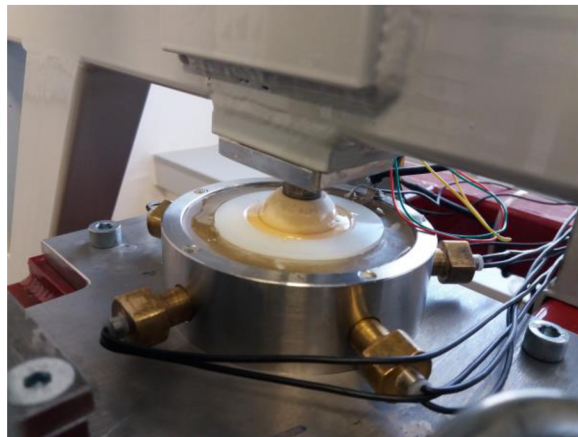
Figure 5.4. Ball on cup configuration in Pendulum hip simulator

The other two ball-on-cup sets are made from two types of ceramics. Alumina ceramic ball was used that is BIOLOX®forte from Zimmer- sulox (28mm), and the cup of the same component was used from smith and nephew.

And the set of ball and cup is of zirconia toughened alumina ceramic to be precise BIOLOX®delta (28mm), and the cup was also made from the same component. Both ball and cup of BIOLOX®delta are used from Zimmer.

5.2.2 Model fluid lubricants

Within hip replacement to observe the chemical reaction occurring on implant surfaces 25% BSA, albumin (28.0 mg/ml), γ-globulin (11.0 mg/ml) and HA (2.0 mg/ml) separately and three types of model SFs were used as lubricants within the ball on cup configuration.

These model fluid were prepared according to the concentration of the components of real physiological SFs evaluated by Galandakova et al. [17]. The types of model fluids used here are respectively the mimic of SF of healthy or physiologic joint (SF1), SF of total joint replacement (SF2) and SF within a joint with OA (SF3) [17, 71]. In the model fluids, the concentration of albumin, γ-globulin, HA and phospholipids were maintained within the range of the situation of human joints described in Table 1.

Table 5.1. Composition and concentration of the applied test lubricants.

Test Fluid	Bovine serum albumin (mg/ml)	Albumin (mg/ml)	γ-globulin (mg/ml)	Hyaluronic Acid (mg/ml)	Phospholipids (mg/ml)
BSA	25%	-	-	-	-
Albumin	-	28	-	-	-
γ-globulin	-	-	11	-	-
Hyaluronic Acid (HA)	-	-	-	2	-
Healthy Joint (SF1)	-	20	3.6	2.5	0.15
After Total Joint Replacement (SF2)	-	26.3	8.2	0.87	0.35
Joint with Osteoarthritis (SF3)	-	24.9	6.1	1.49	0.34

Albumin, γ-globulin, HA and phospholipids were dissolved in PBS, which will be used as the base fluid, for overnight at 4 oC while employing laboratory rocker-shaker (MR-12, Biosan, Riga, Latvia).

The next step of preparation is mixing each of the individual components' solutions in the same solution in order albumin, γ-globulin, HA, phospholipids. The product specifications of the components applied are as stated here. BSA (powder, >96%; A2153, Sigma-Aldrich, St. Louis, MO, USA), γ-globulin from bovine blood (powder, >99%; G5009, Sigma-Aldrich, St. Louis, MO, USA), HA = Sodium Hyaluronate HySilk (powder, quality class—cosmetic; molecular weight = 820–1020 kDa, Contipro, Dolní Dobrouč, Czech Republic), and PHs = L-α-Phosphatidylcholine (powder, Type XVI-E, lyophilized powder; >99%; vesicles form; P3556, Sigma-Aldrich, St. Louis, MO, USA). Lubricant solutions were preserved in -22 oC after preparation.

5.2.3 Test conditions

Within pendulum hip joint simulator set up:

- The temperature was maintained 37 ^{o}C throughout all the experiments.
- 15 kg weight was used on the simulator during these experiments.
- 5-6 minutes to observe the tribological effect of each of the lubricants to obtain the chemical impact on the ball surface.
- The lubricants were collected from the cup after tribological tests for analysis.

To obtain the Raman data:

- The green laser with 532 nm excitation was used.
- On the surfaces of metal and ceramic ball, 1 mW laser power was used with the exposure time of 100 s.
- The lubricants fingerprints before and after tribological tests were realized with 100 mW laser power and 20 s exposing time.

5.3 Experiment design

In the initial stage to acquire the understanding of the methodology, 25% BSA was used as the lubricant and as a ball-on-cup setup with Co-Cr-Mo ball in contact with a tailor-made acetabular cup from optical glass (BK7) were used. But in recent time, the use of BS is discouraged since there are variations in content, fluid characteristics, and nonhuman origin [17]. Thus, we tried to substitute BS with model SF as lubricating fluid in the next steps of the experimental setup.

Therefore, to achieve more realistic environment of the replaced joint, we used commercially available Co-Cr-Mo ball against UHMWPE cup. This arrangement seems more rational as in metal on PE combination used in replaced joint, while albumin and γ-globulin were used as lubricants. In the hip, joint simulator tribological tests were done to observe the formation of lubricating film. After this tribological experiment, the lubricants were collected from the cup. Then Raman spectroscopic analysis carried out for the surface of the Co-Cr-Mo ball and also lubricants without tribological test and after the tribological test to compare the difference of the chemical structure occurring on the ball surface and lubricants due to the tribological test. The microscopic image of the surface of the metal heads were also taken during Raman analysis. These results were published in Paper A, including a systematic review.

Consequently, for more appropriate lubrication that mimics human SF, three types of model SFs were used respectively imitating of SF of healthy or physiologic joint (SF1), SF of total joint replacement (SF2), SF within a joint with OA (SF3) and also HA separately. Furmann et al. [71] used similar lubricants of physiologic concentration and osteoarthritic concentration in the study of frictional behaviour of articular cartilage. Similarly, the tribological test and Raman analysis took place for these lubricants with Co-Cr-Mo ball and UHMWPE cup contact pairs.

(a)   (b)
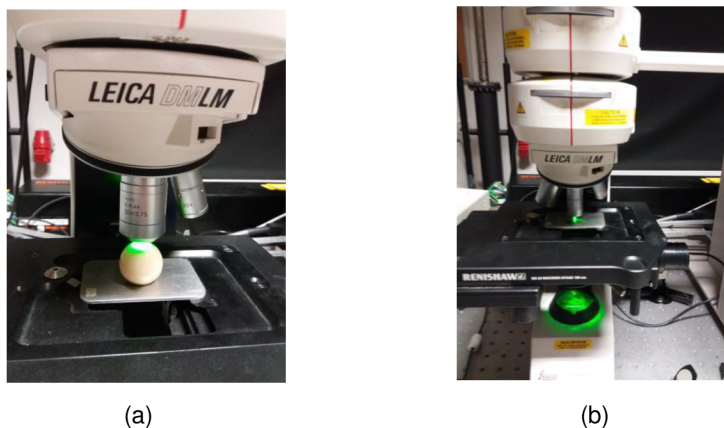
Figure 5.5. (a) Raman spectroscopic measurement of the ceramic ball surface (b) Raman spectroscopic measurement of the lubricant in capillary.

The coefficients of frictions were also measured for each type of lubricants in the contact pair by pendulum hip simulator. Raman analysis were done for the lubricants before and after experiment in the hip simulator and formed film on the implant surface.

Thus, we have Raman data of separate components of SF such as albumin, γ-globulin and HA, as well as the Raman data of the model SFs, where each component, including phospholipids, were mixed in an appropriate ratio of the different joint condition. The microscopic image of the formed film on the surface after tribological experiments were collected to define the visual nature of the films. These results of Co-Cr-Mo implants are published in Paper B.

In the same manner, contact pairs of alumina ceramic, namely BIOLOX®forte and zirconia toughened alumina ceramic called BIOLOX®delta were involved in the tribological experiments within the pendulum hip simulator, including coefficient of friction measurement followed by Raman analysis. As before, separately albumin, γ-globulin, HA and all three types of model SF were exploited for these both types of ceramic contact pairs. Microscopic image of the formed film on ceramic heads with different fluids are also available for these experiments. These results consist of in the latest part of the dissertation in Paper C. Nevertheless, several combinations of test fluids and implant materials usage may help to unveil the chemistry of the film formation perspective in many different points of view.

6 RESULTS AND DISCUSSION

The concern with lubricant film formation in total joint replacement has been studied extensively at the Institute of Machine and Industrial Design (IMID) by other researchers. However, introducing Raman spectroscopy in this area of research is quite a novel approach due to its expedient advantages as non-destructiveness, contactless measurements, without the demand for sample preparation and rapidity. These features of Raman spectroscopy present it as an effective, convenient and desirable method [69], which is efficient to measure the secondary structure of proteins only with a small volume of solution over a range of temperatures [47]. Derivatives of HA in shape of film were also analyzed previously by using Raman [72].

While using Renishaw inVia Raman spectrometer BSA, albumin and γ-globulin film formation on the Co-Cr-Mo metal ball spectra have been obtained (Paper A). It was observed that after the tribological test, lubricants spectra showed verily different fingerprints compared to before test lubricants spectra. The fingerprints of the film on the Co-Cr-Mo ball surfaces of each type of lubricant proteins were also varied than the before test or after test protein spectra. Crystallization of proteins on the metal surfaces could provide differences. Also, there is a possibility of the existence of chemisorbed transition state within protein lubricants and metal surfaces, in case of the metal surface is playing a role of heterogeneous or contact catalyst to change the chemical structure of proteins. It is assumed that the formation of synovial protein films are chemisorbed transition state, those changing the secondary structural composition of protein molecules within the artificial joint replacement. The phenomena can be explained as due to heterogeneous catalysis process, the activation barriers of protein bond formation or breaking might be reduced [73-76].

The spectra of BSA and albumin after test did not show well-defined peak, that can be concluded as the distortion of α-helical structure due to tribological effect, thus denaturation of proteins. In contrast, γ-globulin shows definite peaks in the after-test spectra, which differs from before-test fingerprints; it may presume β-sheet structure is changing its structure due to tribological effect within γ-globulin. The microscopic images of different structures of the formed film produced by different proteins are evidence of chemisorption on the metal surface by protein molecules during film formation.

During these experiments, we could not define each peak due to less experiences on Raman spectroscopy. We assumed that the mixture of different components of SF might expose the fact that which elements are the cause for forming films on implant materials.

Further, in the following experiment (Paper B) we used three types of model SFs, respectively simulating SF of healthy or physiologic joint (SF1), SF of total joint replacement (SF2), SF within a joint with OA (SF3) as lubricants of the setup. HA also used separately, within a physiological concentration with Co-Cr-Mo ball and UHMWP cup to perceive the film formation in hip joint replacement more precisely with this implant combination. Coefficient of friction measurement took place for each of the lubricants with metal and PE contact pairs.

From the Raman spectra of model fluid films on the Co-Cr-Mo ball surface Amide I band for α-helix, ranging within 1645-1660 cm^{-1} [49], were observed, this can emphasis albumin absorption taking place on the Co-Cr-Mo ball surface from the model SFs. CH_2/CH_3 deformation were also observed for all three fluids on the implant surface. SF2 and SF3 fingerprint expressed the presence of CH_2-CH_3 wagging, did not show by the film formed by SF1 and only SF3 exposed α-helix range of the Amide III band. On the other hand, SF2 displays peak at the range of protein backbone vibrations: C-C, C-OH, C-N stretch, C-O-C and glycosidic linkage. Peak ranged near 1000 cm^{-1} due to ring breathing on the metal surface is showed by all three model fluid films [20, 70]. Including some other peaks, the peak ranges showed by the spectra of all three model fluids on the Co-Cr-Mo ball surface expresses several α-helix related features determining the adsorption of mainly albumin from the model fluids after tribological functions. Raman spectra of HA on Co-Cr-Mo ball surface indicated peaks due to C-N stretching and C-H deformation, C-C and C-O stretching, and CH_2/CH_3 deformation, which revealed chemisorption of HA at physiological concentration alone on the Co–Cr–Mo surface. At the same time, there are no similarities with the Raman peaks of Co-Cr-Mo ball clear surface.

From the microscopic image of the film, no remarkable film structure was found for model SF of healthy joint SF1. On the other hand, very thick and branched film were exposed for the model SF after total joint replacement SF2. Similarly, SF3 forms branched film on the implant surface, but the pattern was unlike SF2. Model SFs of joint after replacement and osteoarthritic joint are chemically more reactive and thus adsorbable to Co–Cr–Mo surface than SF healthy joint SF, demonstrating by Raman peaks and significantly visible in the microscope.

The frictional coefficient of the proteins and HA independently within Co–Cr–Mo ball and PE cup are lesser than the coefficient of friction of all three types of SF model fluids. When HA individually used as lubricant, the coefficient of friction showed the lowest value among all the fluids.

However, we could not find any relationship between the coefficient of friction measurement and chemical structural changes for model fluids, proteins and HA due to tribological effect of Co–Cr–Mo and UHMWPE.

In our subsequent approach, we used ceramic contact pairs (Paper C) instead of metal and PE. Two types of commercially available ceramic balls and cups were used, alumina ceramic pair of BIOLOX®forte and zirconia toughened alumina ceramic to be precise BIOLOX®delta pair. Albumin, γ-globulin and HA individually and all three types of model fluid lubricants used previously, were repeated with the ceramic ball-on-cup set up for tribological test following Raman analysis as well as coefficient of friction measurements.

There were no remarkable chemical changes by individual protein (albumin and γ-globulin) fluids on the BIOLOX®delta ball surface. Very thin film was observed, in the microscopic image of the BIOLOX®delta surface for both albumin and γ-globulin, assumed almost no chemisorption to the BIOLOX®delta surface. At the same time, BIOLOX®forte surface Raman fingerprint shows CH_2/CH_3 deformation for albumin and C-C skeletal deformation of both protein molecules. These peaks are evidence of adsorption of albumin and γ-globulin on BIOLOX®forte surface chemically.

Raman fingerprint of HA after tribological test with BIOLOX®delta exposed chemical structural changes due to the experiment. Mainly ring-breathing mode alteration and C-OH bending peak shifts and disappearing 879 cm^{-1} peak from before test spectra manifest the chemical change within HA molecule due to tribological effect of BIOLOX®delta. On the other hand, after test with BIOLOX®forte, HA shift of C-N stretching peak and invisibility of the 879 cm^{-1} band were observed.

In case of BIOLOX®forte with HA film on the surface, C-C skeletal deformation was found, which peak is also detectable on the BIOLOX®forte surface after testing with albumin and γ-globulin. In addition, peaks defining CH_2/CH_3 deformation and C=O stretch on the surface of BIOLOX®forte were marked after testing with HA, which are absent in clear ball. Consequently, both of the ceramic balls are adsorbing HA chemically with a different pattern. HA exposed different spectra after reacting with two different ceramic contact pairs. Microscopic images are also visual as evident of forming different film pattern by BIOLOX®forte and BIOLOX®delta.

With all three model fluids, BIOLOX®delta ball surface shows merely any change. With SF2 and SF3, slight shifting of peaks were observed.

However, BIOLOX®forte surface shows noticeable changes after test with SF2 and SF3. Peaks defining CH_2/CH_3 deformation were observed for these two fluids which were also exposed while reacting with HA on BIOLOX®forte surface. Moreover, CH_2-CH_3 wagging and Amide I expressing of the β-sheet structure were found on BIOLOX®forte that proves the existence of γ-globulin for SF mimicking a total joint replacement fluid and an osteoarthritic joint fluid.

From microscopic images on ceramic ball surfaces, SF1 provides uneven films on both ceramic balls. BIOLOX®forte surface exhibits some clear area without any visible film. However, SF2 shows fluid film with uniform distribution on both ceramic ball surfaces. Lastly, SF3 exposed with inconsistent compilation of fluid on the surface of the ball.

The coefficient of friction for BIOLOX®delta contact pair was observed higher in case of γ-globulin, HA and little higher in case of osteoarthritic model SF than BIOLOX®forte contact pair. On the contrary, the BIOLOX®forte contact pair shows a higher value coefficient of friction for albumin, SF imitating healthy joint and SF imitating total joint replacement.

Nevertheless, no correlation was observed with the frictional coefficient of both ceramic contact pairs and SF lubricants chemisorption features, same as that of Co–Cr–Mo and UHMWPE contact pairs.

In summary, comparing with chemical reactivity within metal-PE and ceramic contact pairs, it has been postulated that albumin and γ-globulin are active elements to form film on Co-Cr-Mo surface and on BIOLOX®forte. In contrast, BIOLOX®delta surfaces were merely affected by albumin and γ-globulin while using them individually. While HA used as a separate lubricant, chemisorption were evident by Raman fingerprints on all three types of hip implant balls. However, the absorption patterns were different for Co-Cr-Mo, BIOLOX®forte and BIOLOX®delta balls. After-test HA lubricant displayed changes of chemical structural change due to tribological effect with ceramic contact pairs contrasting metal-PE contact pairs.

In case of model fluids, after tribological tests with each types of contact pairs remarkable changes within the liquids were not observed. But when we conducted Raman analysis on the ball surfaces after-test with model fluids, we could reach some conclusions.

Albumin adsorption on Co-Cr-Mo surface were taking place for all three types of model fluids. Model fluid imitating healthy joint fluid are less reactive to form film on Co-Cr-Mo. On the other hand, model fluids imitating total joint replacement fluid and OA joint are attached with more bonds on Co-Cr-Mo surface compared to the healthy model SF.

It could be also asserted that BIOLOX®forte chemically adsorbed these two types of model fluids alike Co-Cr-Mo. Although this implant made from pure alumina showed almost no chemisorption of SF elements, after tribological test with healthy model SF. In contrast, BIOLOX®delta surface were almost inert with three types of model SF.

Comparing coefficient of friction values of separate lubricant components, albumin showed close values for all three contact pairs and γ-globulin exhibits the highest value for BIOLOX®delta contact pair and the lowest for BIOLOX®forte contact pairs. Again, HA showed very low value for Co–Cr–Mo and UHMWPE contact pairs and highest for BIOLOX®delta. Thus, there is no consistency for frictional coefficients of different contact pairs with each individual component of the SF.

Similarly, the coefficient of friction measurement for model SF with all three contact pairs disclosed close values for healthy model SF. For SF1 within BIOLOX®forte contact pair value was highest. For SF simulating total joint replacement showed the highest value for Co–Cr–Mo and UHMWPE contact pair and the lowest for BIOLOX®delta. Conversely, model SF simulating OA displayed very high value for Co–Cr–Mo and UHMWPE contact pair than ceramic contact pairs. Likewise, individual components of SF, all three types of model SF do not maintain a consistent value of the frictional coefficient for three types of contact pairs.

Therefore, it can be revealed that the coefficient of friction is not an influencing factor of the chemisorption process of SF on the metal and ceramic surface. Rather elevated concentration of proteins and/or HA in SF could be the influencing factor of chemical adsorption on the metal and ceramic surface on hip implant materials. Among Co–Cr–Mo, alumina and zirconia toughened alumina implant balls, zirconia toughened alumina could be assumed as the most inert and Co–Cr–Mo is found to be the most reactive in case of chemisorption and tribo-film formation of SF and its components.

RESEARCH ARTICLE - LS

WILEY

A systematic review on correlation between biochemical and mechanical processes of lubricant film formation in joint replacement of the last 10 years

Risha Rufaqua[1] (iD) | Martin Vrbka[1,2] | Dipankar Choudhury[3] | Dušan Hemzal[4] | Ivan Křupka[1,2] | Martin Hartl[1]

[1] Faculty of Mechanical Engineering, Brno University of Technology, Brno, Czech Republic

[2] CEITEC - Central European Institute of Technology, Brno University of Technology, Brno, Czech Republic

[3] Nano Mechanics and Tribology Laboratory, Department of Mechanical Engineering, University of Arkansas, Fayetteville, Arkansas, USA

[4] Department of Condensed Matter Physics, Faculty of Science, Masaryk University, Brno, Czech Republic

Correspondence
Risha Rufaqua, Faculty of Mechanical Engineering, Brno University of Technology, Technicka 2896/2, 616 69, Brno, Czech Republic.
Email: risha.rufaqua@vut.cz

Funding information
Ministry of Education, Youth and Sports of the Czech Republic

Abstract

This study provides a systematic review of the synovial and simulated body fluid research for the last 10 years (2006 to 2016). In particular, biochemical and mechanical properties of synovial fluid after joint replacement are focused, namely, the chemical composition of the formed lubricating film and structural changes of the associated proteins under mechanical loading. In summary, the formation of the film depends on pH, viscosity, and concentration of the solution, static, sliding, and rolling conditions and other factors related to the joint replacement. However, chemical changes of the synovial fluid proteins after the joint replacement are rarely addressed and require further attention. To this end, we provide a preliminary study of selected proteins within the synovial fluid using Raman spectroscopy. We conclude that chemical analysis together with the analysis of mechanical and biological properties of the synovial fluid after total joint replacement will help in comprehension of the process.

KEYWORDS

bio-tribology, film formation, Raman spectroscopy, synovial fluid, tribo-chemistry

1 | INTRODUCTION

Synovial fluid (SF) of an articulating joint is a complex biological composite fluid enriched with protein that derived from the blood plasma and cells within the joint tissues (such as synovium, cartilage, ligament, and meniscus) are contained in SF of an articulating joint.[1] This highly efficient water-based tribological system is optimised to provide low friction and wear protection at both low pressures and high contact pressures. The protection is maintained through the entire life of a human across various sliding velocities including during the resting periods.[2] Concerning mobility of the skeletal system,

synovial joints act as bearings and SF is responsible for the lubrication of these bearings, adhering to various mechanisms.[3] The molecules participating in joint lubrication are engaged mainly in providing an effective surface lubricant to reduce the friction and minimising wear damage to the rubbing or shearing surfaces.[2]

The naturally occurring components of SF can vary in concentration. In addition, differences in SF composition were observed for normal knee joint, patients without replacement of joint, patients with primary arthroplasties, and patients with revisions of total hip and knee arthroplasties.[4] In particular, hyaluronic acid, proteins, and phospholipid concentrations varied widely in

patients undergoing the joint replacement.[5,6] The thickness of lubricant film within hip prostheses is hypothesised to influence particular proteins.[7] It has also been stated that concentrations of bovine serum albumin (BSA) and γ-globulin manipulate the frictional behaviour of the CoCr femoral head.[8] The optimum tribological performance of joint replacement would also be subject to the combination of composition, microstructural condition, and manufacturing process of the used alloy.[9]

Pursuing biochemical reactions underlying the formation of the lubricating film, vibrational fingerprint provided by Raman spectroscopy can be used to identify the components present and analyse the chemical bonding among them.[10] In addition, the correlation between the level of phospholipids and proteins exists and can be deduced from Raman spectra.[11] The technique has also been previously used to distinguish between healthy SF and SF changes in osteoarthritis (OA) patients as well as to OA subchondral bone matrix change detection.[10,12]

The objectives of this study are to review and clarify the chemical reactions of SF components during the formation of the lubricating film on the joint replacement along with the focus on mechanical properties of the film. The selection of the review literature is described in Section 2, the result obtained is described in Section 3, while Section 4 contains the review itself. In Section 5, the discussion is provided including the preliminary Raman study on the behaviour of the selected SF proteins when subject to tribological experiment.

2 | METHODOLOGY

2.1 | Search strategy and eligibility criteria

Peer review articles published from 2006 to 2016 were searched for the review. To address both chemical and mechanical properties of the film that forms within artificial joints, articles subject to "SF film formation of artificial joints" or "protein film chemistry of SF" topics were considered. However, articles focused on biotribology in dental and optical science or protein film formation chemistry of outside synovial joint areas and/or mathematical modelling were excluded from the search.

The search explored online citation indexing services such as Web of Science and Scopus and the data range was limited to 2006 to 2016, considering this era most effective for research in this field. The search criteria were "film formation" And "artificial joint," "synovial fluid" And "lubrication," and "synovial fluid" And "protein" And "chemistry."

2.2 | Study selection and data extraction

The selection of articles for the review was independently performed by two researchers. First, duplicate results coming from different keywords or different citation database searches were merged. In the next step, the title and abstract of the obtained citations were screened to exclude work with low relevance to the topic. In particular, exclusion criteria were chosen to exempt articles on dental and optical tribology, on film formation other than on joint replacement, and on mathematical modelling of joint replacement. In result, articles dealing with mechanical or biochemical properties of film formation within the synovial joint, in particular dealing with lubrication mechanism, protein concentration and adsorption, film composition, usage of spectroscopy in this field, or pH and buffer of protein films, were accepted as relevant for the review.

3 | RESULT

In the below flowchart, the journal selection process has been demonstrated, using inclusion and exclusion method. Initially, 1138 articles were found in online citation databases, 676 in Scopus, and 462 in Web of Science. Duplicate items were merged by using Endnote and, reviewing title and abstract, the article extraction continued via the inclusion and exclusion criteria. Finally, two more articles were added explicitly. In result, 14 articles were selected for review in this section (Tables 1 and 2).

4 | BIOCHEMICAL AND MECHANICAL PROPERTIES OF SF AND JOINT REPLACEMENTS

4.1 | Properties of SF

The SF constitutes a complex mixture of large and surface-active molecules, such as proteins, phospholipids, hyaluronic acid, cholesterol, and glycoproteins.[18,20] However, the proteome composition of healthy SF and cellular origins of its components are yet to be understood completely.[1]

The prominent functions of SF within the joint lies in its biological lubrication, but SF also acts as a biochemical pool for nutrients and regulatory cytokines outpour. Of course, the tribological performance of cartilage cannot be featured with a single mechanism. Rather, multiple functions of lubrication take place mutually. When lubrication is optimum, normal loads, shear stresses, and rates change are provided at articulating cartilage

TABLE 1 Inclusion and exclusion process of article selection for the systematic review [Colour table can be viewed at wileyonlinelibrary.com]
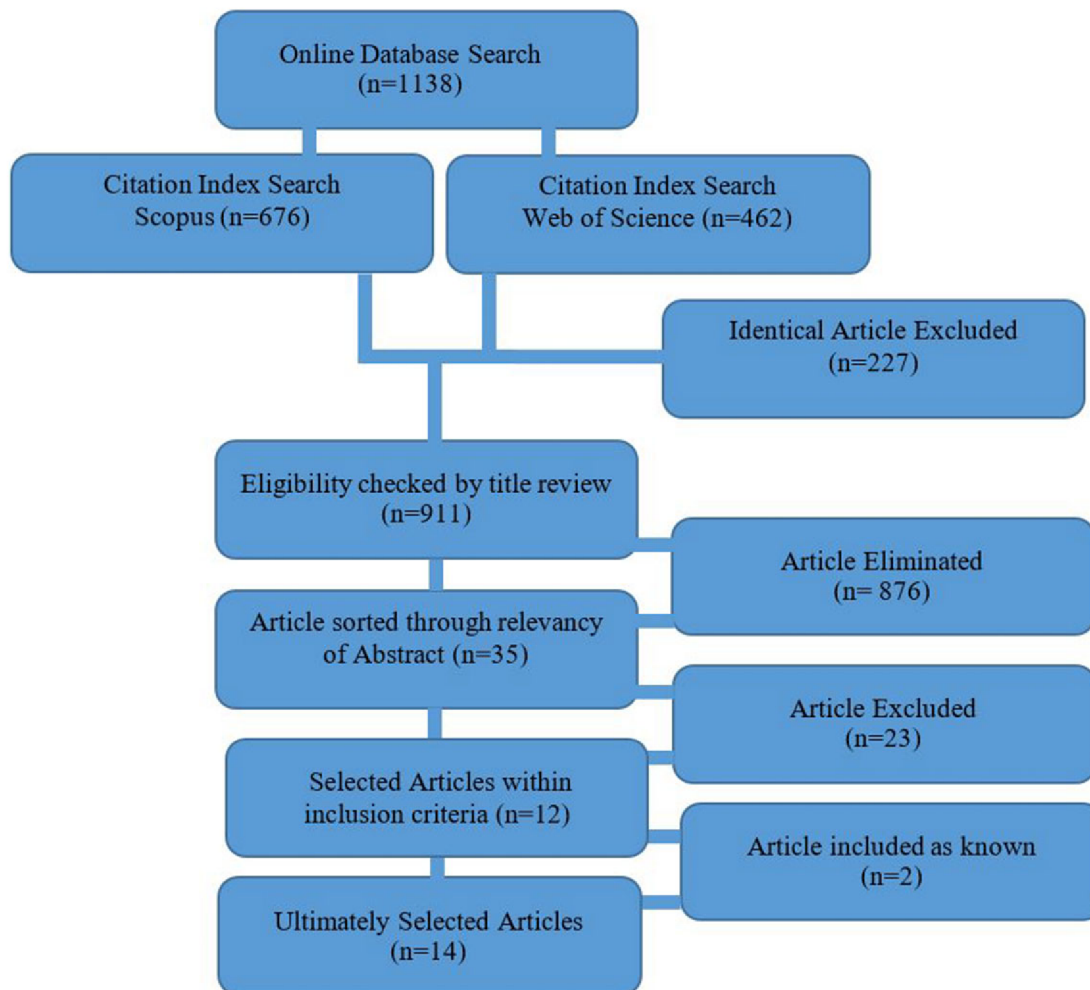
surfaces, yielding low-friction, and low-wear properties.[2] Erosion of articulating cartilage surfaces may occur due to arthritis if there is a lack of proper SF lubricating system or any disruption of chemical environment within synovial joint takes place. In damaged joint SF normal electrostatic interactions are not workable, probably due to chemical-change-induced secondary structure modification of the proteins.[12,21]

Within the synovial space, SF is accumulated and separated by the semipermeable synovial lining. The chemical regulation is assumed to be controlled by lubricant concentration, as secreted by chondrocytes and synoviocytes.[21] Therefore, SF also plays a transporting role of the boundary lubricant to its site of adsorption.[5]

At the beginning of bio-tribology research, Dowson et al[22] had provided the idea that the cartilage surfaces are prevented from contacting each other primarily because of the formation of trapped pools of lubricant.

Due to compression and concentration of the fluid between the cartilage surfaces, an acid-protein complex is formed as a protective gel. While proteoglycan 4, hyaluronic acid (HA), and surface active phospholipids (SAPL) contribute to the total arrangement of the system.[21] Walker et al[22] termed this combination of trapped pool and fluid concentration as "boosted lubrication." The proteins are produced from synovium, cartilage, ligament, and meniscus,[1] and their structural and functional properties are directly connected with the phospholipids.[11] On the other hand, HA contributes more as a potential boundary lubricant for cartilage and shows a small amount of lubrication activity.[2]

In a model described by Blewis et al,[21] SF is compared with an ultrafiltrate of plasma, which has the ability of filtration through the synovial membrane with chondrocytes in articular cartilage and synoviocytes in synovium secrete lubricants (Figure 1).

TABLE 2 Summary of the systematic review, with characteristics of the eligible studies

Characteristics of the Eligible Studies (Continued)				
Reference	Area of Research	Conditions of Analysis	Focused Parameters	Key Results
David Nečas et al[7]	The thickness of lubricant film for specific proteins on hip joint replacements and interfacial lubrication process.	Thin-film colorimetric interferometry and fluorescent microscopy in combination with the optical method were used to measure film thickness. Metal femoral head and glass disc were used in different conditions. Test lubricants were albumin and γ-globulin (2:1) with saline solution.	Kinematic conditions such as, under pure rolling, partial negative, and partial positive sliding on film formation and film thickness	γ-globulin forms a thin protein layer. Albumin absorbs onto that layer. In most cases, albumin contributes to increasing the total film thickness.
Adela Galandáková et al[4]	Differences of compositions and the constituents of synovial fluid extracted from respectively, patients of primary arthroplasties and revision arthroplasties and without joint replacement.	Synovial fluid collected from 152 patients was categorised into four different groups depending on their conditions of osteoarthritis and joint replacements. Kinsley method, quantitative colorimetric kit, enzyme-linked immunosorbent assay, and Vibro-viscometer SV-1A were used respectively to determine the concentration of proteins, phospholipid, hyaluronic acid, and viscosity of synovial fluids. For statistical analysis IBM SPSS Statistics 22 software was used.	Concentration of components, viscosity, and statistical analysis of constituents for diversified patient characteristics	Albumin and γ-globulin readily adsorbed on artificial materials, whereby have an influence on the frictional properties of the lubricating surface. The γ-globulin concentration found remarkably higher and concentration of phospholipid observed significantly lower with the revision of joint replacement patients and with patients without joint replacements. Hyaluronic acid and viscosity of different groups were observed unchanged.
Maria Parkes et al[13]	Film formation impact of the protein content of model synovial fluids under the static and rolling condition and correlation with changing properties.	Adsorption of bovine serum albumin (BSA) and bovine gamma globulin on silica and chromium surface was observed at pH 7.4 and 8.1. Quartz crystal microbalance and ball on the flat device were used for adsorption measurement in the static condition. Under the pure rolling condition, optical interferometry was used to observe the effect of protein content on lubricant film thickness on silica/CoCrMo interface.	Film thickness, pH, adsorption, under static and rolling conditions, and different composition of proteins	Protein layers are thicker under rolling than the statical condition. Film formation depends on protein content and the pH of the solution in both conditions. Bovine gamma globulin and mixed protein bounds more strongly than bovine serum albumin. Bovine gamma globulin forms much thicker deposited layers compare to BSA.

(Continues)

TABLE 2 (Continued)

Characteristics of the Eligible Studies (Continued)				
Reference	**Area of Research**	**Conditions of Analysis**	**Focused Parameters**	**Key Results**
Nakashima Kazuhiro et al[14]	Adsorption and frictional property of bovine serum albumin in the rubbing condition of ultra-high molecular weight polyethylene and CoCrMo alloy.	Reciprocating pin-on-disk tribometer with the electrochemical cell was used to measure the frictional property during friction. Open circuit potential condition technique was used to cover friction force and electric potential. But −0.2 applied potential condition also measured electric current and friction force.	Adsorption and desorption behaviour of the protein, frictional property, the coefficient of friction during rubbing condition, shear force, and protein concentration. The transition of potential, frictional force and normal loading force, current measurement was recorded.	BSA film is reconstructed during rubbing on CoCrMo alloy surface, under rubbing condition. The absorbed film formed become strong and stable and optimally adapted structure for shear force by receiving shear force.
Jong Bong Park et al[15]	Boundary lubrication ability of retrieved CoCrMo head within hyaluronic acid and phospholipid.	Atomic force microscopy technique was used, including a rectangular silicon cantilever integrated with sharp silicon tips. Hyaluronic acid and phospholipid of various concentrations were used with retrieved CoCrMo head.	Boundary lubrication, microscale frictional coefficients, and concentration	Retrieved CoCrMo heads. The microscale frictional response has the dependency on the concentration of HA and phospholipid. The optimal concentration that ranges to maximise frictional behaviour is similar to the concentration of HA and phospholipid of human synovial fluid.
Martin Vrbka et al[16]	Observation of film formation and measurement of film thickness of bovine serum through various test configurations.	Ball on disc and lens on disk configuration were used for metal and ceramic ball with silica and chromium layer on glass respectively, for bovine serum lubricant considering as a function of the artificial hip joint. Film thickness was measured by optical interferometry as a function of time.	Film thickness, hydrophilicity, hydrophobicity, surface geometry, concentration, wettability, conformity, kinematic condition, temperature, material, time, and hydrodynamic effect	Glass disc covered by a chromium layer showing hydrophobic behaviour formed a thicker lubricating film, on the other hand, silica layer in the same condition showed hydrophilic behaviour. Due to hydrodynamic effect, a thin film was formed on the silica layer. Wettability has no effect on protein film formation, while kinematic condition and conformity of contact surface has the fundamental effect. Due to protein aggregation film formed within ball on disc configuration. On the contrary ball on lens configuration, hydrodynamic effect leads to film formation.

(Continues)

TABLE 2 (Continued)

Characteristics of the Eligible Studies (Continued)

Reference	Area of Research	Conditions of Analysis	Focused Parameters	Key Results
Maria Parkes et al[17]	Buffer selection and pH impact on the protein adsorption kinetics and film formation respectively under static and rolling conditions.	BSA with respect to different buffer solutions was utilised to observe the adsorption properties by means of quartz crystal microbalance. Under static condition adsorption of proteins were investigated on silica coated quartz crystal. Under the rolling condition, the ball-on-flat device was used and film thickness or protein solution was measured by a thin film optical interferometry.	Solution buffer, pH, film thickness, viscoelasticity, adsorption, static, and rolling condition	The aspect of the buffer depends on pH within static condition. Both in static and rolling conditions pH has an impact on film formation. At lower pH, protein adsorption observer initially rigid and relaxed, with time rate increased. At pH 7.4 or lower, thicker protein film formed in rolling condition. The film found nonuniform and irregular deposition of protein. At higher pH initially, viscoelasticity is higher, also uniform and a consistent film formed at static condition.
Jemma G Kerns et al[10]	The molecular structural change occurrence, in the subchondral bone matrix, due to osteoarthritis.	By using Raman spectroscopic technique, differences of molecular structures between tibial plateaus of respectively healthy joints and joints with total replacements due to osteoarthritis were compared. Also, comparison of medial and adjacent compartments of subchondral bones was observed as different load bearing sites.	Molecular structure and load baring	Medial and lateral for both bone matrix significant chemical structural changes appear due to osteoarthritis. Whereas spectral differences were not found between the medial and lateral compartment of the subchondral bone matrix.
Zhang Z et al[3]	Interfacial rheology and bulk rheology of model synovial fluid effect by the proteins and hyaluronic acid for respectively various shear rates, strains and frequencies.	A model synovial fluid was utilised for the experiment that contained hyaluronic acid, BSA, and γ-globulin within pH 7.4. A double wall ring geometry and AR-G2 stress controlled TA instruments rheometer were used to measure interfacial rheology and bulk rheology respectively.	Interfacial rheology, bulk rheology, pH of the solution, oscillation shear rate, strain, and frequency	In the steady and oscillatory condition of the model synovial fluid composed of hyaluronic acid, BSA and γ-globulin interfacial rheology occur due to protein adsorption at the interface are rejected. On the contrary, bulk rheology is controlled wholly by the hyaluronic acid of model synovial fluid in the difference of shear rate, strains and frequencies.

(Continues)

TABLE 2 (Continued)

Characteristics of the Eligible Studies (Continued)				
Reference	**Area of Research**	**Conditions of Analysis**	**Focused Parameters**	**Key Results**
Duong Cong Truyen et al[8]	The concentration levels of BSA and γ-globulin influence on the lubricating ability of CoCrMo hip prostheses.	Sections of the retrieved CoCrMo femoral head from revision surgery were lubricated with several concentrations of BSA and γ-globulin. Atomic force microscopy was used to measure applied normal force and surface roughness. Friction coefficients were calculated afterward.	Frictional coefficients, the concentration of lubricant, boundary lubrication, applied normal force, and surface roughness	A maximum level of BSA and optimal concentration of γ-globulin leads to effective boundary lubrication. Thus, the concentration of BSA and also γ-globulin control the friction of CoCrMo head.
Fan Jingyun et al[18]	Film thickness and wear measurements for various model synovial fluids solutions of different pH.	Thin-film optical interferometric test device was used to analyse film thickness and wear tests. The experiment conducted within glass disc and CoCrMo surface for a range of model synovial fluids of the variety of pH.	Film thickness, pH, and wear measurement	Film formation signifies two distinct mechanisms: the boundary lubrication mechanism and high viscosity gel mechanism. Wear mechanism is designated through the tribocorrosion process, with higher pH, wear increases. The chemistry within synovial fluid has a significant effect on wear and failure of joint replacements.
George W Greene et al[2]	Frictional experiment on porcine cartilage and enzymatic digestion of hyaluronic acid to disclose the lubrication mechanism.	The effect of enzymatic digestion of hyaluronic acid with hyaluronidase was investigated. Using surface force apparatus SFA 2000 equipped with friction device attachment normal and frictional force was measured under various loading conditions.	Friction, wear, lubrication, pressure, time duration, shearing force, and concentration	Hyaluronic acid and glycoprotein lubricin complex as HA-LUB, trapped at the interface to form a cross-linked network, which plays a role of boundary lubricant and prevent wear mechanism.
Karen A Esmonde-White et al[12]	Investigation of differences between biochemical compositions of healthy joint synovial fluids and synovial fluids of osteoarthritis patients.	Drop deposition/Raman spectroscopy protocol was utilised as an evaluation tool to distinguish between osteoarthritis patients' synovial fluid and healthy joint synovial fluid. The light microscope was used for coarse separation from the dried drop. From knee joint x-rays Kellgren/Lawrence (K/L) scores were used, for grouping individual patients.	Chemical structural analysis, K/L score, and microscopic image	Drop deposition/Raman spectroscopy method can be used as an appropriate detector of synovial fluids of osteoarthritis patients, namely the Raman band describes protein secondary structure. Raman data clarified that disorder within normal electrostatic interactions of synovial fluid occurs due to osteoarthritis.

TABLE 2 (Continued)

	Characteristics of the Eligible Studies (Continued)			
Reference	Area of Research	Conditions of Analysis	Focused Parameters	Key Results
Tannin A Schmidt et al[19]	The contribution of boundary lubrication of various constituents of synovial fluids separately and also collectively.	ELF 3200 (Bose EnduraTEC, Minnetonka, MN) equipment set up was used for the performance of cartilage boundary lubrication tests with fresh bovine osteochondral samples. Effect of graded dilutions was determined by the test lubricants prepared in PBS and different percentage of SF.	Boundary lubrication, frictional coefficients (static and kinetic), and concentration.	Both at physiologic and pathophysiologic concentrations, constituents of SF contribute to the boundary lubrication of the apposing articular cartilage surface. The contribution found individually and also in combination with the constituents of SF.

4.2 | Biochemical composition of SF

The principal element of SF is phospholipids, amounting to about 61% in the normal joint constitution. Being the main phospholipid component, phosphatidylcholine is extremely surface-active due to large saturation of joint phospholipids. Another element abundant in SF is the SAPL. These small molecules function as binders of amino acid groups.[5]

Albumin, the most abundant protein of SF, shows affinity to hydrophobic surfaces such as OH-terminated surfaces. Adherence of albumin to artificial surfaces may thus be regulated by altering the pH value. Therefore, for lubrication of articular surfaces and interaction with other components, albumin plays an important role. On the other hand, globulin activity is more focused on boundary lubrication. At low speeds, globulin plays the role of pH-independent boundary lubricant. When speed is higher, boundary lubrication by globulin depends on pH, which in turn helps in producing hydrodynamic or mixed lubrication.[23]

Being another essential element of SF, HA produces a cross-linked network by complexing with the glycoprotein lubricin, whose solutions are slippery to the touch. This network provides wear prevention mechanism of joints and is also (chemically) responsible for boundary lubrication.[2,5] Lubricin is formed by a long, heavily glycosylated, mucinous domain, separating two somatomedin domains at the N-terminus and a haemopexin region at the C-terminus. The total amount of lubricin in SF is small but assists in a substantial amount in the boundary lubrication as well as lubrication properties, transporting, anchoring of phospholipids to the cartilage surface, and the friction coefficient of the different area of articular cartilage. In addition, lubricin contributes essentially to chondroprotective properties of articular cartilage; by interaction with HA via dissipation of shear-induced energy, this activity is further increased. Thus, effective biolubrication is provided by lubricin in the presence of other major components in SF.[5,23]

In result, the chemical behaviour, friction, and wear properties of the joints are controlled by prime constituents of human SF, which are proteins such as serum albumin and γ-globulin, phospholipids, and HA.[4,15]

4.3 | Synovial liquid content correlated to joint replacement

The levels of different components within SF may differ with the person and age, and they also depend on the

FIGURE 1 (A) Synovial joints composed of cartilage, synovium, and synovial fluid; (B) communicating compartments are present in synovial fluid, while lubricant secretion is regulated by chemical and mechanical factors.[21] Reprinted from Journal: European Cells and Materials, Vol. 13; Authors: Blewis ME, GE Nugent-Derfus, TA Schmidt, BL Schumacher and RL Sah; Title of article: A model of synovial fluid lubricant composition in normal and injured joints, Page: 26–38, Copyright (2007), reproduced with kind permission from eCM journal (www.ecmjournal.org) [Colour figure can be viewed at wileyonlinelibrary.com]
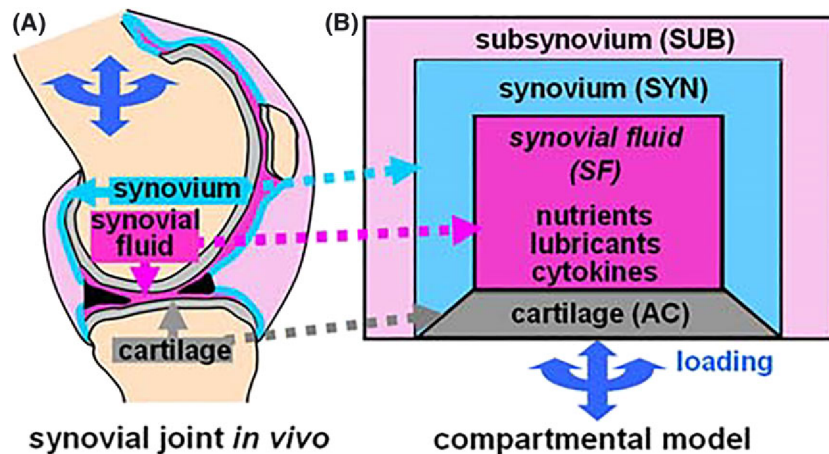
presence of disease. The total volume of SF, protein concentration, pH value, viscosity, and other properties are known to vary between healthy persons and patients with OA at different stages.[4,23] The concentration of proteins and other components differs for diseased and periprosthetic SF, and the condition includes decreased effective viscosity, increased protein content, and increased pH.[4,18,20]

In case of inflammation, stimulation of tissue protective and regenerative mechanisms takes place to prevent collateral damage to periprosthetic tissues. The tissue architecture is balanced by various hormones such as cytokines, chemokines, and specific cell populations, including macrophages, dendritic, and stem cells to minimise inflammation. As a result of the failure of local tissue homeostatic mechanism, periprosthetic osteolysis may arise.[24]

The bulk properties of the SF may control the film lubrication as proposed by Mazzuccoa et al[6] some connections between the composition of the joint fluid and the tribology of joint replacement prostheses in vivo. Determination of protein, phospholipid, and hyaluronic acid contents of joint fluid samples obtained from patients undergoing total knee arthroplasty and revision total knee arthroplasty reveals that despite normal total protein content, the individual protein concentrations deflect in the diseased joints from that in healthy joints. To the implant wear and failure of joint replacement, patient SF chemistry plays an important role.[18]

From the experiment of Galandáková et al,[4] four types of sample were collected as below:

Group I. Patient with aseptic loosening of total joint replacement

Group II. Patient with total joint replacement but without any sign of aseptic loosening

Group III. Patient without total joint replacement and the end stage of OA

Group IV. Healthy SF

In the experiment, γ-globulin concentration was found significantly higher in patients with the revision of total joint replacement compared with patients without total joint replacement. On the other hand, the concentration of phospholipid was found to be significantly lower: on average 0.312 mg/mL for healthy SF and 0.154 mg/mL in the patient with aseptic loosening of total joint replacement. No significant difference was found among the groups in HA concentration and viscosity.

The average concentrations of different components of the joint fluid in the four distinct groups are summarised in Figure 2.

Galandáková et al[4] concluded that lubricant film is predominantly formed because of bovine serum proteins. Duong et al[8] stated that the concentration of BSA and γ-globulin regulates the frictional behaviour of the CoCr femoral head.

The protein concentration dependent lubrication system could be the result of the difference in the adsorption strength of BSA and γ-globulin. The α-helix structure of albumin causes low adsorption strength of this protein and the bearing surface, while the β-sheet structure of γ-globulin rather plays a role in its strong adsorption on the rubbing surfaces[8] (and the references cited therein[8]), which leads to the formation of large cohesive and/or adhesive forces on the bearing surface within a mixed or boundary lubrication regime. At high concentrations, BSA seems to act as an effective boundary lubricant, but in the physiological concentration range of the human
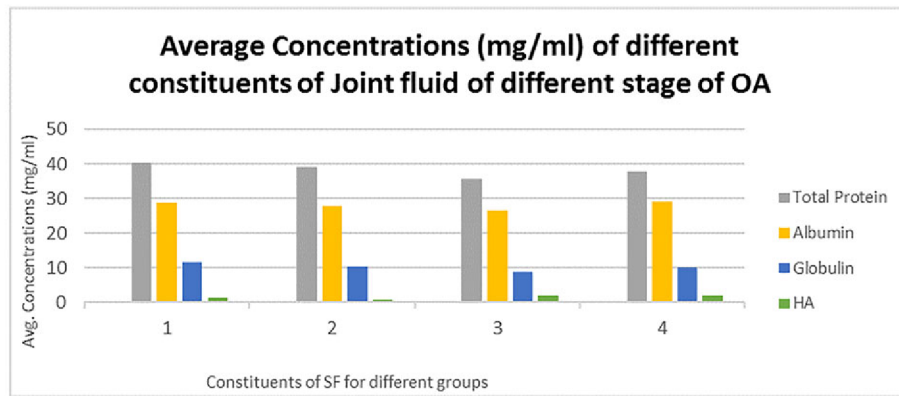
FIGURE 2 The average concentrations of the constituents of the joint fluid from the different stages of osteoarthritis. Average total concentration of protein found 40.3–35.5 mg/mL, average concentration of albumin 29.1–26.7 mg/mL, average concentration of globulin 11.5–8.7 mg/mL, and HA 0.8–2.0 mg/mL for different groups of patients as described above[4] [Colour figure can be viewed at wileyonlinelibrary.com]

SF, the lubricating ability of γ-globulin for boundary lubrication is most effective.[8]

4.4 | SF lubricant film formation on artificial joint replacement

The SAPL provides a thin hydrophobic outermost lining to the normal articular surface. Through SAPL, the boundary lubricant reduces friction to significantly lower levels.[5]

Optimal concentrations of HA and phospholipids, such as dipalmitoylphosphatidylcholine, for effective lubrication are equivalent to those observed in normal human SF. These concentrations regulate the microscale frictional response of the retrieved CoCr femoral head.[15] In case of arthritis, injury, and artificial joint failure, the friction between the articulating surfaces is enhanced through concomitant erosion of the load-bearing elements.[21,25] On the other hand, Parkes et al[17] stated that under static conditions, the lubrication properties of proteins are only partially governed by their adsorption properties.

The corrosion-enhanced wear occurs mainly due to the presence of the proteins. More precisely,[26,27] the presence of the proteins increases wear component; probably, adsorption of proteins in the particle entrainment also enhance the rolling efficiency of the abrasives. The CoCrMo implanted into the human body (pH 7.4) within a tribological contact of a knee or a hip is known to be susceptible to corrosion. In particular, Co^{2+} and Cr^{2+} ions in acidic conditions and CoO and CrO species at neutral pH are produced as a result of initial corrosion of CoCrMo alloy. Actually, the wear-corrosion behaviour of the cast CoCrMo alloy can be deflected noticeably with a minor alteration in test solution chemistry[26,27] (Figure 3).

4.5 | pH dependency of protein film formation

Parkes et al stated[13,17] that film formation within protein solutions is dependent on both the protein content and pH of the solution. When the film thickness during and after rolling tests was compared, it shows that the deposited films formed by bovine γ-globulin (BGG) and mixed proteins were quite strongly bound. The BSA films were, however, only weakly bound. Comparing BSA and BGG deposited layers, the BGG films were much thicker. In the case of mixed proteins, the ability of BGG to form thick layers was decreased. Therefore, the interaction between the proteins influences the process of film formation.[13]

At physiological pH, the films are formed by large irregular deposits in solutions. However, both the protein adsorption kinetics and the formation of tribofilms are influenced by the solution pH, whether statically or under the rolling conditions. At the lower pH, the adsorbed protein layers are initially rigid and relaxed over time to form viscoelastic layers, while the rate of adsorption also increases with time. At higher pH, even the initially adsorbed films are found to be substantial viscoelastic.[17] However, for the solutions tested in different buffer chemistry, no significant changes to protein adsorption were observed. In particular, for all buffer chemistry, the rate of protein adsorption and the viscoelastic properties of the adsorbed layer are similar. In buffers with pH 7.4 or lower, thicker protein films were formed in a rolling contact than under static conditions.[17]

Fan et al[18] examined an inlet reservoir of viscous material produced from high concentration protein fluids and stated that film formation mechanisms can happen in two distinct ways: boundary and "gel" hydrodynamic deposition. According to the boundary lubrication
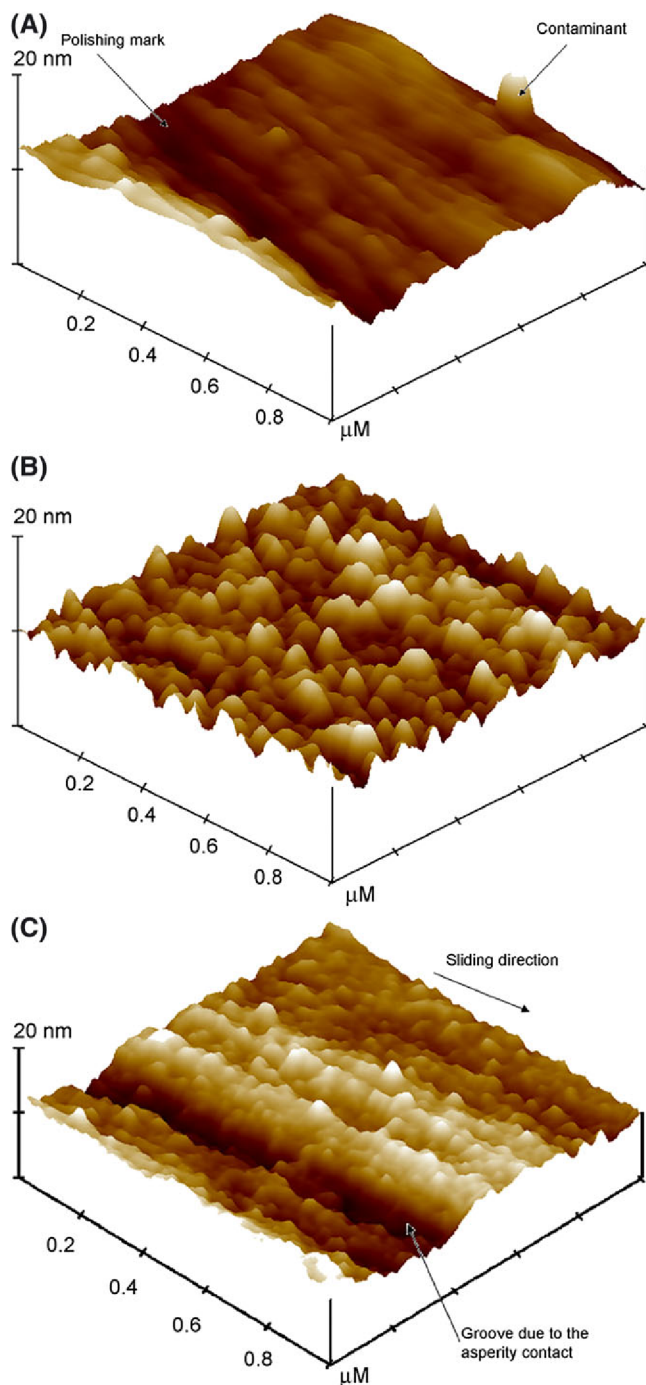
FIGURE 3 Atomic force microscopy study of the CoCrMo surface (A) as polished, (B) after immersion in 25% BS for 30 min at 37°C, and (C) after Sc test in 25% BS at 37°C.[26] Reprinted from Journal: Tribology International, Vol. 42(1); Authors: Sun D., J.A. Wharton, R.J.K. Wood, L. Ma & W.M. Rainforth; Title of article: Microabrasion–corrosion of cast CoCrMo alloy in simulated body fluids, Page: 99–110, Copyright (2009), with permission from Elsevier [Colour figure can be viewed at wileyonlinelibrary.com]

mechanism, the proteins adsorb at the CrCoMo surface to form thin, discontinuously deposited films. These films appear to survive rubbing. On the other hand, fluids with high-concentration protein form an inlet reservoir of viscous material that is entrained into the contact forming a separating film of agglomerated proteins on implant surfaces. In the fluid environment, these deposits act as viscous and possible to easily removed by surface scratches. Once removed from the fluid, they dry to form highly adherent, solid films.

Wear mechanisms occur through tribocorrosion processes, and with increasing pH, the wear of CoCrMo increases as well.

The wear scar width pH 7.4 < pH 8.5, pH 7.4 < pH 8.0, and BCS25 < pH 8.5.

Toshio et al[20] stated that variation of protein content may affect the pH and viscosity dependency. At low speed, the presence of albumin, the lubricant promotes pH dependence and viscosity independence of the tribological properties. On the other hand, globulin promotes pH and viscosity independence at low speed and promotes pH and viscosity dependence at high speed in the lubrication of ultrahigh molecular weight polyethylene against stainless steel (SUS). Therefore, the effect of constituents and pH variation in the periprosthetic fluid can lead to different lubrication results.

4.6 | Composition of formed protein films

From the above discussion, it is clear that the film formation on the joint replacement depends on pH, concentration, and viscosity of the solution, but the chemical composition of the formed film remains yet unknown.

The noticeable influence of the electrolyte composition on the passivation behaviour of Co-based alloys has been observed several times. The adsorbed organic species of the SF are assumed attached to this passivation film, altering their surface reactions. In result, adsorption of proteins disrupts the biocompatibility of the metallic materials used and accelerated metal dissolution may occur. At the same time, a protein (or amino acid) biofilm on the surface behaves as a lubricant film reducing friction and thus leads to reduced mass lost.[28,29] The chemical composition of the biofilm is yet to be clarified.

Milošev and Strehblow[30] used electrochemical oxidation to observe the composition, thickness, and structure of the oxide layer formed on the CoCrMo alloy in simulated physiological solution at various passivation potentials. Remarkable changes were found in the oxide layer found depending on the applied passivation potential. Presumably, the structure of the SF film could be analysed in a similar way (Figure 4).

Fan et al examined an inlet reservoir of viscous material produced from high concentration protein fluids. It is stated that an organic deposit forms on the surface,
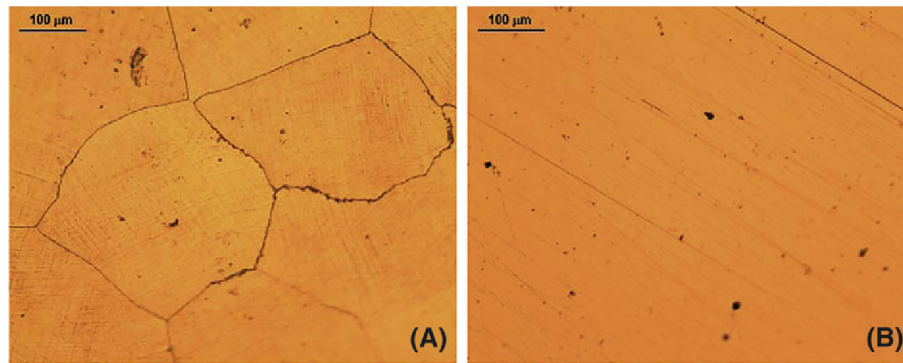
FIGURE 4 Optical images of the CoCrMo alloy microstructure: (A) grain boundaries and (B) carbide content.[28] Reprinted from Journal: Electrochimica Acta, Vol. 55(28); Authors: Valero Vidal C. & A. Igual Muñoz; Title of article: Study of the adsorption process of bovine serum albumin on passivated surfaces of CoCrMo biomedical alloy, Page: 8445–8452, Copyright (2010), with permission from Elsevier [Colour figure can be viewed at wileyonlinelibrary.com]

yielding from agglomerated proteins. The organic deposit remains viscous in a fluid environment, and it is possible to abolish this layer by surface scratches. After drying, a highly adherent solid film is formed.[18]

Nečas et al[7,31] used a model fluid to study the impact of protein content on the lubrication of joint replacements. For lubricant with albumin and γ-globulin content in concentrations 2:1, the film thickness increased with increased sliding speed. The effect was attributed mainly due to the presence of γ-globulin, although the film formation was very complex and both time and distance dependent. The film developed gradually under purely rolling conditions, and there was no substantial scatter formation. Under partial negative sliding, where the ball was faster than the disc, the film was generally very thin. Under positive sliding, the most scattered results were obtained when the disc was faster than the ball. Increase in mean speed usually resulted in an increase of the film thickness, although under positive sliding the effect of speed was opposite. Namely, for the speed of 5.7 mm/s, the film thickness was more than 120 nm, while for higher speeds, it was only around 40 nm. The thickness of the lubricating film can be assumed to scale specifically with the deposited amount of albumin. Presumably, a thin layer of γ-globulin is adsorbed primarily on to rubbing surfaces, enabling subsequent adsorption of albumin to create a layer structure.[7] Thus, this model fluid can be used for chemical composition analysis.

Parkes et al[13] also stated that under the rolling condition, protein layers are much thicker compared with statically adsorbed layers. From the study of Fan et al,[18] it was also found that much thicker films were formed in case of γ-globulin occurrence, although by monolayer or multilayer adsorbed protein forms a thin residual film. Hence, if the chemistry of γ-globulin film formation is analysed separately, most likely, it can provide an interesting result.

Nakashima et al[14] studied the adsorption of BSA through measurement of friction force and electric potential under open circuit potential condition in the rubbing combination of ultrahigh molecular weight polyethylene and CoCrMo alloy. The results show the onset of BSA desorption at first rubbing with the gradual decline of desorption. During rubbing, BSA film on the metal surface is reconstructed and observed stable with the structure optimally adapted with respect to the shear force.

Vrbka et al[32] used the pendulum simulator in combination with optical measurement of film thickness, which seems to imitate the lubrication processes within artificial hip joints. They show the model able to consider different loading and kinematic conditions, the influence of geometry, clearance, and material combination of contact pairs.

Despite all efforts, the role of proteins in the electrochemical behaviour of bio-metallic surfaces is yet to be comprehended.[28] Addressing this unknown area of biofilm chemistry simultaneously with consideration of mechanical properties could, hence, bring a significant advance in this research field.

5 | DISCUSSION

The principal causes of OA are assumed to be classified into two main classes. The first one is the mechanical loading change, which leads to the total joint replacement of patients due to the stiffer structure. The other one could be articulated as a change of chemical composition of the bone matrix and the SF. Most likely, the secondary structures of SF proteins and tropocollagen are affected in OA.[4,10,12] Most of the studies found are concerned with adsorption and desorption of proteins in different kinematic conditions and film thickness in different pH, buffer, and concentration of proteins.[7,13,14,16-19] Frictional

coefficients, frictional force, shear force, wear measurement, boundary lubrication, surface geometry, rheology of various constituents are also considered in connection with proteins and other SF components to explore the knowledge in this area.[2,3,8,14,15,19,23] To take into account the mechanical and chemical environment of human synovial joint, the viscosity of various modal fluids and wettability of various surface materials were also considered[4,15-17,23] with respect to their duration in time and under varying temperature and pressure.[2,16]

Esmonde-White et al[12] considered the change of chemical structure in SF under OA and total joint replacements and concluded that differences occurred in diseased SF compared with healthy SF. In addition, Kerns et al[10] confirmed that the subchondral bone matrix also altered its chemical structure due to OA. Both above observations of chemical structural changes were investigated by means of Raman spectroscopy. Nevertheless, the structural changes of individual protein components must be addressed to understand these chemical changes thoroughly. The sought for information on protein film chemical composition should be revealed through simultaneous consideration of mechanical properties and control of temperature, pressure, and frictional force.

The optical method of Raman spectroscopy provides information relying on the change of bond polarisability of a molecule through inelastic probing of its vibrations. Although the cross section of Raman scattering is low, it is extremely sensitive to intramolecular conditions. In addition, although water is always present as one of the elements of the biological materials, it does not affect the Raman spectroscopic fingerprint of biomolecules too much.[11]

Within the Raman spectrum, there are several qualitative and quantitative indicators of a peptide conformation. In particular, the hydrogen bond stabilised secondary structural motifs of peptides such as α-helix or β-sheet structures have well-defined imprints on the Raman spectrum. As an example, the position of Amide I band (describing the C=O stretching, contributions from C—N stretching, and N—H deformation) for the α-helical peptide is 1645 to 1660 cm^{-1}, while for β-sheet peptide, the band is located at 1665 to 1680 cm^{-1}. In addition, Amide III band (describing the vibrational coupling between adjacent C—H and N—H deformation) is observed at 1265 to 1300 cm^{-1} for α-helix, while β-sheet structure shifts the band to 1230 to 1240 cm^{-1}. Therefore, the changes of a peptide conformation, that through
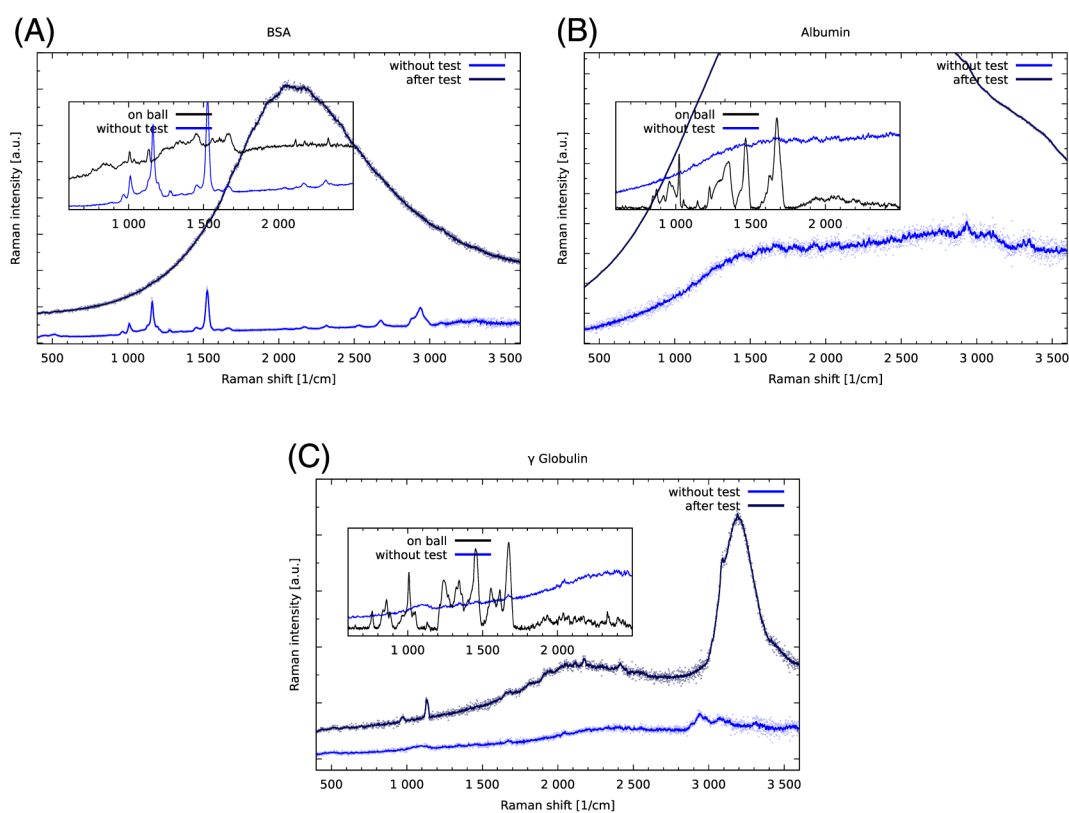

FIGURE 5 Raman fingerprint spectra of solutions without tribological test and after tribological experiment together with Raman spectra of the film formed on CoCrMo ball with lubricants (A) BSA, (B) albumin, and (C) γ-globulin [Colour figure can be viewed at wileyonlinelibrary.com]

chemical reactions or denaturation can even be the reason of loss of biological activity of proteins,[33] are easily monitored using Raman spectroscopy.

Indeed, Raman spectroscopy was successfully used in the study of Depciucha et al[11] to evaluate the balance between phospholipids and proteins in blood serum with the conclusion that the method provides quick measurement results for analysis of biological material.

Using Renishaw inVia Raman spectrometer, the below spectra have been obtained for solutions of γ-globulin, albumin, and BSA before and after the tribological experiment. In addition, optical images of the film formed on CoCrMo metal ball were taken. The tribological experiment was conducted within pendulum hip simulator with the ball on the disc configuration by metal prosthesis head of CoCrMo ball (28 mm) ISO 5832-12.[16,31,34]

The first experiment was conducted with 25% BSA as the lubricant. Then 28 mg/mL of albumin solution and 11 mg/mL of γ-globulin were respectively prepared as the lubricant with phosphate buffer solution and the experiments continued.

In the above Raman spectra, the buffer correction was applied (Figure 5). The spectra found on the metal ball for all lubricants were quite different from the spectra of without-test liquid of the same protein. The reason for the difference could be due to the crystalline form of the protein on the metal ball (see Figure 6). There could also be a chemisorbed transition state within protein lubricants and metal surfaces. The after-experiment protein solution spectra for BSA and albumin have similarities but did not show appropriate spectra, although after-test γ-globulin shows well-defined peaks. Most probably the β-sheet structure of γ-globulin is affected by chemical reactions. The α-helical structure of BSA and albumin become distorted. The result of the tribological effect of joint replacement can be more evident if we can use mixtures of different proteins for the experiment.

To study the protein changes in more detail, one of plasmonic-enhanced Raman modalities could be used.
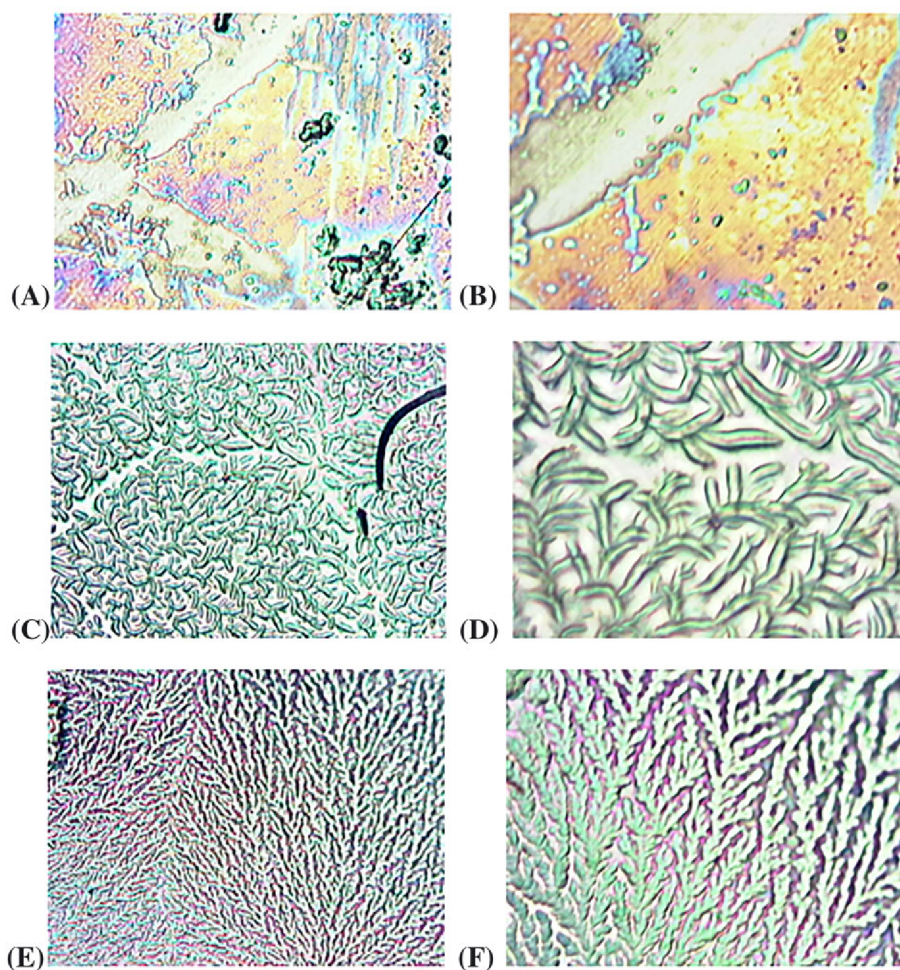

FIGURE 6 Film formation viewed with Raman microscope on the ball by respectively (A) BSA and (B) BSA enlarged view, (C) albumin and (D) albumin enlarged view, and (E) γ-globulin and (F) γ-globulin enlarged view. The horizontal size of panels are 180 μm (a, c, and e) and 70 μm (b, d, and f) [Colour figure can be viewed at wileyonlinelibrary.com]

In particular, surface-enhanced Raman scattering (SERS)–based biosensors are developing rapidly for the applications of chemical analysis, nanostructure characterisation, and for biomedical sectors.[35] Making use of high increase of Raman signal after protein binding to the metallic nanoparticle(s), SERS is a very effective technique.[35-37] In another SERS study of protein-nanoparticle interaction, bio-conjugated silver nanoparticles were used by Reymond-Laruinaz et al.[38] In summary, SERS has been recognised as a very successful operative analytical tool due to its high sensitivity, high selectivity, and fluorescence-quenching properties.[35,38]

The formed film structures on CoCrMo ball surface for BSA, albumin, and γ-globulin were observed during the Raman experiment in order to investigate the biochemical influence of protein lubricant on the metal surface.

The different structures of the formed film produced by different proteins are clearly visible from Figure 6. These observations could also play an important role in the biochemical explanation of adsorption, which takes place on the metal surface by protein molecules during film formation.

From the above discussion, it could be assumed that the CoCr femoral head could act as a heterogeneous or contact catalyst by forming synovial protein films as chemisorbed transition state and changing the secondary structural composition of protein molecules within artificial joint replacement. That is, the activation barriers might be reduced by the process of heterogeneous catalysis.[39-42]

6 | CONCLUSIONS

From the systematic review of last 10 years (2006–2016) contribution, it has been observed that research on protein film formation of SF beneath the artificial joint is mostly concentrated on mechanical properties such as kinematic conditions, film thickness, frictional coefficients, frictional force, shear force, wear, boundary lubrication, surface geometry, rheology, and wettability of different modal fluids and different surface materials. The influences of some physical chemistry parameters like pH, buffer, viscosity, and concentration of proteins, temperature, pressure, and time dependence were also investigated. However, analysis of chemical changes induced within artificial joint and chemical composition of the formed films is yet to be revealed.

- Therefore, to describe the condition of joint replacement and to increase the longevity of the replaced area, the chemical changes taking place in the proteins of SF need to be observed to explain the

biochemical behaviour of the materials using in joint replacement.
- Raman spectroscopy is a good technique to understand clearly the changes of the chemical structure, as the vibrational fingerprint of each compound reveals the specific chemical structure of the compound within the formed film in the Raman spectrum.
- The Raman spectroscopic differences obtained for each of the protein lubricants before use and after experiment within the simulator of the ball on disc set up can explain the chemical reactions that are occurring within artificial joint replacement.
- Also, by observing the Raman spectra of lubricant film formed on the ball, one can address the chemical structural changes that are taking place due to bond breaking or formation within the proteins of SF.
- There could also be a possibility of heterogeneous catalysis process occurring among proteins within joint replacement in case of using CoCrMo alloy as a metal prosthesis.
- Furthermore, using mixtures of different synovial proteins in appropriate ratios as lubricants may show significant spectroscopic differences, and thus, it would be possible to understand the lubrication chemistry and mechanism of synovial liquid proteins within artificial prosthesis more explicitly.

ORCID

Risha Rufaqua https://orcid.org/0000-0002-2261-966X

REFERENCES

1. Bennike T, Ayturk U, Haslauer CM, et al. A normative study of the synovial fluid proteome from healthy porcine knee joints. *J Proteome Res*. 2014;13(10):4377-4387. https://doi.org/10.1021/pr500587x
2. Greene GW, Banquy X, Lee DW, Lowrey DD, Yu J, Israelachvili JN. Adaptive mechanically controlled lubrication mechanism found in articular joints. *Proc Natl Acad Sci*. 2011;108(13):5255-5259. https://doi.org/10.1073/pnas.1101002108
3. Zhang Z, Barman S, Christopher GF. The role of protein content on the steady and oscillatory shear rheology of model synovial fluids. *Soft Matter*. 2014;10(32):5965-5973. https://doi.org/10.1039/C4SM00716F

4. Galandáková A, Ulrichová J, Langová K, et al. Characteristics of synovial fluid required for optimization of lubrication fluid for biotribological experiments. *J Biomed Mater Res B Appl Biomater.* 2017;105(6):1422-1431. https://doi.org/10.1002/jbm.b.33663

5. Hills BA, Crawford RW. Normal and prosthetic synovial joints are lubricated by surface-active phospholipid. *J Arthroplasty.* 2003;18(4):499-505. https://doi.org/10.1016/S0883-5403(03)00072-X

6. Mazzucco D, Scott R, Spector M. Composition of joint fluid in patients undergoing total knee replacement and revision arthroplasty: correlation with flow properties. *Biomaterials.* 2004;25(18):4433-4445. https://doi.org/10.1016/j.biomaterials.2003.11.023

7. Nečas D, Vrbka M, Urban F, Křupka I, Hartl M. The effect of lubricant constituents on lubrication mechanisms in hip joint replacements. *J Mech Behav Biomed Mater.* 2016;55:295-307. https://doi.org/10.1016/j.jmbbm.2015.11.006

8. Duong CT, Lee JH, Cho Y, et al. Effect of protein concentrations of bovine serum albumin and γ-globulin on the frictional response of a cobalt-chromium femoral head. *J Mater Sci Mater Med.* 2012;23(5):1323-1330. https://doi.org/10.1007/s10856-012-4603-9

9. Cawley J, Metcalf JEP, Jones AH, Band TJ, Skupien DS. A tribological study of cobalt chromium molybdenum alloys used in metal-on-metal resurfacing hip arthroplasty. *Wear.* 2003;255(7-12):999-1006. https://doi.org/10.1016/S0043-1648(03)00046-2

10. Kerns JG, Gikas PD, Buckley K, et al. Evidence from raman spectroscopy of a putative link between inherent bone matrix chemistry and degenerative joint disease. *Arthritis Rheum.* 2014;66(5):1237-1246. https://doi.org/10.1002/art.38360

11. Depciuch J, Sowa-Kućma M, Nowak G, et al. Phospholipid-protein balance in affective disorders: analysis of human blood serum using Raman and FTIR spectroscopy. A pilot study. *J Pharm Biomed Anal.* 2016;131:287-296. https://doi.org/10.1016/j.jpba.2016.08.037

12. Esmonde-White KA, Mandair GS, Raaii F, et al. Raman spectroscopy of synovial fluid as a tool for diagnosing osteoarthritis. *J Biomed Opt.* 2009;14(3):034013. https://doi.org/10.1117/1.3130338

13. Parkes M, Myant C, Cann PM, Wong JSS. Synovial fluid lubrication: the effect of protein interactions on adsorbed and lubricating films. *Biotribology.* 2015;1–2:51-60. https://doi.org/10.1016/j.biotri.2015.05.001

14. Kazuhiro N, Sawae Y, Murakami T, Mischler S. Behavior of adsorbed albumin film on CoCrMo alloy under in-situ observation. *Tribology Online.* 2015;10(2):183-189. https://doi.org/10.2474/trol.10.183

15. Park JB, Duong CT, Chang HG, et al. Role of hyaluronic acid and phospholipid in the lubrication of a cobalt–chromium head for total hip arthroplasty. *Biointerphases.* 2014;9(3):031007. https://doi.org/10.1116/1.4886255

16. Vrbka M, Křupka I, Hartl M, Návrat T, Gallo J, Galandáková A. In situ measurements of thin films in bovine serum lubricated contacts using optical interferometry. *Proc. Inst. Mech. Eng. H J. Eng. Med.* 2014;228(2):149-158. https://doi.org/10.1177/0954411913517498

17. Parkes M, Myant C, Cann PM, Wong JSS. The effect of buffer solution choice on protein adsorption and lubrication. *Tribol. Int.* 2014;72:108-117. https://doi.org/10.1016/j.triboint.2013.12.005

18. Fan J, Myant C, Richard Underwood R, Cann P. Synovial fluid lubrication of artificial joints: protein film formation and composition. *Faraday Discuss.* 2012;156:69-85. https://doi.org/10.1039/C2FD00129B

19. Schmidt TA, Gastelum NS, Nguyen QT, Schumacher BL, Sah RL. Boundary lubrication of articular cartilage: role of synovial fluid constituents. *Arthritis Rheumatol.* 2007;56(3):882-891. https://doi.org/10.1002/art.22446

20. Kitano T, Ateshian GA, Mow VC, Kadoya Y, Yamano Y. Constituents and pH changes in protein rich hyaluronan solution affect the biotribological properties of artificial articular joints. *J Biomech.* 2001;34(8):1031-1037. https://doi.org/10.1016/S0021-9290(01)00058-6

21. Blewis ME, Nugent-Derfus GE, Schmidt TA, Schumacher BL, Sah RL. A model of synovial fluid lubricant composition in normal and injured joints. *Eur. Cell. Mater.* 2007;13:26-38. https://doi.org/10.22203/eCM.v013a03

22. Walker PS, Sikorski J, Dowson D, Longfield MD, Wright V, Buckley T. Behaviour of synovial fluid on surfaces of articular cartilage. A scanning electron microscope study. *Ann Rheum Dis.* 1969;28(1):1-14.

23. Ghosh S, Choudhury D, Das NS, Pingguan-Murphy B. Tribological role of synovial fluid compositions on artificial joints—a systematic review of the last 10 years. *Lubr. Sci.* 2014;26(6):387-410. https://doi.org/10.1002/ls.1266

24. Gallo J, Goodman SB, Konttinen YT, Raska M. Particle disease: biologic mechanisms of periprosthetic osteolysis in total hip arthroplasty. *Innate Immun.* 2013;19(2):213-224. https://doi.org/10.1177/1753425912451779

25. Buckwalter JA, Mankin HJ. Articular cartilage. Part II: degeneration and osteoarthrosis, repair, regeneration, and transplantation. *J. Bone Joint Surg. Ser a.* 1997;79(4):612-632. https://doi.org/10.1007/978-1-4471-5451-8_98

26. Sun D, Wharton JA, Wood RJK, Ma L, Rainforth WM. Microabrasion–corrosion of cast CoCrMo alloy in simulated body fluids. *Tribology Int.* 2009;42(1):99-110. https://doi.org/10.1016/j.triboint.2008.05.005

27. Contu F, Elsener B, Böhni H. Characterization of implant materials in fetal bovine serum and sodium sulfate by electrochemical impedance spectroscopy. II. Coarsely sandblasted samples. *J Biomed Mater Res a.* 2003;67(1):246-254. https://doi.org/10.1002/jbm.a.10113

28. Valero Vidal C, Igual Muñoz A. Study of the adsorption process of bovine serum albumin on passivated surfaces of CoCrMo biomedical alloy. *Electrochim Acta.* 2010;55(28):8445-8452. https://doi.org/10.1016/j.electacta.2010.07.028

29. Yan Y, Neville A, Dowson D. Biotribocorrosion of CoCrMo orthopaedic implant materials—assessing the formation and effect of the biofilm. *Tribol. Int.* 2007;40(10–12):1492-1499. https://doi.org/10.1016/j.triboint.2007.02.019

30. Milošev I, Strehblow HH. The composition of the surface passive film formed on CoCrMo alloy in simulated physiological

solution. *Electrochim Acta*. 2003;48(19):2767-2774. https://doi.org/10.1016/S0013-4686(03)00396-7

31. Nečas D, Vrbka M, Křupka I, Hartl M, Galandáková A. Lubrication within hip replacements—implication for ceramic-on-hard bearing couples. *J Mech Behav Biomed Mater*. 2016;61:371-383. https://doi.org/10.1016/j.jmbbm.2016.04.003

32. Vrbka M, Nečas D, Hartl M, Křupka I, Urban F, Gallo J. Visualization of lubricating films between artificial head and cup with respect to real geometry. *Biotribology*. 2015;1-2:61-65. https://doi.org/10.1016/j.biotri.2015.05.002

33. Max Diem. *Modern vibrational spectroscopy and microspectroscopy: Theory, instrumentation and biomedical applications*. John Wiley & Sons003A Hoboken, NJ 2015.

34. Choudhury D, Urban F, Vrbka M, Hartl M, Krupka I. A novel tribological study on DLC-coated micro-dimpled orthopedics implant interface. *J Mech Behav Biomed Mater*. 2015;45: 121-131. https://doi.org/10.1016/j.jmbbm.2014.11.028

35. Han XX, Zhao B, Ozaki Y. Surfarational spectroscopy and microce-enhanced Raman scattering for protein detection. *Anal Bioanal Chem*. 2009;394(7):1719-1727. https://doi.org/10.1007/s00216-009-2702-3

36. Zou S, Weaver MJ. Surface-enhanced Raman scattering on uniform transition-metal films: toward a versatile adsorbate vibrational strategy for solid-nonvacuum interfaces? *Ana Chem*. 1998;70(11):2387-2395. https://doi.org/10.1021/ac9800154

37. Shanmukh S, Jones L, Driskell J, Zhao Y, Dluhy R, Tripp RA. Rapid and sensitive detection of respiratory virus molecular signatures using a silver nanorod array SERS substrate. *Nano Lett*. 2006;6(11):2630-2636. https://doi.org/10.1021/nl061666f

38. Reymond-Laruinaz S, Saviot L, Potin V, Marco De Lucas MC. Protein–nanoparticle interaction in bioconjugated silver nanoparticles: a transmission electron microscopy and surface enhanced Raman spectroscopy study. *Appl Surf Sci*. 2016;389:17-24. https://doi.org/10.1016/j.apsusc.2016.07.082

39. Hughes DO. Catalysis in Practice. *Chemsa*. 1982;8:114-116.

40. Thompson DT. Some basic research in coordination chemistry and catalysis, related to applications for industry. *Coord Chem Rev*. 1996;154:179-192. https://doi.org/10.1016/0010-8545(96)01282-9

41. Sachtle WMH, De Boer NH. Chemisorption as a prerequisite to heterogekeous catalysis. *J Phys Chem*. 1960;64(10):1579-1580.

42. Barth JV. Fresh perspectives for surface coordination chemistry. *Surf Sci*. 2009;603(10–12):1533-1541. https://doi.org/10.1016/j.susc.2008.09.049

Raman Analysis of chemisorbed tribo-film for metal-on-polyethylene hip joint prostheses.

Risha Rufaqua[1*], Martin Vrbka[1], Dušan Hemzal[2], Dipankar Choudhury[3], David Rebenda[1], Ivan Křupka[1], Martin Hartl[1].

[1]Faculty of Mechanical Engineering, Brno University of Technology, Technická 2896/2, 616 69, Brno, Czech Republic.
[2]Department of Condensed Matter Physics, Faculty of Science, Masaryk University, Kotlářská 2, 611 37, Brno, Czech Republic.
[3]Nano Mechanics and Tribology Laboratory, Department of Mechanical Engineering, University of Arkansas, Fayetteville, Arkansas, USA.
[*]Risha.Rufaqua@vut.cz

Abstract

The study aims to understand the biochemical reaction during formation of lubricating film between the head and the cup of a joint replacement. Three types of model synovial fluids and hyaluronic acid at physiological concentrations were used in the experiment. The experiment was conducted with a cobalt-chromium ball on ultra-high molecular weight polyethylene cup setup in a hip joint simulator. The frictional coefficient for each type of lubricant was measured and Raman spectroscopy was used to perceive the chemical reactions between the synovial fluid and implant material. The Raman spectra evidenced that the three model fluids and the HA chemisorbed onto the Co-Cr-Mo surface. An α-helix structure of the model fluid components was proposed on the surface of Co-Cr-Mo. However, there was no correlation between chemisorption and the coefficient of friction.

Keywords
synovial fluid, film formation, Raman spectroscopy, bio-tribology, tribo-chemistry.

1. Introduction

In clinical applications, Co–Cr alloys are used in form of wrought and cast alloys. In combination with polyethylene, Co–Cr alloys have been effectively used to fabricate artificial disc prostheses. The Co–Cr–Mo alloy (ASTM F75) was introduced in hip prostheses during the late 1960s. This alloy is widely used in orthopaedic implants, such as hip and knee joint replacements [1].

Due to presence of mechanically enhanced electrochemical processes, cobalt–chromium (Co-Cr-Mo) alloys release ions in the human body. The resulting tribocorrosion is strongly affected by biological reactions. In the same time, protein lubricated metal-on-metal (MoM) sliding contact is predicted to undergo tribochemical reactions, which significantly improve its performance. A protective layer is formed by the reaction, generally denoted as a carbonaceous 'tribofilm.' Using scanning electron microscopy and Raman

1

spectroscopy reveals that formation of the tribofilm is influenced by the contact load. Thus, the film is postulated as protective in nature, facilitating reduction of material loss during sliding. A vital role in this tribochemical reaction is played by proteins contained within the synovial fluid (SF) of human joints, together with other organic components such as hyaluronic acid (HA) and lubricin [2, 3].

In the study by Necas et al. [4], Co-Cr-Mo and polyethylene contact pair showed coefficient of friction dependent on both protein concentration and kinematic conditions in case of albumin and γ-globulin mixture. The film thickness and the structure of the adsorbed proteins were evaluated using spectroscopic ellipsometry and FT-IR, respectively. The total protein concentration and adsorbed film thickness noticeably affect friction. Also, the structure of the protein adsorbed on the ultra-high molecular weight polyethylene (UHMWPE) surface exhibits a particular impact of kinematic conditions on the frictional behavior of the contact couple. The native structure of adsorbed molecules was retained at high sliding speed, while denaturation of adsorbed proteins was found when sliding speed was lower. Cr-Co-Mo hip joint Prostheses with micro-dimples in bovine serum lubricant developed remarkably increased film thicknesses and shortened the transition period [5].

Impact of model SFs protein content on the film formation under static and rolling condition was studied by Parkes et al. [6]. Two different pH and six different compositions of SFs were used to track the film thickness and kinetics of its formation. It was confirmed that film formation depends on the protein content and the pH of the solution under both conditions. Protein layers were found thicker under rolling than statical condition. Bovine γ-globulin deposits were thicker compared to bovine serum albumin (BSA). For low pH, a relaxed protein adsorption process was noticed in the initial stage, while with time the adsorption rate increased. A thicker non-uniform and irregular deposition protein film formed in the rolling condition was observed at pH 7.4 or lower. At the primary stage viscoelasticity is higher with higher pH and under static condition, and uniform and consistent film was formed [7]. Due to protein occurrence, the total specific wear rate is increased under abrasion corrosion test conditions. Correspondingly, formation of metal-protein complexes has been predicted in Bovine Serum solutions under enhanced corrosion rate [8].

Formation of the passivation film on Co-Cr-Mo orthopaedic alloy has been studied in simulated physiological solution by X-ray photoelectron spectroscopy. A formation of a complex layer was found using electrochemical oxidation process, where the applied potential was manipulating both composition and thickness of the formed film [9]. The electrochemical corrosion resistance is one of the vital factors to biocompatibility of metals. Within the body environment, surgical alloys achieve an exceptionally high electrochemical corrosion resistance. For the further improvement of the biocompatibility of metal components, reduction of metal ion release is anticipated [10].

In another study, two distinct mechanisms of film formation were studied: boundary lubrication and high viscosity gel mechanism. As agglomerated protein forms organic deposits on the surface of implants, the wear is inflicted through the tribocorrosion process;

with higher pH wear also increases. In general, the chemistry within SF has a substantial impact on wear and failure of joint replacement [11].

Concerning lubrication of Co-Cr-Mo hip prostheses, influence of BSA and γ-globulin concentration was focused along with the frictional coefficient. It was uncovered that sufficient boundary lubrication is maintained by maximum BSA levels and optimal concentration of γ-globulin. Thus, the concentration of BSA and also of γ-globulin control the friction of the Co-Cr-Mo head. These optimal concentrations of BSA and γ-globulin can be manipulated to increase the lubricating ability of Co-Cr-Mo hip prostheses via altering the surface roughness and coating of the bearing surface [12].

Boundary lubrication ability was also determined for the retrieved Co-Cr-Mo head regarding HA and phospholipids, along with microscale frictional coefficients. Retrieved Co-Cr-Mo head's microscale frictional response shows a dependence on the concentration of HA and phospholipids. The optimal concentration to maximize lubrication is similar to the concentration of HA and DPPC of human SF [13].

Contribution to boundary lubrication of various constituents of SF separately and collectively was also focused. Graded concentrations of SF constituents (HA, PRG4, and SAPL) and their combinations were utilized for cartilage boundary lubrication tests. It was exposed that both at physiologic and pathophysiologic concentrations, the constituents of SF contribute to boundary lubrication of the articular cartilage surface. The contribution was specified individually and in the combination of the SF constituents [14]. In addition, HA and glycoprotein lubricin form a complex HA-LUB, trapped at the interface to form a cross-linked network, which plays a role of boundary lubricant and prevents wear mechanism [15].

Using the electrochemical method, the area of adsorption and frictional property of BSA under rubbing condition with UHMWPE and Co-Cr-Mo alloy were explored *in-situ*. Using the real-time information on adsorption and desorption of proteins, it was disclosed that during rubbing, the BSA film is reconstructed on the Co-Cr-Mo surface by the shear force. By acquiring the shear force, the adsorbed film becomes a strong, stable and optimally adapted structure [16].

Interfacial and bulk rheology for model SF were focused for various shear rates, strains and frequencies as an effect due the proteins and HA. In the steady and oscillatory condition of the model SF composed from HA, BSA and γ-globulin, at the interface interfacial rheology are rejected due to protein adsorption. On the contrary, bulk rheology was controlled wholly by HA of model SF for various shear rate, strains and frequencies [17].

Infrared Reflection-Absorption Spectroscopy analysis during the wear test of Co-Cr-Mo material pairs showed deposits formed predominately by proteins and implying denaturation of the proteins. During rubbing, denatured proteins turned out to be adherent. Thus, the rubbing process forms insoluble agglomerates, which are deposited and contribute to reduced wear [18]. Consequently, surface protection during rubbing is

3

contributed by this insoluble, denatured protein films as primary lubrication mechanism [19].

For model fluids it is found that higher concentration of HA and phospholipids causes reduction of the film thickness in the case of metal-head [20]. It is also shown that, compared to the ceramic heads, metal-heads form thicker films during articulation [21].

Concerning the effect of friction, it is stated that implant material is the fundamental parameter. Usually, friction is increased twice by implementation of the metal pair compared to ceramic. In the case of hard-on-hard pairs, addition of protein to the lubricant exposed a positive result on friction, while adding protein to the hard-on-soft pairs shows barely any response [22].

Not many studies concentrate on biochemical composition of the synovial joints, where the spectroscopic technique was used as an analyzing tool. Using Raman spectroscopy, variations of molecular structures between tibial plateaus of healthy joints and joints with total replacements due to osteoarthritis were evaluated. Also, a comparison of medial and adjacent compartments of subchondral bones was observed to compare different load baring sites [23]. Investigation of differences between biochemical compositions of healthy joint SFs and SFs of OA patients was carried out in [24]. Galandakova et al. [25] revealed that adsorption of albumin and γ-globulin on artificial materials takes place instantaneously, impacting also the frictional properties of the lubricating surface.

In summary, it is necessary to observe the biochemical reactivity of the SF on the implant materials to increase the depth of knowledge on joint replacement procedure and to enhance the longevity of the orthopaedic implantations. Studying different synovial components in appropriate ratios, instead utilization of BS, may uncover more practical results to understand the lubrication chemistry and mechanism of SF within the prosthesis [26].

2. Materials and methods

2.1. Pendulum hip simulator
The Pendulum hip simulator, imitating 'flexion and extension' of artificial hip joints together with their real geometry, body temperature and loads, is an exclusive and unique bio-tribological instrument. It is efficient in measuring the real-time velocity profile, average friction coefficients and the viscous effect (an indicator of lubrication film formation). Vrbka et al. [27] conducted an experiment with this simulator to visualize the lubricating films between artificial head and cup in real geometry and Necas et al. [21] utilized the same instrument to understand the effect of diameter, clearance and material during in situ observation of lubricant film formation. Dipankar et al. used this simulator to understand a significant reduction of friction coefficient for 'dimpled a-C:H/ceramic' prosthesis compared to a 'Metal (Co-Cr)/ ceramic' prosthesis. In result, it is indicated that the simulator can be utilized as an advanced bio-tribometer. [21, 27, 28].

4

The simulator comprises of a base frame with the acetabular cup and a swinging pendulum with the femoral head. The pendulum is driven by electromagnetic motors that allow its continuous motion in the flexion-extension plane [21]. It is supposed that this kind of instrumental setup could help in determination of the chemical reactions within SF after artificial joint replacement along with the frictional coefficient of individual contact pairs.
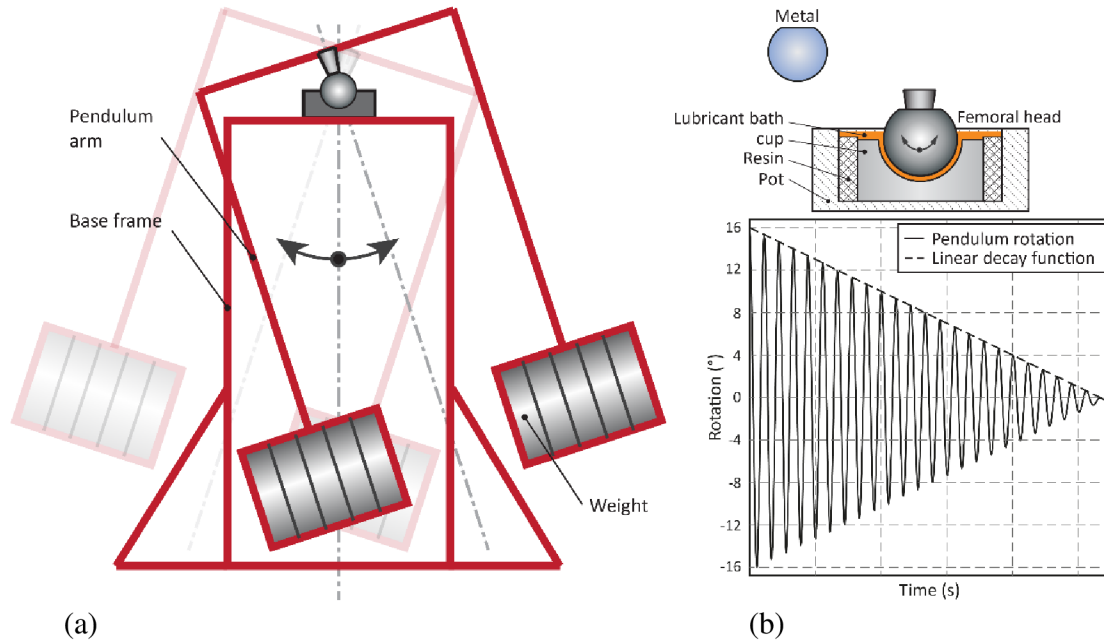

Fig. 1 *(a) A schematic illustration of the pendulum hip joint simulator (b) Overview of the tested femoral components, detail of the contact couple, and representative linear decay signal.*

2.2. Ball-on-cup configuration

To clarify the lubrication processes considered within artificial joints, the experiments were conducted in a ball-on-cup configuration, where the contact couple was Co-Cr-Mo (the ball) and polyethylene (the acetabular cup). In particular, metal hip prosthesis head of Co-Cr-Mo ball (28mm) from Zimmer was used in accordance with ISO 5832-12, which contains cobalt-chromium casting alloy. The cup used was made from polyethylene by Smith and Nephew (28mm).

2.3. Model fluid lubricants

To observe the chemical reaction occurring within hip replacement, three types of model SFs were used as lubricants in the ball-on-cup configuration. These model fluids were prepared with concentrations of the components at real physiological values, as evaluated by Galandakova et al. [25]. In particular, the three types of model fluids used here are the mimic of SF of healthy or physiologic joint (SF1), SF of total joint replacement (SF2) and SF within a joint with osteoarthritis (SF3) [25, 30]. In the model fluids the concentrations of albumin, γ-globulin, HA and phospholipids were maintained within the range observed in the human joints, as described in Table 1.

Albumin, γ-globulin, HA and phospholipids were dissolved in PBS with overnight employment of a laboratory rocker-shaker (MR-12, Biosan, Riga, Latvia) at 4 °C. The next step of preparation was mixing the individual components into model fluids in the order albumin, γ-globulin, HA, phospholipids. The lubricant solutions were preserved at -22 °C after preparation.

The product specifications of the applied components applied are: Bovine serum albumin (powder, $\geq$96%; A2153, Sigma-Aldrich, St. Louis, MO, USA), γ-globulin from bovine blood (powder, $\geq$99%; G5009, Sigma-Aldrich, St. Louis, MO, USA), HA = Sodium Hyaluronate HySilk (powder, quality class—cosmetic; molecular weight = 820–1020 kDa, Contipro, Dolní Dobrouc, Czech Republic), and PHs = L-α-Phosphatidylcholine (powder, Type XVI-E, lyophilized powder; $\geq$99%; vesicles form; P3556, Sigma-Aldrich, St. Louis, MO, USA).

Albumin (28.0 mg/ml) and γ-globulin (11.0 mg/ml) were also used as lubricants separately with Co-Cr-Mo ball in our previous experiment [26]. These two lubricants are used individually in this experiment to determine the cofficient of friction within the contact pair. HA (2.0 mg/ml) was tested to observe the chemical reaction occurring with the metal contents of Co-Cr-Mo ball.

To observe the tribological effect within the pendulum hip joint simulator, each experiment was conducted for 5-6 mins to achieve the chemical changes on the ball surface.

Table 1: Composition and concentration of the applied test lubricants.

Test Fluid	Albumin (mg/ml)	γ-globulin (mg/ml)	Hyaluronic Acid (mg/ml)	Phospholipids (mg/ml)
Healthy Joint (SF1)	20	3.6	2.5	0.15
After Total Joint Replacement (SF2)	26.3	8.2	0.87	0.35
Joint with Osteoarthritis (SF3)	24.9	6.1	1.49	0.34
Hyaluronic Acid	-	-	2	-

After the tribological experiment, the fluids were collected for analysis. All experiments were performed at 37 °C and the weight used on the simulator was 15 kg.

2.4. Raman Spectroscopy

Concerning characterization and structure analysis of the samples, Raman spectroscopy is a fast and non-destructive method [31]. The differences in Raman spectra acquired for each of the lubricants before use and after experiment within the simulator clarify that chemical reactions are taking place within the artificial joint replacement. Through Raman spectrum,

the obtained vibrational fingerprints expose the specific chemical structure of the individual lubricant components within the formed films [26].

To obtain the fingerprints of different lubricants before and after tribological experiment in the simulator, Renishaw inVia Raman spectrometer was used with 532 nm excitation. The surfaces of the balls were observed to determine the chemical changes due to the tribological process. On the surface of Co-Cr-Mo ball, 1 mW of laser power was used with the exposure time of 100 s. The fingerprints of the lubricants before and after tribological tests were achieved with 100 mW laser power and 20 s exposure.

2.5. Coefficient of friction measurement

Coefficient of friction for the Co-Cr-Mo and polyethylene contact pair was also determined for each of lubricants. Within the pendulum hip joint simulator, the acetabular cup is installed using resin in a stainless-steel pot. This set up is mounted to the base frame. The swinging arm is connected to the head using a cone. When the experiment starts, the pendulum arm is deflected to the primary position and then released. The swinging is then damped due to friction between the ball and the cup. Instant deflection of the pendulum is recorded via angular velocity sensor. Consequently, the recorded signal is evaluated using linear model of damping to obtain the friction coefficient [29].

3. Results

3.1. Raman Analysis

Co-Cr-Mo surface before and after tribological test with different model fluids resulted in Raman spectra shown in Figure 2.
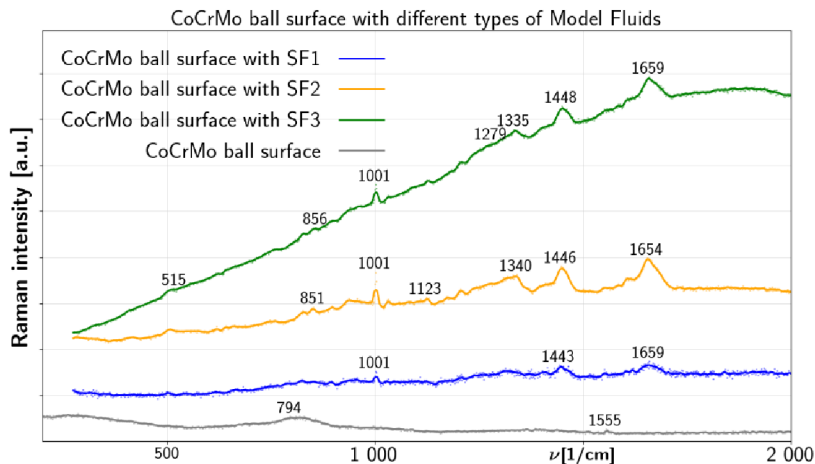

Fig. 2 Raman Spectroscopic data of Co-Cr-Mo ball surface with SF1, SF2 and SF3 respectively.

The spectra for model fluid SF1 and SF3 are showing peak on 1659 cm^{-1}, while for SF2 it shifted to 1654 cm^{-1}. Another peak is showing at 1443 cm^{-1}, 1446 cm^{-1} and 1448 cm^{-1} for SF1, SF2 and SF3, respectively, film on the surface. SF2 and SF3 on the surface are

showing peaks at 1340 cm^{-1} and 1335 cm^{-1}, respectively, while SF1 is not showing any peak in this range. A peak at 1001 cm^{-1} is found for all three lubricants.

Fig. 3 Raman Spectroscopic data for SF1 model synovial fluid liquid before-test and after test with Co-Cr-Mo.

SF1 liquid spectra without test and after test with Co-Cr-Mo are compared in Figure 3. Before test, SF1 showed a prominent peak at 1651 cm^{-1}, which shifted after the tribological test to 1654 cm^{-1}. The peaks at 1449 cm^{-1} and 1336 cm^{-1} shifted to 1451 cm^{-1} and 1340 cm^{-1} after the test, while peak at 1211 cm^{-1} and the sharp peak at 1003 cm^{-1} remained essentially unchanged. The peak at 945 cm^{-1} before testing is positioned at 953 cm^{-1} after the test. Finally, a broader band near 450 cm^{-1} is observed in both spectra.
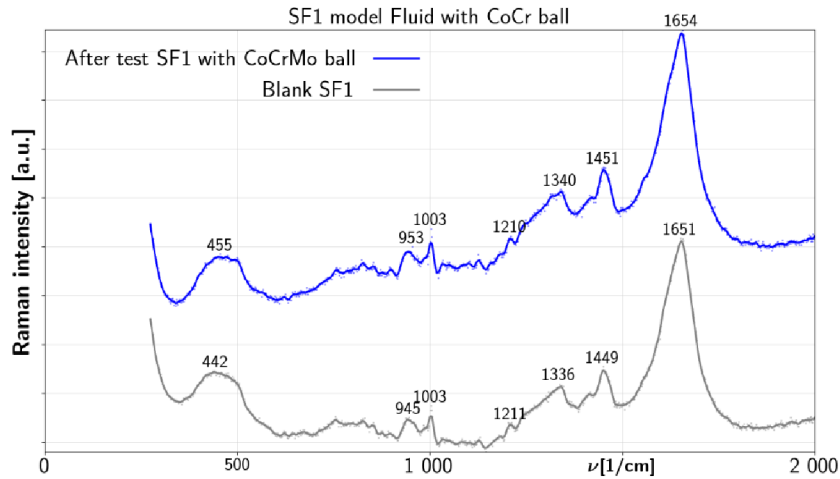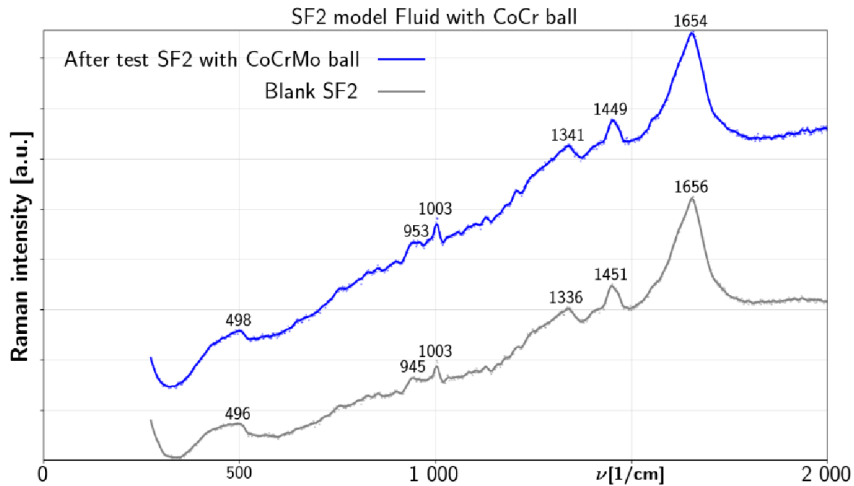

Fig. 4 Raman Spectroscopic data for SF2 model synovial fluid liquid before-test and after test with Co-Cr-Mo.

SF2 liquid spectra without test and after test with Co-Cr-Mo are compared in Figure 4; most of the data in this figure are comparable with Figure 3 for SF1. Without test, the SF2

8

prominent peak at 1656 cm⁻¹ was at 1651 cm⁻¹ for SF1, while after the test with the metal ball, both fluids exhibit this peak at 1654 cm⁻¹. The before-test SF2 peaks at 1451 cm⁻¹ and 1336 cm⁻¹ shift after the test to 1449 cm⁻¹ and 1341 cm⁻¹, respectively. The peak near 1210 cm⁻¹, present in SF1 spectra, is absent for SF2 liquid. Again, a sharp peak is observed for both before and after the test SF2 at 1003 cm⁻¹. The peak at 945 cm⁻¹ for before test is shifting to 953 cm⁻¹ in after-test SF2 liquid, similarly to SF1. A broader band is visible around 490 cm⁻¹ for both before test and after the test SF2 liquid.
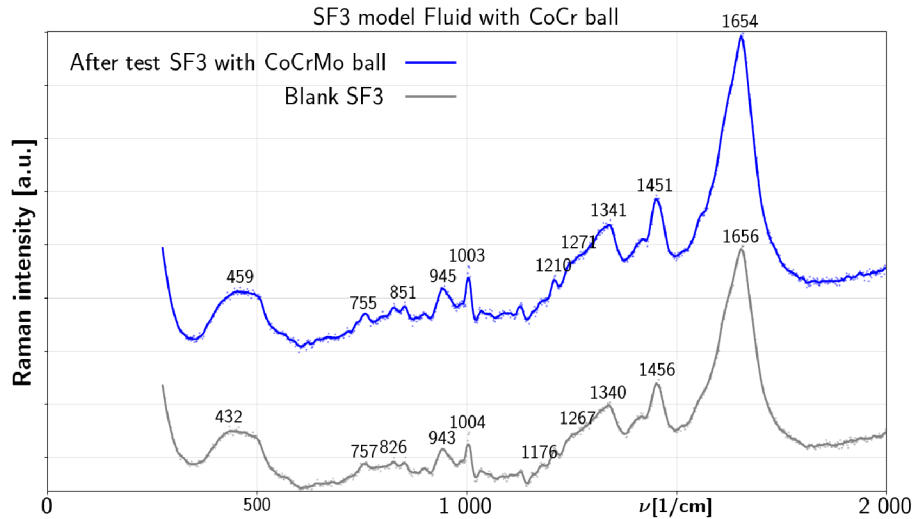

Fig. 5 Raman Spectroscopic data for SF3 model synovial fluid liquid before-test and after test with Co-Cr-Mo.

Raman spectra of SF3 liquid before and after the tribological test with Co-Cr-Mo are presented in Figure 5. Several peaks in Figure 5 are comparable with Figures 3 and 4 for SF1 and SF2 liquids, respectively. Before testing, the SF3 prominent peak at 1656 cm⁻¹ is found in the same position for SF2, but for SF1 the peak is shifted to 1651 cm⁻¹. Nevertheless, all three model fluids show this peak after the test with Co-Cr-Mo at 1654 cm⁻¹. SF3 before-test peaks at 1456 cm⁻¹ and 1340 cm⁻¹ shift to 1451 cm⁻¹ and 1341 cm⁻¹, respectively, after the test. The peaks in these two ranges are also visible for SF1 and SF2 liquids.

The sharp peak at 1004 cm⁻¹ and the peak at 943 cm⁻¹ peak remain essentially unaffected by the test and are thus visible for all three fluids. In contrast, SF3 fluid shows the peak at 1210 cm⁻¹ only after the test, while SF1 fluid shows this peak for both before test and after the test.

At the same time, SF3 is providing two peaks near 830 cm⁻¹ and 850 cm⁻¹ both before test and after the test, which other model fluids did not show. On the other hand, there is a similar peak for the Co-Cr-Mo surface with SF2 and SF3 in Figure 2. Yet another peak at 757 cm⁻¹ and 755 cm⁻¹ is observed for SF3 fluid before test and after the test, respectively, which is not observable for SF1 or SF2 fluids. Finally, broader band near 450 cm⁻¹ is seen also for SF3 fluid both before test and after the test.
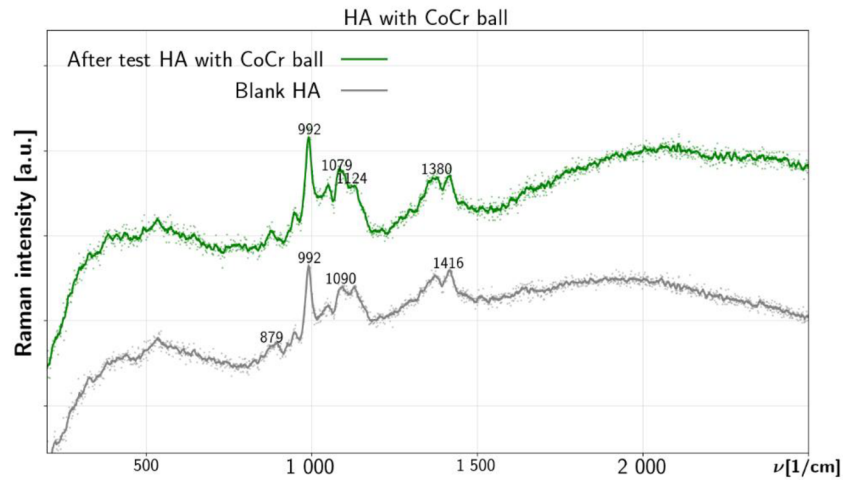
9

Fig. 6 Raman Spectroscopic data for HA liquid before-test and after test with Co-Cr-Mo.

The Raman spectra of HA liquid without test and after the test with Co-Cr-Mo are compared in Figure 6. Both without test and with the test, HA is displaying double peaks near 1400 cm^{-1} and 1100 cm^{-1}. In particular, the peak component at 1090 cm^{-1} in before-test liquid shifts to 1079 cm^{-1} after the test. The strong peak at 992 cm^{-1} is present for both before-test and after the test HA liquid.
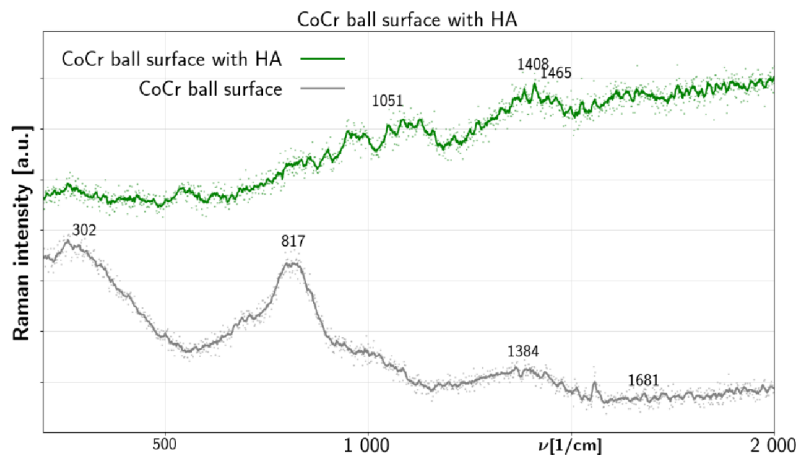
Fig. 7 Raman Spectroscopic data of Co-Cr-Mo ball surface with HA liquid.

Co-Cr-Mo surface spectra are elaborated in Figure 7 both before and after the tribological test with HA acid. The spectrum found for the after-test surface is entirely different from the before-test one. The clean Co-Cr-Mo surface provides peaks at 1681 cm^{-1}, 1384 cm^{-1}, 817 cm^{-1} and 302 cm^{-1}, while after the test with HA, the metal surface provides peaks at 1465 cm^{-1}, 1408 cm^{-1} and 1051 cm^{-1}.

10

3.2. Microscopic view of the formed film

Figure 8 (a to e) provides microscopic photos of the film formed on the Co-Cr-Mo ball with SF1, SF2 and SF3. The 8(a) photo of the Co-Cr-Mo surface after tribological experiment with SF1 (which is the model SF of a healthy joint) shows no noticeable film structure. In contrast, 8(b) and (c) for SF2 (which is the model SF after total joint replacement) show very thick and branched film. A similar branched pattern of the film was found also in our previous experiment with albumin and γ-globulin film on the Co-Cr-Mo surface [26]. Consequently, these films are due to the protein accumulation on the metal surface. Raman spectra were taken for both branched and flat area of the Co-Cr-Mo surface with SF2. The branched area provided more substantial Raman peaks than the flat area. Similalry, SF3 in 8(d) and (e) forms some branched film on the metal surface, but the pattern was not as apparent as for SF2.
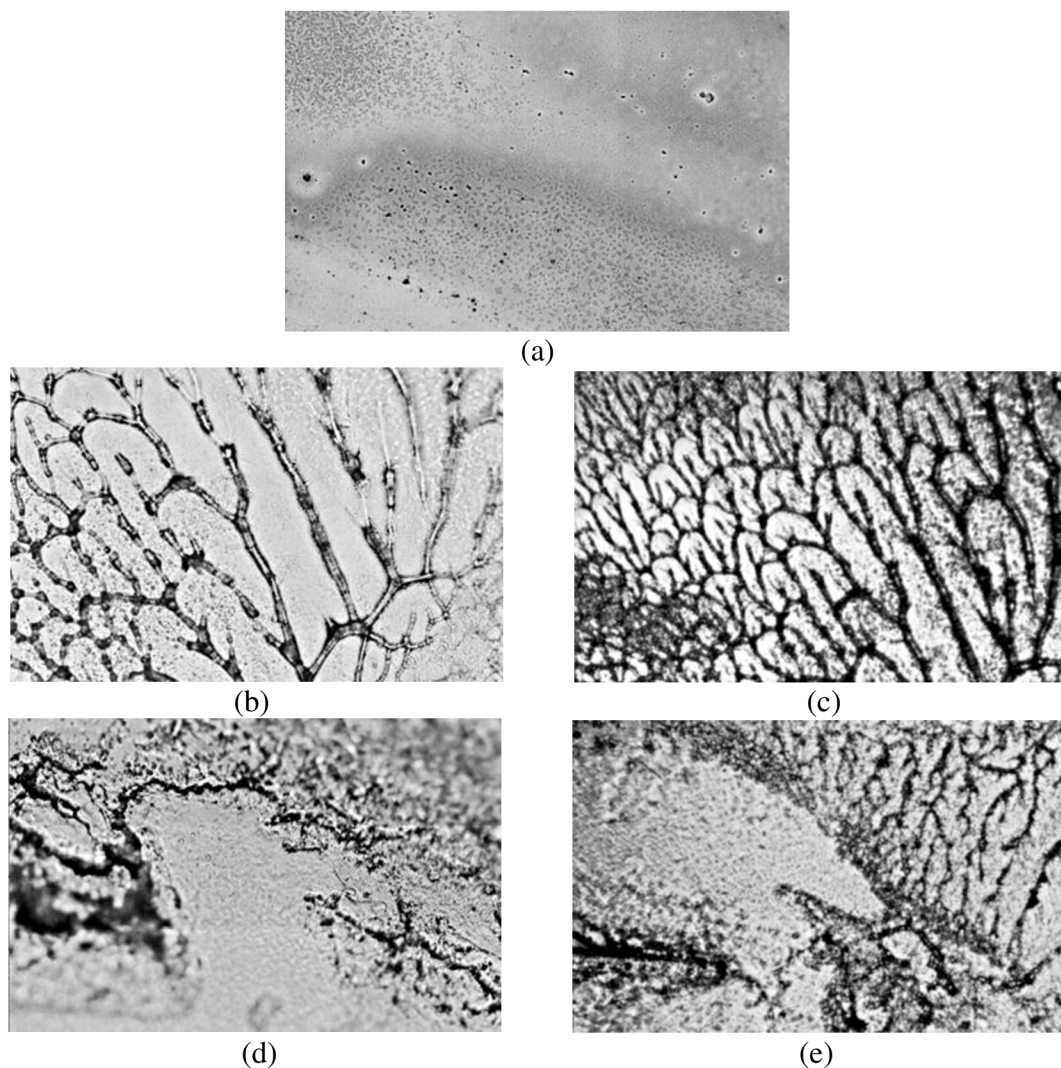

(a)

(b)

(c)

(d)

(e)

Fig. 8 Co-Cr-Mo ball viewed by Raman Microscope respectively (a) SF1 on the surface, (b) and (c) SF2 on the surface, (d) and (e) SF3 on surface. The horizontal size of the panels is 20 μm for (a), (b), and (d) and 5 μm for (c) and (e).

11

In summary, it could be determined that the type of the model fluid changes the characteristics of the film on the metal ball surface: when concentrations of the SF elements changes, so does the pattern of the developed film.

Figure 9 shows the film on Co-Cr-Mo formed by HA. It also exhibits some kind of pattern, but this pattern was not visible on the metal surface before Raman emission.

| (a) | (b) |
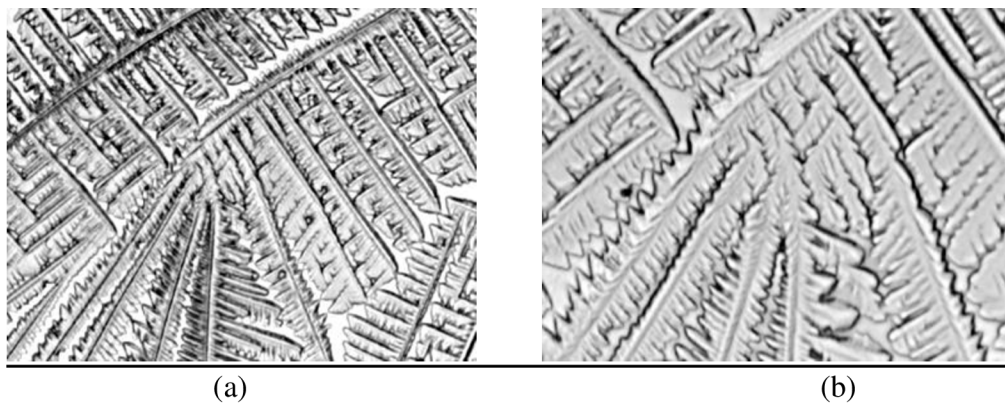
Fig. 9 Co-Cr-Mo ball viewed by Raman Microscope after test with HA. The horizontal size of the panels is 20 µm (a) 5µm (b).

3.3. Coefficient of friction analysis

The friction coefficient of all three types of model fluid with Co-Cr-Mo ball was found above 0.23. The highest value of 0.2365 was showed by SF2, and the lowest value was 0.2308 for SF1. When measuring the coefficient of friction separately for the components, albumin, γ-globulin and HA, all values were lower than that of the model SFs. HA shows coefficient of friction as low as 0.072, while γ-globulin shows the highest value of 0.208 among the SF components. In the used Co-Cr-Mo ball and polyethylene cup setup, albumin shows coefficient of friction 0.1969. The values are summarised in Figure 10.

Fig. 10 Coefficient of friction for Co-Cr-Mo and Polyethylene contact pairs for albumin, γ-globulin, HA and SF1, SF2 and SF3 model synovial fluids.

4. Discussion

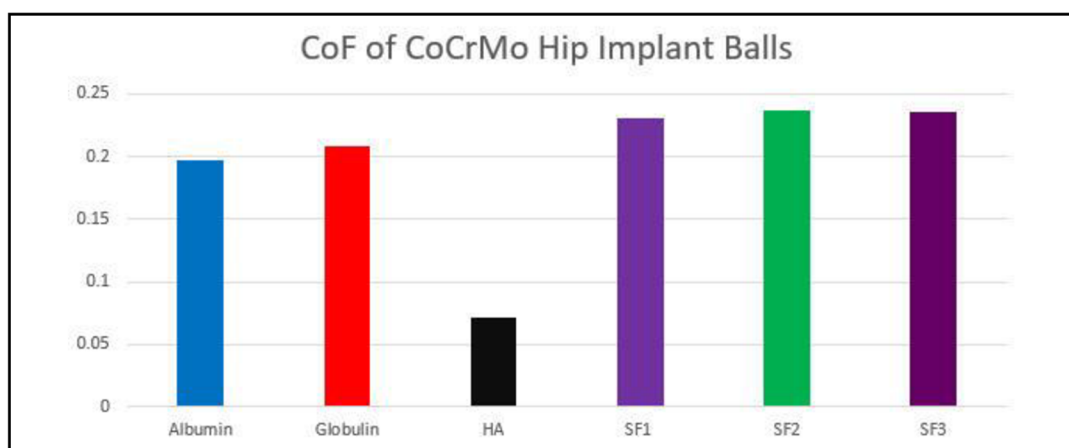This contribution aims at clarification of the chemical reactions taking place between several model SFs and the Co-Cr-Mo joint replacement during formation of the tribofilm along with study of the frictional properties. To track the state of the SF components, vibrational fingerprints provided by Raman spectroscopy are used.

The Raman analysis of the Co-Cr-Mo surface after the tribological test with all model fluids are described as below. The prominent peak near 1660 cm^{-1} is due to water; it is found at 1659 cm^{-1} for model fluids SF1 and SF3, while for SF2, it is shifted to 1654 cm^{-1}. Since however, these positions constitute a significant shift from the usual water peak position at 1642 cm^{-1}, it is possible that convolution with α-helix Amide I band, ranging within 1645-1660 cm^{-1} [32], takes place, which could facilitate albumin adsorption on Co-Cr-Mo surface for the model fluids we used. The peak at 1443 cm^{-1}, 1446 cm^{-1} and 1448 cm^{-1} for SF1, SF2 and SF3, respectively, is due to CH$_2$/CH$_3$ deformation [24, 33]. In addition, SF2 and SF3 exhibit peaks at 1340 cm^{-1} and 1335 cm^{-1}, respectively. This range provides information regarding CH$_2$-CH$_3$ wagging [24, 33]. It is noticeable that SF1 did not provide any peak nearby this area. SF3 also provides a peak at 1279 cm^{-1}, which is within the α-helix range of the Amide III band [32], supporting the conclusion that from SF3, albumin is adsorbing on the Co-Cr-Mo. In comparison, SF2 exhibits peak at 1123 cm^{-1}, in the range of protein backbone vibrations: C-C, C-OH, C-N stretch, C-O-C, glycosidic linkage [24]. All three fluids on Co-Cr-Mo show a sharp peak near 1000 cm^{-1}, which is due to benzene ring breathing [24, 33]. The peak at 851 cm^{-1} and 856 cm^{-1} provided on the surface by SF2 and SF3, respectively, is in the range of C-C skeletal stretch [33, 34]; it is not provided by SF1. After all, 515 cm^{-1} peak showing in SF3 could be due to the tertiary and quaternary branched carbon atom next to the tertiary carbon atom [33].

As the above described peaks do not match any peaks of the Co-Cr-Mo substrate (such as 1681 cm^{-1}, 1555 cm^{-1}, 1384 cm^{-1}, 817 cm^{-1}, 794 cm^{-1} and 302 cm^{-1}) and several α-helix related features were observed, we suggest that adsorption of (mainly helical) albumin to the Co-Cr-Mo surface is taking place from all model fluids. In addition, SF3 (which mimicks osteoarthritic joint) is attached with more bonds to Co-Cr-Mo surface than SF1, while for SF2 (mimicking the SF of total joint replacement) the protein backbone vibrations also show. It should be noted that maximum amount of albumin is present in SF2 (that is in the model fluid of total joint replacements), but the ratio of the model fluid components present in SF3 (osteoarthritic SF) is more favourable for film formation on the Co-Cr-Mo surface. In diseased joints, the amount of protein is altered naturally [25], and more protein is involved in the formation of the film on the metal surface. The film changes on the surface of Co-Cr-Mo, particularly for SF2 and SF3, are also remarkable in the microscopic pictures. The SF2 is forming a branched film, and it seems from the microscopic pictures that SF3 is also forming a thicker film compared to SF1.

Raman spectra of SF1 liquid with Co-Cr-Mo present before testing and after the test the water peak at 1651 cm^{-1} and 1654 cm^{-1}, respectively, which again seems to include a contribution from α-helix Amide I band [32], as described above. The peak at 1449 cm^{-1} before testing, shifted to 1451 cm^{-1} after the test, is in the range of CH$_2$/CH$_3$ deformation [24, 33]. In contrast, the peak provided by SF1 at 1336 cm^{-1} before testing and at 1340 cm^{-1}

[1] after the test, is due to CH$_2$-CH$_3$ wagging [24, 33]. The C-C stretching region [35] is covered by the peak at 1211 cm^{-1} and 1210 cm^{-1} before testing and after the test, respectively. The benzene ring breathing peak at 1003 cm^{-1} appears for both SF1 liquids without shifting [35]. The SF1 liquid peak at 945 cm^{-1} before testing, and shifted to 953 cm^{-1} after the test, is in the range of α-helix C-C skeletal stretching [35]. The peak at 442 cm^{-1} before testing and at 455 cm^{-1} after the test shows C-C skeletal deformation [33].

SF2 liquid before testing and after the test shows similarities to SF1 liquids data. The water peak range 1645-1660 cm^{-1} seems to also include the α-helix Amide I band contribution [32]. The CH$_2$/CH$_3$ deformation peak [24, 33] is visible for SF2 before testing at 1451 cm^{-1} and after the test at 1449 cm^{-1}. The SF2 peak at 1341 cm^{-1} after the test, which appeared at 1336 cm^{-1} before testing, expresses CH$_2$-CH$_3$ wagging [24, 33]. The benzene ring breathing mode peak [35] is visible for both SF2 liquids at 1003 cm^{-1}. The C-C skeletal stretching of α-helix [35] is proven in SF2 by presence of the peak at 945 cm^{-1} before testing and at 953 cm^{-1} after the test. Thus, Figures 3 and 4 for SF1 (healthy SF) and SF2 (SF after joint replacement) are comparable with exception of the SF1 1210 cm^{-1} peak, which is not visible for SF2.

Raman spectra of SF3 before testing and after the tribological process in Figure 5 are also equivalent to Figures 3 (SF1) and 4 (SF2). The SF3 water peak including α-helix Amide I band contribution was found at 1656 cm^{-1} before testing and at 1654 cm^{-1} after the test. Similarly, to SF1 and SF2, the peak providing information for CH$_2$/CH$_3$ deformation is present for SF3 at 1456 cm^{-1} before testing and at 1451 cm^{-1} after the test. At the same time, SF3 CH$_2$-CH$_3$ wagging appears at 1340 cm^{-1} before testing and at 1341 cm^{-1} after the test.

The weak SF3 liquid peak in 1270 cm^{-1} range is found both before testing and after the test. Consequently, we assign this peak to α-helix range (1265-1300) of the Amide III band [32].

The C-C stretching [35] in SF3 is attributed to the peak at 1210 cm^{-1} after the test, similarly to SF1. The SF3 benzene ring breathing mode shows peak near 1003 cm^{-1} both before testing and after the test. The α-helix C-C skeletal stretching is observed at 943 cm^{-1} before testing and at 945 cm^{-1} after the test for SF3 liquid. The peak at 826 cm^{-1} before testing and at 851 cm^{-1} after the test provides information on C-C skeletal stretch [33, 34]. SF2 and SF3 provide similar peak on the ball surface, at 851 cm^{-1} and 856 cm^{-1}, respectively, but SF2 does not provide this peak in the liquid. C-C, C-O skeletal deformation is expressed in SF3 fluid by the peak at 757 cm^{-1} before testing and at 755 cm^{-1} after the test. In addition, the peak at 432 cm^{-1} before testing and at 459 cm^{-1} after the test indicates C-C skeletal deformation [33].

Turning to HA, the liquid before testing and after the test with Co-Cr-Mo (in Figure 6) exhibits similar characteristics. The double peak near 1400 cm^{-1} is due to C-N stretching and C-H deformation. The peak at 1090 cm^{-1} before testing and at 1079 cm^{-1} after the test is due to C-OH bend in the acetyl group [34, 36]. The sharp HA peak at 992 cm^{-1} is due to ring breathing [33], and the additional peak at 879 cm^{-1} is observable also in other literature [34]. After the test HA shows a peak at 1380 cm^{-1}, which provides information about C-H

bend [34]. Another peak is noticeable after the test at 1124 cm^{-1}, which could be due to C-C stretch [33].

The Co-Cr-Mo surface exhibited Raman peaks at 1681 cm^{-1}, 1555 cm^{-1}, 1384 cm^{-1}, 817 cm^{-1}, 794 cm^{-1} and 302 cm^{-1}. Not much literature was found for the characteristics of these peaks. Liao et al. [37] describe peaks at 1383 cm^{-1} and 1567 cm^{-1} as correlated to disordered sp2-carbon and sp3-bonded carbon in Co-Cr-Mo. However, the spectra of the Co-Cr-Mo surface observed after the tribological test with HA varied from the clean surface. After-test surface exhibited a peak in 1408 cm^{-1}, which is in literature due to C-N stretching and C-H deformation [34, 36]. Another peak of the after-test surface at 1051 cm^{-1} is likely due to C-C and C-O stretching [34, 36]. Finally, the peak at 1465 cm^{-1} demonstrates CH$_3$ deformation within the Co-Cr-Mo surface [33].

Observing film thickness of HA on Co-Cr-Mo implants, Necas et al. [20] concluded, that HA is not an effective lubricant on Co-Cr-Mo. In Figure 7, HA after the test shows on the metal surface peaks due to C-N stretching and C-H deformation, C-C and C-O stretching, and CH3 deformation. Thus, it can be predicted that, when using HA at physiological concentration alone, its chemisorption is taking place on the Co-Cr-Mo surface.

While Co-Cr-Mo in the synovial model fluid containing physiologically relevant concentrations of albumin and HA was evaluated non-destructive electrochemical measurements. A complexation of degenerated HA molecular chains with chromium ions released from the metallic surface was postulated, which may decrease corrosion resistance of the alloy. This attribution is described as essential in building the protective oxide film. Therefore, corrosion of Co-Cr-Mo implants is enhanced by HA in the presence of strong inflammation [38].

In our experiments, HA peaks are not observed in the spectra of the model fluids and neither the surface of Co-Cr-Mo with SF1, SF2 and SF3 model fluids shows peaks relevant to HA. Thus, all the spectra for the model fluids were missing HA contribution, which is, however, in agreement with results by Esmonde et al., who used Raman spectroscopy to assess SF in both healthy and osteoarthritic patients [24]. Nevertheless, it should be noted that HA formed a patterned film on Co-Cr-Mo when the tribological test was executed separately for HA.

In a study of Metal-on-metal (MoM) hip retrievals, electrochemically induced film formation showed the presence of carbonaceous tribofilms derived from synovial proteins, particularly on the articulating surfaces. It is evident that the films decrease corrosion and wear and thus are potentially able to increase the corrosion resistance of biomedical implants. However, it is suggested that mechanical characterization is necessary for estimation of the total performance of the generated film [39].

The coefficient of friction calculated for all model fluids with Co-Cr-Mo ball and polyethylene cup is higher than the frictional coefficient of the proteins and HA separately. In addition, HA showed lower coefficient of friction compared to the other components. Although molecular weight of HA has vital impact on its rheological properties, the HA molecular weight and its coefficient of friction were found to have no mutual dependency

[40]. Also, only limited effect on friction was found when protein-based lubricants were applied with variation of fluid constituents' concentration in the range corresponding to physiologic and osteoarthritic SF [30]. Dependence between the coefficient of friction for model fluids, proteins and HA with chemical changes of Co-Cr-Mo could not be identified.

5. Conclusions

This research provides a joint study of frictional and chemical conditions occurring within the artificial joint replacement. Raman spectroscopy was used to determine the chemisorption of the model fluids on the Co-Cr-Mo ball surface. Simultaneously, measurement of the frictional coefficient took place to reveal the relationship with chemical reactions. The key results from the investigation can be articulated as below:

- Chemisorption occurs on the Co-Cr-Mo surface with all the three types of model SF representing physiologic, total joint replacement and osteoarthritic SF and also with HA as separate lubricant.

- When using albumin, γ-globulin, HA and phospholipid concentrations appropriate to healthy human, total joint replacement and a joint with osteoarthritis SF, the model fluids are attached chemically to the Co-Cr-Mo surface through proteins rather than HA.

- Vibrational traces of α-helix structure are found on the surface of Co-Cr-Mo, which favours albumin as a binding protein.

- Model SFs emulating osteoarthritic joint and joint after replacement are chemically more adsorbable to Co-Cr-Mo surface than SF imitating a healthy joint; the film formed using these two SF types is distinctly visible in the microscope.

- The coefficient of friction with Co-Cr-Mo ball and polyethylene cup showed for all the model fluids higher value then in the case of protein and HA separately. The lowest coefficient of friction was obtained for HA.

- The coefficient of friction for model fluids, proteins or HA could not be significantly correlated with chemical changes of Co-Cr-Mo.

In summary, utilization of various model fluids within ball-on-cup configuration provided clear information about chemistry of the lubricant film formation. Furthermore, the used methodology enables to observe chemical reactions of specific components of SF with implant material. Thus, this procedure can be exploited to determine the chemical changes within artificial hip implants to introduce improved implant materials.

16

Reference

1. Navarro, M., Michiardi, A., Castano, O., et al.: 'Biomaterials in orthopaedics', Journal of the royal society interface, 2008, 5, (27), pp 1137-58

2. Wimmer, M. A., Laurent, M.P., Mathew, M.T., et al.: 'The effect of contact load on CoCrMo wear and the formation and retention of tribofilms', Wear, 2015, 332, pp 643-649

3. Yan, Y., Neville, A., Dowson, D., 'Biotribocorrosion of CoCrMo orthopaedic implant materials—assessing the formation and effect of the biofilm', Tribology international, 2007, 40, (10-12), pp 1492-1499

4. Nečas, D., Sawae, Y., Fujisawa, T., et al.: 'The influence of proteins and speed on friction and adsorption of metal/UHMWPE contact pair', Biotribology, 2017, 11, pp 51-59

5. Choudhury, D., Rebenda, D., Sasaki, S., et al.: 'Enhanced lubricant film formation through micro-dimpled hard-on-hard artificial hip joint: An in-situ observation of dimple shape effects', Journal of the mechanical behavior of biomedical materials, 2018, 81, pp 120-129

6. Parkes, M., Myant, C., Cann, P. M., et al.: 'Synovial fluid lubrication: The effect of protein interactions on adsorbed and lubricating films', Biotribology, 2015, 1, pp 51-60

7. Parkes, M., Myant, C., Cann, P. M., et al.: 'The effect of buffer solution choice on protein adsorption and lubrication', Tribology International, 2014, 72, pp 108-117

8. Sun, D., Wharton, J. A., Wood, R. J., et al.: 'Microabrasion–corrosion of cast CoCrMo alloy in simulated body fluids', Tribology International, 2009, 42, (1), pp 99-110.

9. Milošev, I., Strehblow, H. H.: 'The composition of the surface passive film formed on CoCrMo alloy in simulated physiological solution', Electrochimica Acta., 2003, 48, (19), pp 2767-2774.

10. Dorner-Reisel, A., Schürer, C., Irmer, G., et al.: 'Electrochemical corrosion behaviour of uncoated and DLC coated medical grade Co28Cr6Mo', Surface and Coatings Technology, 2004, 177, pp 830-837

11. Fan, J., Myant, C., Underwood, R., et al.: 'Synovial fluid lubrication of artificial joints: protein film formation and composition', Faraday discussions, 2012, 156, (1), pp 69-85

12. Duong, C. T., Lee, J. H., Cho, Y., et al.: 'Effect of protein concentrations of bovine serum albumin and γ-globulin on the frictional response of a cobalt-chromium femoral head', Journal of Materials Science: Materials in Medicine, 2012, 23, (5), pp 1323-1330

13. Park, J.B., Duong, C. T., Chang, H. G., et al.: 'Role of hyaluronic acid and phospholipid in the lubrication of a cobalt–chromium head for total hip arthroplasty', Biointerphases, 2014, 9, (3), pp 031007

14. Schmidt, T. A., Gastelum, N. S., Nguyen, Q. T., et al.: 'Boundary lubrication of articular cartilage: role of synovial fluid constituents', Arthritis & Rheumatism, 2007, 56, (3), pp 882-891

15. Greene, G. W., Banquy, X., Lee, D. W., et al.: 'Adaptive mechanically controlled lubrication mechanism found in articular joints', Proceedings of the National Academy of Sciences, 2011, 108, (13), pp 5255-5259.

16. Nakashima, K., Sawae, Y., Murakami, T., et al.: 'Behavior of adsorbed albumin film on CoCrMo alloy under in-situ observation', Tribology Online, 2015, 10, (2), pp 183-189

17. Zhang, Z., Barman, S., Christopher, G. F.: 'The role of protein content on the steady and oscillatory shear rheology of model synovial fluids' Soft matter, 2014, 10, (32), pp 5965-5973

18. Stevenson, H., Parkes, M., Austin, L., et al.: 'The development of a small-scale wear test for CoCrMo specimens with human synovial fluid', Biotribology, 2018, 14, pp 1-10

19. Stevenson, H., Jaggard, M., Akhbari, P., et al.: 'The role of denatured synovial fluid proteins in the lubrication of artificial joints', Biotribology, 2019, 17, pp 49-63

20. Nečas, D., Vrbka, M., Rebenda, D., et al.: 'In situ observation of lubricant film formation in THR considering real conformity: The effect of model synovial fluid composition', Tribology International, 2018, 117, pp 206-216

21. Nečas, D., Vrbka, M., Urban, F., et al.: 'In situ observation of lubricant film formation in THR considering real conformity: The effect of diameter, clearance and material', Journal of the Mechanical Behavior of Biomedical Materials, 2017, 69, pp 66-74

22. Nečas, D., Vrbka, M., Křupka, I., et al.: The effect of kinematic conditions and synovial fluid composition on the frictional behaviour of materials for artificial joints, Materials, 2018,11, (5), pp 767

23. Kerns, J. G., Gikas, P. D., Buckley, K., et al.: 'Evidence from Raman spectroscopy of a putative link between inherent bone matrix chemistry and degenerative joint disease', Arthritis & Rheumatology, 2014, 66, (5), pp 1237-1246

24. Esmonde-White, K. A., Mandair, G. S., Raaii, F., et al.: 'Raman spectroscopy of synovial fluid as a tool for diagnosing osteoarthritis', Journal of biomedical optics, 2009, 14, (3), pp 034013

25. Galandáková, A., Ulrichová, J., Langová, K., et al.: 'Characteristics of synovial fluid required for optimization of lubrication fluid for biotribological experiments', Journal of Biomedical Materials Research Part B: Applied Biomaterials, 2017, 105, (6), pp 1422-1431

26. Rufaqua, R., Vrbka, M., Choudhury, D., et al.: 'A systematic review on correlation between biochemical and mechanical processes of lubricant film formation in joint replacement of the last 10 years', Lubrication Science, 2019, 31, (3), pp 85-101

27. Vrbka, M., Nečas, D., Hartl, M., et al.: 'Visualization of lubricating films between artificial head and cup with respect to real geometry', Biotribology, 2015, 1, pp 61-65

28. Choudhury, D., Urban, F., Vrbka, M., et al.: 'A novel tribological study on DLC-coated micro-dimpled orthopedics implant interface', Journal of the mechanical behavior of biomedical materials, 2015, 45, pp 121-131

29. Nečas, D., Usami, H., Niimi, T., et al.: 'Running-in friction of hip joint replacements can be significantly reduced: The effect of surface-textured acetabular cup', Friction, 2020, pp 1-6

30. Furmann, D., Nečas, D., Rebenda, D., et al.: 'The Effect of Synovial Fluid Composition, Speed and Load on Frictional Behaviour of Articular Cartilage', Materials, 2020, 13, (6), pp 1334

31. Papež, N., Sobola, D., Škvarenina, Ľ., et al.: 'Degradation analysis of GaAs solar cells at thermal stress', Applied Surface Science, 2018, 461, pp 212-220

32. Diem, M.: 'Modern vibrational spectroscopy and micro-spectroscopy: theory, instrumentation and biomedical applications' (John Wiley & Sons, 2015), pp. 204-219

33. Lin-Vien, D., Colthup, N. B., Fateley, W. G., and Grasselli, J. G., 'The handbook of infrared and Raman characteristic frequencies of organic molecules' (Elsevier, 1991)

34. Essendoubi, M., Gobinet, C., Reynaud, R., et al.: 'Human skin penetration of hyaluronic acid of different molecular weights as probed by Raman spectroscopy', Skin Research and Technology, 2016, 22, (1), pp 55-62

35. Chourpa, I., Ducel, V., Richard, J., et al.: 'Conformational modifications of α gliadin and globulin proteins upon complex coacervates formation with gum arabic as studied by Raman microspectroscopy', Biomacromolecules, 2006, 7, (9), pp 2616-2623

36. Kotzianová, A., Řebíček, J., Pokorný, M., et al.: 'Raman spectroscopy analysis of biodegradable electrospun nanofibers prepared from polymer blends', Monatshefte für Chemie-Chemical Monthly, 2016, 147, (5), pp 919-923

37. Liao, Y., Hoffman, E., Wimmer, M., et al.: 'CoCrMo metal-on-metal hip replacements', Physical Chemistry Chemical Physics, 2013, 15, (3), pp 746-756

38. Radice, S., Yao, J., Babauta, J., et al.: 'The effect of hyaluronic acid on the corrosion of an orthopedic CoCrMo-alloy in simulated inflammatory conditions', Materialia, 2019, 6, pp 100348

39. Kerwell, S., Baer, D., Martin, E., Liao Y, et al.: 'Electrochemically Induced Film Formation on CoCrMo Alloy for Hip Implant Application', Journal of Bio-and Tribo-Corrosion, 2017, 3, (1), pp 4

40. Rebenda, D., Vrbka, M., Čípek, P., et al.: 'On the Dependence of Rheology of Hyaluronic Acid Solutions and Frictional Behavior of Articular Cartilage', Materials, 2020, 13, (11), pp 2659

Analysis of chemisorbed tribo-film for ceramic-on-ceramic hip joint prostheses by Raman spectroscopy

Risha Rufaqua[1*], Martin Vrbka[1], Dušan Hemzal[2], Dipankar Choudhury[3], David Rebenda[1], Ivan Křupka[1], Martin Hartl[1]

[1]Faculty of Mechanical Engineering, Brno University of Technology, Technická 2896/2, 616 69, Brno, Czech Republic.
[2]Department of Condensed Matter Physics, Faculty of Science, Masaryk University, Kotlářská 2, 611 37, Brno, Czech Republic.
[3]Nano Mechanics and Tribology Laboratory, Department of Mechanical Engineering, University of Arkansas, Fayetteville, Arkansas, USA.
*Corresponding author. Tel.: +420541143238; Email: Risha.Rufaqua@vut.cz

Abstract: Biochemical reactions of the synovial fluid and the corresponding frictional coefficients were studied to understand the possible lubricant mechanism in ceramic-on-ceramic hip joint prosthessess. The experiments were performed in a hip joint simulator with the ball-on-cup configuration. The balls and the cups were made from two types of ceramics, BIOLOX®forte and BIOLOX®delta. Different lubricants such as albumin, γ-globulin, hyaluronic acid, and three model synovial fluids were used in the experiments. Raman spectroscopy was used to analyze the biochemical responses of the lubricants at the interface. BIOLOX®delta surface was found less reactive to proteins and model fluid lubricants. In contrast, BIOLOX®forte ball surface has shown chemisorption with both proteins, hyaluronic acid and model fluids, thus imitating total joint replacement and osteoarthritic joint. There was no direct correlation between the measured frictional coefficient and the observed chemical reactions.

Keywords
synovial fluid, film formation, Raman spectroscopy, bio-tribology, tribo-chemistry.

1. Introduction

A healthy synovial joint is essential for a comfortable and active function of the natural musculoskeletal system [1]. Skeletal organs are consisting of multiple tissues and structures, these structures allow synovial joints for smooth movement [2]. In the same time, millions of people in the whole world suffer from bone and joint degenerative and inflammatory problems - about half of all chronic diseases in population over 50 years of age in the developed countries is due to bone diseases [3].

To improve life quality of these patients, hip joint arthroplasty is an available surgery, proficient to significant extent [4]. It is a safe process for medicating severe degenerative, post-traumatic and end-stage diseases of the hip joint [5]. Consequently, elements from orthopaedic biomaterials are implanted through the surgeries within the human body. These elements are designed to execute specific biological functions by altering and deflecting different tissues (such as bones, cartilage or ligaments and tendons), also pursuing bone repairment when required [3]. Substantial service-life of the implants is requisite to repeal their failure [6]. To this end, aseptic loosening accompanied by osteolysis is considered the primary reason for defection of total hip arthroplasty, causing instability and infection [5].

1

Ceramic on ceramic bearings for implants were introduced more than four decades ago. Since then, three generations of Biolox ceramics were explored with progression in density, grain size and purity. In result, current alumina ceramic (introduced as BIOLOX®forte) and zirconia toughened alumina ceramic (BIOLOX®delta) can both be exposed to wider range of residual stress upon wear compared to the first generation of Biolox. In addition, Raman experiments demonstrate compositional enhancement of BIOLOX®delta [7]. It is also proclaimed that model synovial fluids (SF) produce thicker adsorbed films on alumina ceramic than on zirconia toughened alumina ceramic [8].

As an advancement of ceramic-on-ceramic couplings in total hip arthroplasty, alumina-zirconia composite was introduced to the market in 2000 [9]. The zirconia-toughened alumina (ZTA) phase transformation has been observed by fluorescence piezo-spectroscopy and X-ray diffraction. Subject to residual stress state, the tetragonal zirconia (t-zirconia) transforms to monoclinic zirconia (m-zirconia), where monoclinic content and the residual stress found linearly correlated. This transformation is influenced in different stages of processing, thus increasing its tensile stress [10].

It is validated that under hydrothermal conditions the transformation occurs as well. Comparing monoclinic content and surface roughness of the retrieved heads with wear testing in a hip simulator, it is observed that worn areas of the retrieved heads show higher surface roughness than heads that have undergone hip simulation [11].

The wear was confirmed as the main reason for the in vivo tetragonal-to-monoclinic transformation in zirconia. Micro-Raman mapping of the fractured articulating surface found the tetragonal-to-monoclinic transformation involved extensively within the region [9]. Observed Vm (volume fraction) monoclinic zirconia content was higher near center of the articulating surface and in the metal transfer area compared to the border control area of the retrievals. Different thicknesses of the transformation were found in other samples through Vm depth-profiling analyses [12].

The stress-induced tetragonal-to-monoclinic polymorphic transformation of zirconia results in high flexural strength and fracture toughness. These features occur because of the microscopic crack-tip shielding mechanism of ZTA [13]. Therefore, to investigate the changes in material properties of BIOLOX®delta femoral heads, Raman spectroscopy proves an effective technique [9, 11-13].

Within the contact of a hip replacement, lubrication mechanisms and film formation depend on the composition of SF. Eventually, the SF composition affects tribological performance of the contact couple, thus impairing the service-life of the implant [8]. Synovium, cartilage, ligament and meniscus are the tissues, that produce proteins of SFs within an articulating joint [14]. Chemical variations occurring within the synovial joint environment in result of injury or disease were predicted to modify its lubricant concentration [15].

Natural SF contains proteins (albumin and γ-globulin) as lubricants. In albumin, the α-helix structure is present to large extent, whereas β-sheet structure prevails in γ-globulin. The boundary film is affected by change of the protein lubricants - a lubricant containing albumin provides lower friction than lubricant comprising only γ-globulin [16].

2

On the other hand, the major hydrodynamic nonprotein component of joint SF is Hyaluronan or hyaluronic acid (HA). High concentration of HA in SF is essential for normal joint function; HA provides necessary lubrication for the joint and serves as a shock absorber, reducing friction of the moving bones and diminishing wear of the joint. The viscous and elastic properties both depend on size, interactions and concentration of HA molecules in the fluid. Furthermore, the molecular weight of HA is significantly related to its rheological properties. Due to the existence of several acid and hydroxyl groups in the molecule, HA can be chemically modified. Under specific conditions, an acid-protein complex forms a protective gel of concentrated fluid compressed between the cartilage surfaces. Under inflammatory conditions of arthritic diseases (such as osteoarthritis or rheumatoid arthritis), high molar mass HA is degraded by reactive oxygen species, though in the case of OA patients, the percentage of proteins increases. In result, the viscosity of SF is reduced together with HA lubricant and shock absorbing properties, leading to deteriorated joint movement and pain. [17-23].

Another substantial component of human SF, besides serum albumin, γ-globulin, and HA are the phospholipids, which can have a considerable effect on the friction and wear properties of the joints [24]. The largely saturated phospholipids content is present in a typical joint; hence it is more surface-active [25]. The presence of phospholipids also directly affects the structure of the proteins and their function [26].

The detected concentration of HA and phospholipids in normal human SF is similar to optimal concentration of HA and DPPC (dipalmitoyl phosphatidylcholine) needed for sufficient lubrication [27]. Within replaced joints, lower hydrophobicity of articular surfaces is found than in the normal joint, which exposes insufficiency of the surface-active phospholipids. High contact angle is observed in recovered prosthetic knees at revision, defining the adsorption of the recovered surface-active phospholipids [25].

On the contrary, improved lubrication conditions are obtained by adding phospholipids to the γ-globulin based fluid. A combined effect of HA and phospholipids caused more accrued lubricant film in the case of a complex fluid [28].

The significance of lubrication lies in minimizing friction between the surface of the joint. In the case of boundary lubrication, friction force depends on the properties of the thin-film formed on the surface of the solids, often biased by additives introduced into the lubricants. Dowson et al. [29] mention HA as an additive of SFs.

SF components influence essentially the coefficient of friction within the synovial joint, both before and after joint replacement. A comprehensive comparison of frictional behaviour of articular cartilage was conducted considering the speed and load by Denis et al., contemplating the effect of SF composition [30]. It was stated that no variations in the friction coefficient are displayed by protein-based solutions, while adding HA and phospholipids induced its change. It is also concluded that with γ-globulin the friction coefficient decreased noticeably.

From the above studies, it is suggested that correlation between biochemical and mechanical processes during lubrication film formation within hip joint replacement on both types of ceramic implants should be considered and studied. Containing an average total protein concentration of 34 g/L, human SF is considerably different from calf serum [31]. Also, to acquire in vivo conditions,

the impact of protein lubricants, including phospholipids and HA on friction and wear, should be studied [32].

Model fluids of different synovial composition could be an appropriate selection to elaborate the present situation of joint replacements with implants of various materials. Raman spectroscopy-based detection methods surpass conventional analyzes in terms of sensitivity, selectivity, and stability. Thus, Raman spectroscopy could provide practical bio diagnostics under presence of protein interaction [33]. Alumina ceramic implants were analyzed previously by this procedure several times. Hence, Raman Spectroscopy could be the most suitable technique to explain the function of the fluids and the ceramic implant material performance [9, 11-13].

However, the SF components' chemical structural changes with ceramic implants after the joint replacement are rarely addressed and require further attention. For proper understanding of the condition of joint replacement and further improvement of its durability, it is high time to detect the chemical changes of SF. Raman spectroscopy is a unique technique to explain the biochemical behaviour of the materials used in joint replacement. The resulting chemical analysis, including the study of mechanical and biological properties of the SF of joint replacement, will improve the concept of the whole process [34].

2. Materials and methods

In the experiment the ball and cup sets were made from two types of ceramics. Alumina ceramic ball used was BIOLOX®forte from Zimmer-sulox (28 mm), and the cup of the same material was used from Smith and nephew. The other set of ball and cup had zirconia-toughened alumina ceramic BIOLOX®delta (28 mm) ball, and the cup was also made from the same material. In this set, both ball and cup were received from Zimmer.

The artificial hip joint simulator has a base frame with acetabular cup and swinging pendulum with femoral head. The pendulum is driven with an electronic motor, which enables the machine to maintain continuous motion in the flexion-extension plane. The simulator is imitating artificial hip joint conditions, including real geometry, body temperature and load. It is also capable of measuring real-time velocity profile, average friction coefficients and viscous effect. This mechanism was utilized to visualize lubricating films between artificial head and cup in real geometry and to understand the effect of diameter, clearance, and material during in situ observation of lubricant film formation. [35, 36]. The pendulum hip joint simulator was also used to assess the coefficient of friction to evaluate the impact of surface texturing of ultra-high molecular weight polyethylene acetabular cup [37].

4
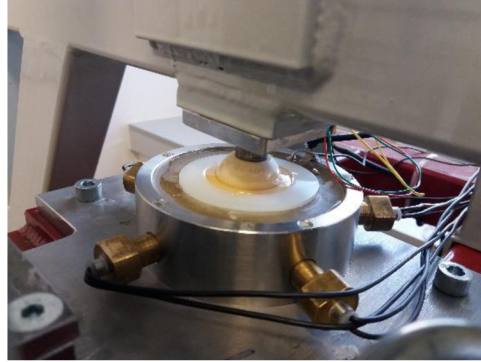
(**a**)
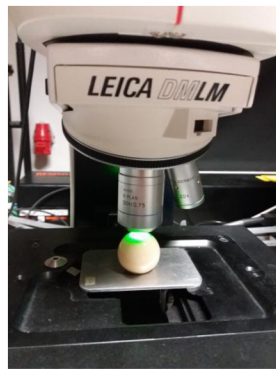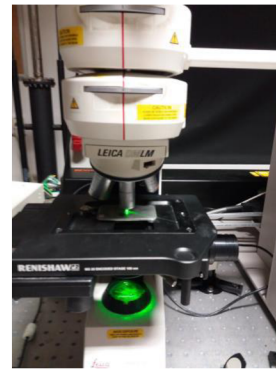
(**b**)   (**c**)

Figure 1. (a) Coefficient of friction measurement in the pendulum hip joint simulator (b) Raman spectroscopic measurement of the ceramic ball (c) Raman spectroscopic measurement of the lubricant in capillary.

The cup is fixed within a stainless-steel pot using resin, the base frame is holding this set up. A rotating arm is linked to the head using a cone. The pendulum arm is pulled from equilibrium position to primary deflection and released. The spontaneous swinging between the ball and cup is then damped due to friction. An angular velocity sensor calculates the rapid deflection of the pendulum. In result, the friction coefficient is acquired from the processed signal. A linear model of damping is applied to assess the coefficient of friction [37]. The described instrumental setup allows to determine the chemical reactions between the ceramic ball surface and SF, along with the frictional coefficient.

Due to the difference in content, fluid characteristics and nonhuman origin, use of Bovine Serum to simulate joint replacement has been reprehended recently. To achieve more accurate lubrication that mimicks human SF, three types of model SFs were used [24]. Using PBS, albumin, γ-globulin and HA solutions were produced as separate lubricants. For model SFs, PBS was used followed by addition of albumin, γ-globulin, HA and phospholipids. The components were dissolved in PBS overnight at 4 ℃ using laboratory rocker-shaker (MR-12, Biosan, Riga, Latvia). After that, each of the individual constituent solutions was mixed into one solution in order albumin, γ-globulin, HA, phospholipids. The specific products of the components used were Bovine serum albumin

(powder, $\geq$96%; A2153, Sigma-Aldrich, St. Louis, MO, USA), γ-globulin from bovine blood (powder, $\geq$99%; G5009, Sigma-Aldrich, St. Louis, MO, USA), HA = Sodium Hyaluronate HySilk (powder, quality class—cosmetic; molecular weight = 820–1020 kDa, Contipro, Dolní Dobrouč, Czech Republic), and phospholipids = L-α-Phosphatidylcholine (powder, Type XVI-E, lyophilized powder; $\geq$99%; vesicles form; P3556, Sigma-Aldrich, St. Louis, MO, USA). Lubricant solutions were preserved at -22 °C after preparation. The types of prepared model SF represent healthy (or, physiologic) total joint replacement and osteoarthritic SF concentrations [24, 30]. The concentration and combination of each of the lubricants used are described in table 1.

Table 1. Composition and concentration of the applied test lubricants.

Test Fluid	Albumin (mg/ml)	γ-globulin (mg/ml)	Hyaluronic Acid (mg/ml)	Phospholipids (mg/ml)
Albumin	28	-	-	-
γ-globulin	-	11	-	-
Hyaluronic Acid (HA)	-	-	2	-
Healthy Joint (SF1)	20	3.6	2.5	0.15
After Total Joint Replacement (SF2)	26.3	8.2	0.87	0.35
Joint with Osteoarthritis (SF3)	24.9	6.1	1.49	0.34

The pendulum hip joint simulator experiment time was set up to 5-6 minutes to observe the tribological effect of each of the lubricants and obtain its chemical impact on the ball surface. The temperature was controlled at 37 °C and weight 15 kg was weight was used on the simulator during all experiments. After the tribological test, lubricants were collected from the cup for analysis.

Raman spectroscopy was found useful for obtaining the changes of lubricants within the simulator. We used this methodology in our previous work [34] to explain the chemical reactions occurring within the artificial joint replacement. To acquire fingerprints of various lubricants before and after tribological experiments in the simulator, inVia Raman spectrometer by Renishaw was employed for analysis of the ball surfaces and lubricants using 532 nm excitation. To obtain Raman data of ceramic balls, 1 mW laser power was used on the surfaces with exposing time of 100 s. To observe the chemical structural changes of the lubricants before and after tribological tests, 100 mW laser power and 20 s exposition were applied. Due to the tribological process, differences in the chemical properties of the ball surfaces were observed.

6

3. Results

Raman fingerprints of BIOLOX®delta and BIOLOX®forte hip implants after tribological test with albumin and γ-globulin are shown in Figure 2.
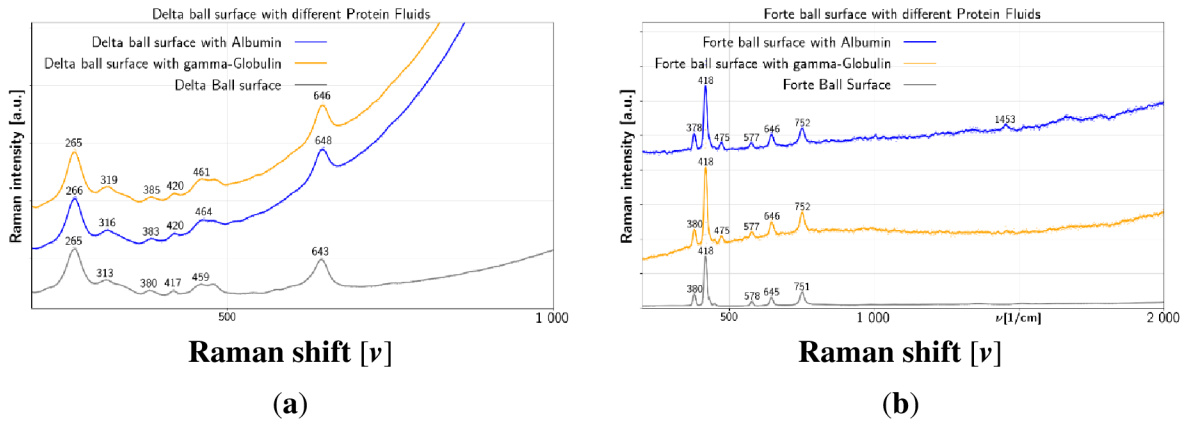

Figure 2. After-test Raman spectra of albumin and γ-globulin on (a) BIOLOX®delta and (b) BIOLOX®forte ball in comparison to clean balls.

Concerning BIOLOX®delta ball surface, a prominent peak at 265 cm^{-1} is observed in Figure 2(a) both before and after tribological tests with albumin and γ-globulin. The second prominent peak of the clean BIOLOX®delta ball surface at 643 cm^{-1} shifts to 648 cm^{-1} after test with albumin and to 646 cm^{-1} after test with γ-globulin. Peaks at 313 cm^{-1}, 380 cm^{-1}, 417 cm^{-1} and 459 cm^{-1} are also visible in the spectrum of a clean BIOLOX®delta ball surface. These peaks shift to 316 cm^{-1}, 383 cm^{-1}, 420 cm^{-1} and 464 cm^{-1}, respectively, after test with albumin and to 319 cm^{-1}, 385 cm^{-1}, 420 cm^{-1} and 461 cm^{-1}, respectively, after test with γ-globulin.

In Figure 2(b), the prominent peak of clean BIOLOX®forte surface at 418 cm^{-1} is unaffected by the tests. Similarly, the other peaks of the BIOLOX®forte surface at 380 cm^{-1}, 578 cm^{-1}, 645 cm^{-1} and 751 cm^{-1} show negligible shifts due to tests with albumin and γ-globulin. On the contrary, the peak at 475 cm^{-1} is visible on the BIOLOX®forte surface only after tests with albumin and γ-globulin. In addition, a small peak appears at 1453 cm^{-1} after test with albumin.
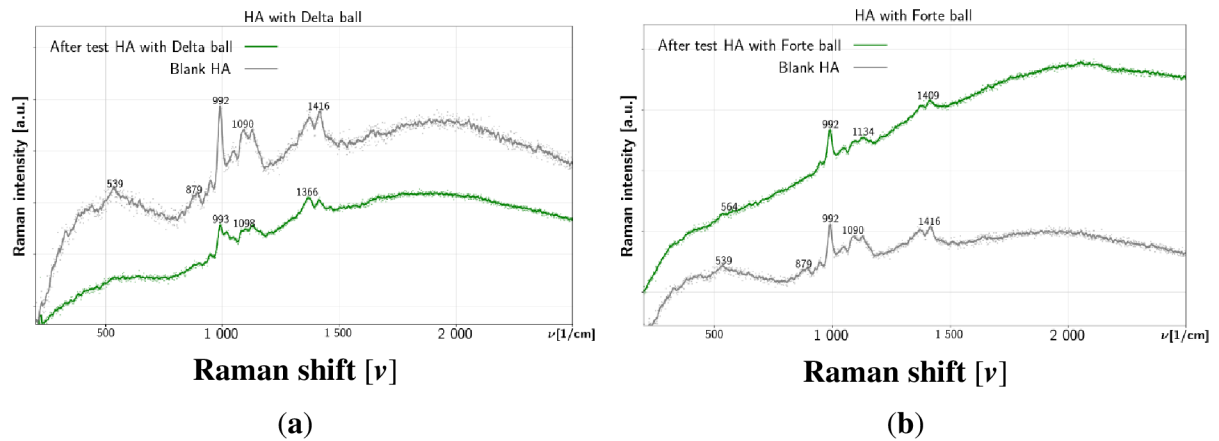
7

Figure 3. Raman spectra of HA liquid before and after test with (a) BIOLOX®delta and (b) BIOLOX®forte ball.

Figure 3 summarizes results of tribological tests for liquid HA. Without test, HA is showing the main peak at 992 cm^{-1} and two double peaks, near 1100 cm^{-1} and near 1400 cm^{-1}. Additionally, two small HA peaks are found before test at 539 cm^{-1} and 879 cm^{-1}. In Figure 3(a) of after-test spectra with BIOLOX®delta most HA liquid peaks are diminished, the exception being the two HA double peaks, and a weaker peak appeared in 993 cm^{-1}. In contrast, after test spectra with BIOLOX®forte in Figure 3(b) preserve the prominent HA liquid peak at 992 cm^{-1} together with most other peaks, the exception being the 879 cm^{-1} peak, which is removed. In particular, the weak HA liquid peak at 539 cm^{-1} before test shifts to 564 cm^{-1} after test with BIOLOX®forte.
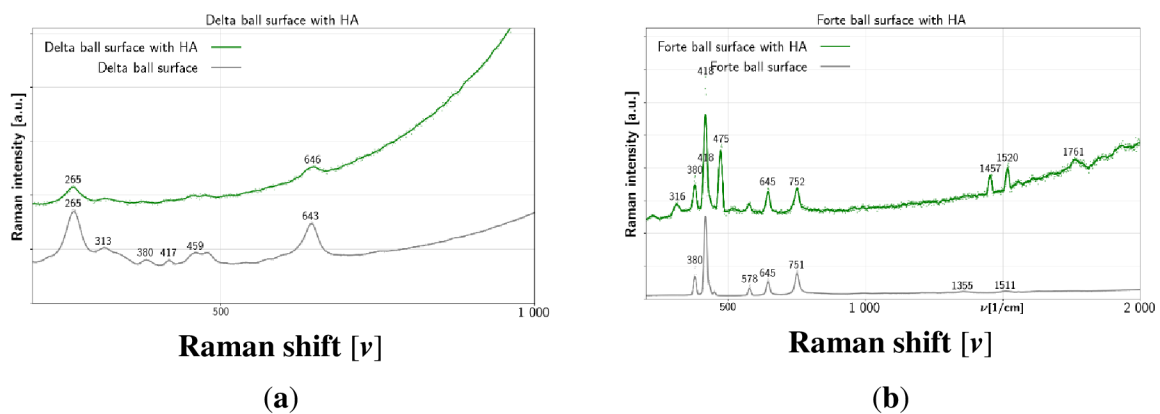

Figure 4. Raman spectra of ceramic surface after test with HA: (a) HA on BIOLOX®delta, (b) HA on BIOLOX®forte.

Figure 4 summarizes changes on the surface of balls after tests with HA. In Figure 4(a), the prominent BIOLOX®delta ball surface peak at 265 cm^{-1} is unaffected by the test with HA. The second prominent peak at 643 cm^{-1} before test is shifted to 646 cm^{-1} after test with HA. The remaining BIOLOX®delta ball surface peaks at 313 cm^{-1}, 380 cm^{-1}, 417 cm^{-1} and 459 cm^{-1} are mostly unaffected by the test with HA. In Figure 4(b) all main peaks of the BIOLOX®forte surface are preserved after test with HA. In addition, there are several new after-test peaks with

8

BIOLOX®forte: a strong peak at 475 cm^{-1}, two peaks near 1500 cm^{-1} and two shoulders, at 316 cm^{-1} and at 1761 cm^{-1}.
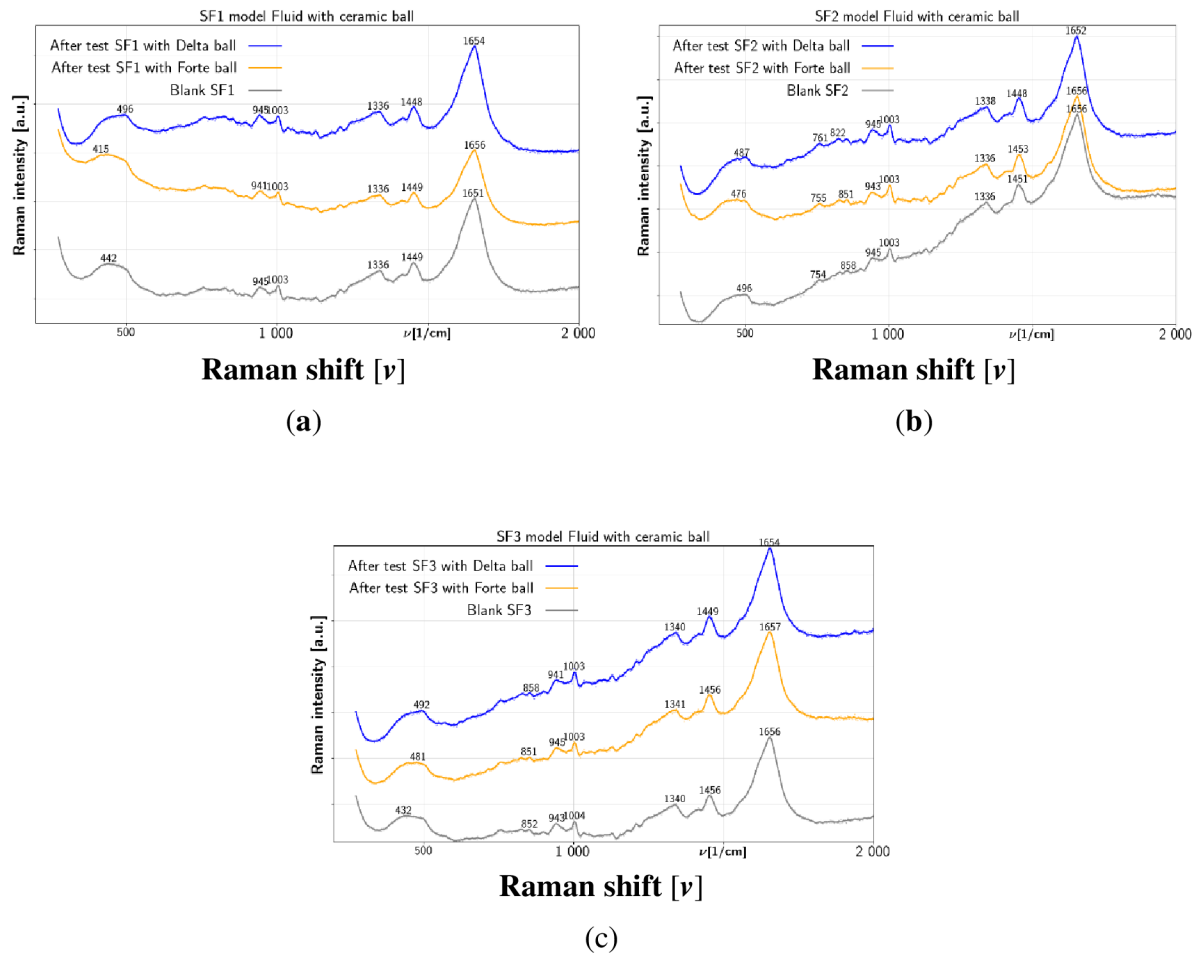

(a)

(b)

(c)

Figure 5. Liquid Raman spectra of model SFs before and after test: (a) SF1 with BIOLOX®delta and BIOLOX®forte (b) SF2 with BIOLOX®delta and BIOLOX®forte (c) SF3 with BIOLOX®delta and BIOLOX®forte.

Figure 5 summarizes changes in model fluids SF1, SF2 and SF3 after tests with both types of ceramic balls. Apart from water peak at 1654 cm^{-1}, the SF1 fluid shows in Figure 5(a) the before-test peaks at 1336 cm^{-1} and 1449 cm^{-1}, together with smaller peaks at 945 cm^{-1} and 1003 cm^{-1}, and a shoulder near 450 cm^{-1}. All these peaks remain mostly unaffected by tests with ceramic balls.

Similar to SF1, the before-test peaks of SF2 are shown in Figure 5(b) at 1336 cm^{-1}, 1451 cm^{-1}, 945 cm^{-1} and 1003 cm^{-1}, including the shoulder near 450 cm^{-1}. In addition, a small peak at 754 cm^{-1} and a double peak near 835 cm^{-1} are visible for SF2 before test. Although the peaks at 945 cm^{-1}, 1003 cm^{-1} and 1336 cm^{-1} remain mostly unaffected by the tests, the peak at 1451 cm^{-1} shifts to 1453 cm^{-1} after test with BIOLOX®forte ball, but to 1448 cm^{-1} after test with BIOLOX®delta ball. The

9

small peak at 754 cm-1 shifts to 755 cm^{-1} after test with BIOLOX®forte ball, but to 761 cm^{-1} after test with BIOLOX®delta ball.

The results shown in Figure 5 (c) for SF3 fluid are similar to the case of SF2. The main SF3 peaks before test are located at 1340 cm^{-1}, 1456 cm^{-1}, 943 cm^{-1} and 1004 cm^{-1}, including the shoulder near 450 cm^{-1} and a small peak 852 cm^{-1}. Most of these peaks remain unaffected by testing, but the 1456 cm^{-1} peak shifts to 1449 cm^{-1} after test with BIOLOX®delta ball. In addition, the peak at 943 cm^{-1} before test shifts to 945 cm^{-1} after test with BIOLOX®forte ball and to 941 cm^{-1} after test with BIOLOX®delta ball.
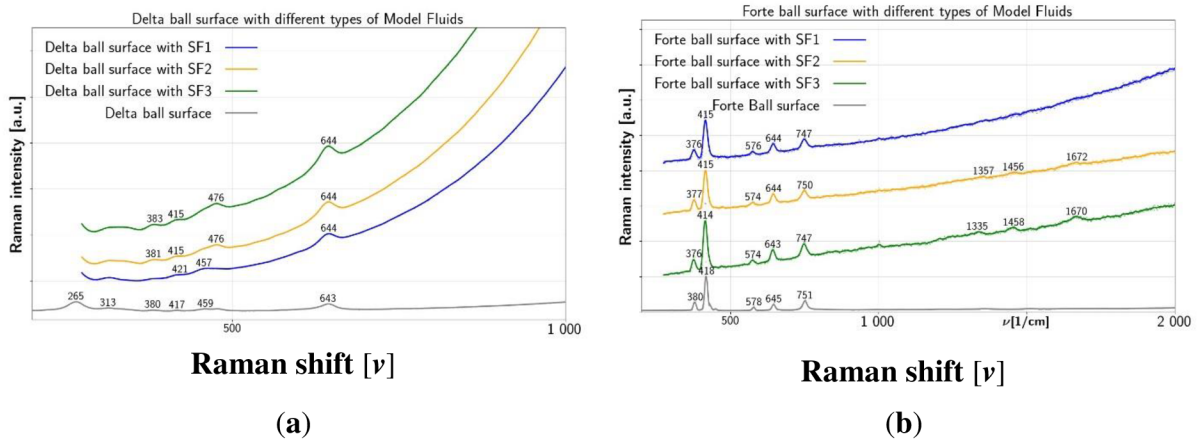

Figure 6. Comparison of Raman spectra on ceramic balls surfaces: (a) SF1, SF2 and SF3 on BIOLOX®delta (b)SF1, SF2 and SF3 on BIOLOX®forte.

Figure 6(a) is showing the BIOLOX®delta ball surface with all three model fluids SF1, SF2 and SF3. The clean BIOLOX®delta surface provides peaks at 265 cm^{-1}, 313 cm^{-1}, 380 cm^{-1}, 417 cm^{-1}, 459 cm^{-1} and 643 cm^{-1}. The peak at 380 cm^{-1} is diminished for SF1 and shifted to 381 cm^{-1} and 383 cm^{-1} for SF2 and SF3, respectively. The peak at 417 cm^{-1} is shifted to 421 cm^{-1} for SF1 while for the other two fluids it is left almost unaffected. The peak at 459 cm^{-1} shifts to 457 cm^{-1} for SF1, but to 476 cm^{-1} for SF2 and SF3.

The BIOLOX®forte ball surface with all three model fluids is shown in figure 6(b). The clean surface shows peaks at 380 cm^{-1}, 418 cm^{-1}, 578 cm^{-1}, 645 cm^{-1} and 751 cm^{-1}. The main peak at 418 cm^{-1} shifts near 415 cm^{-1} for all three fluids. The peak at 380 cm^{-1} downshifts near 376 cm^{-1} for all three fluids. The peak at 578 cm^{-1} shifts to 574 cm^{-1} for SF2 and SF3, but to 576 cm^{-1} for SF1. The peak at 751 cm^{-1} shifts to 747 cm^{-1} for SF1 and SF3, but to 750 cm^{-1} for SF2. The peak at 645 cm^{-1} seems to be almost unaffected by the fluids, but three weak peaks at 1335 cm^{-1}, 1458 cm^{-1} and 1670 cm^{-1} appeared for SF2 and at 1357 cm^{-1}, 1456 cm^{-1} and 1672 cm^{-1} for SF3.
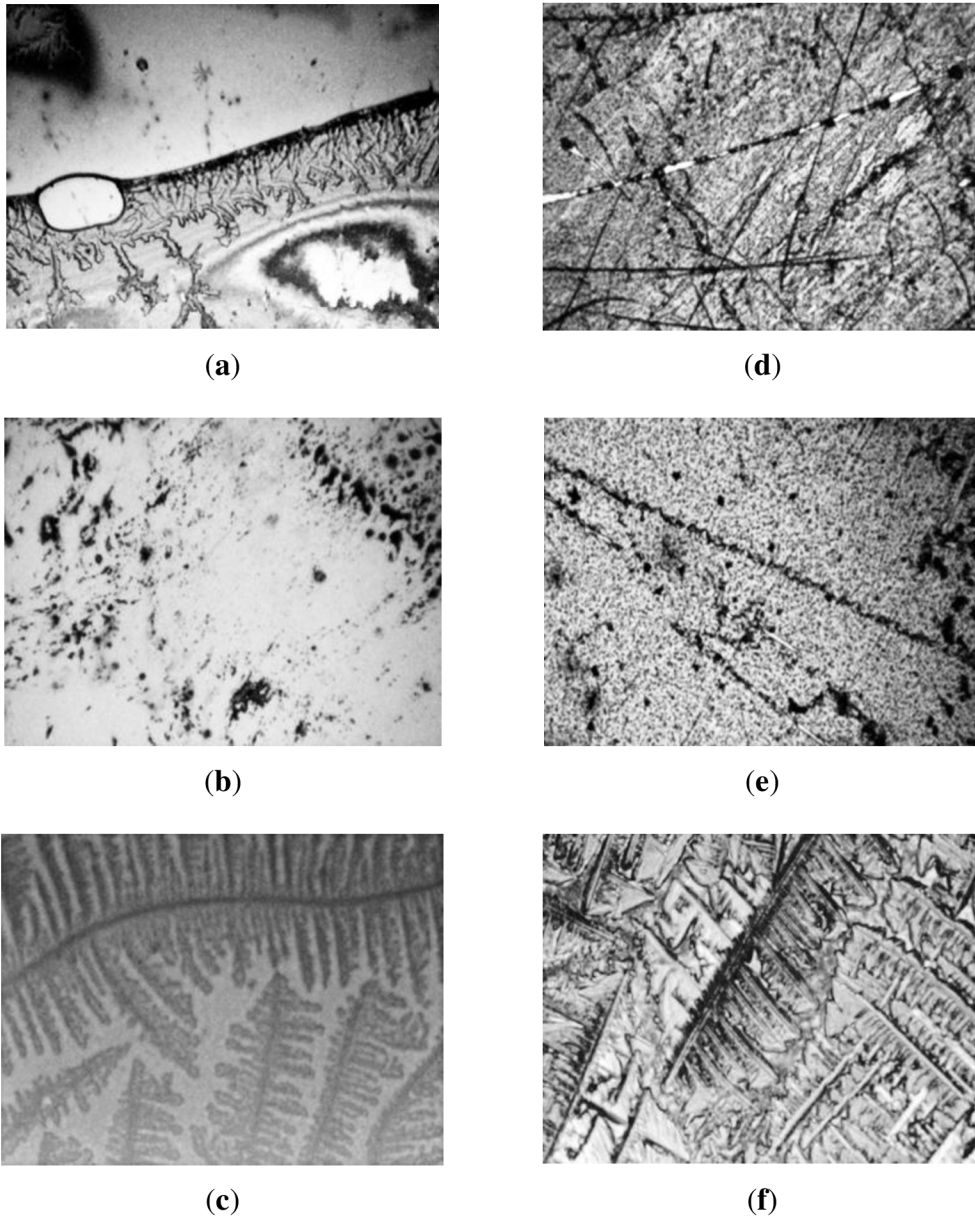
Figure 7. Optical images of ceramic ball: (a) albumin on BIOLOX®delta (b) γ-globulin on BIOLOX®delta (c) HA on BIOLOX®delta (d) albumin on BIOLOX®forte (e) γ-globulin on BIOLOX®forte (f) HA on BIOLOX®forte. The horizontal size of panels are 5 µm for (a), (b), (d) and (e), 50 µm for (c) and 20 µm for (f).

In Figure 7, optical images of the ceramic balls surface after tribological test in the simulator are shown for individual SF components. Less crystallization was observed on ceramic balls for albumin and γ-globulin than in case of metal balls, as found in our previous work [34]. In the case of albumin solution on BIOLOX®delta, a flow of the solution was observed in 7(a). The rest of the balls 7(d), 7(b) and 7(e) show crystallites of the protein molecules. In contrast, in the case 7(f) of HA on both BIOLOX®delta and BIOLOX®forte balls, a patterned film was distinguishable.
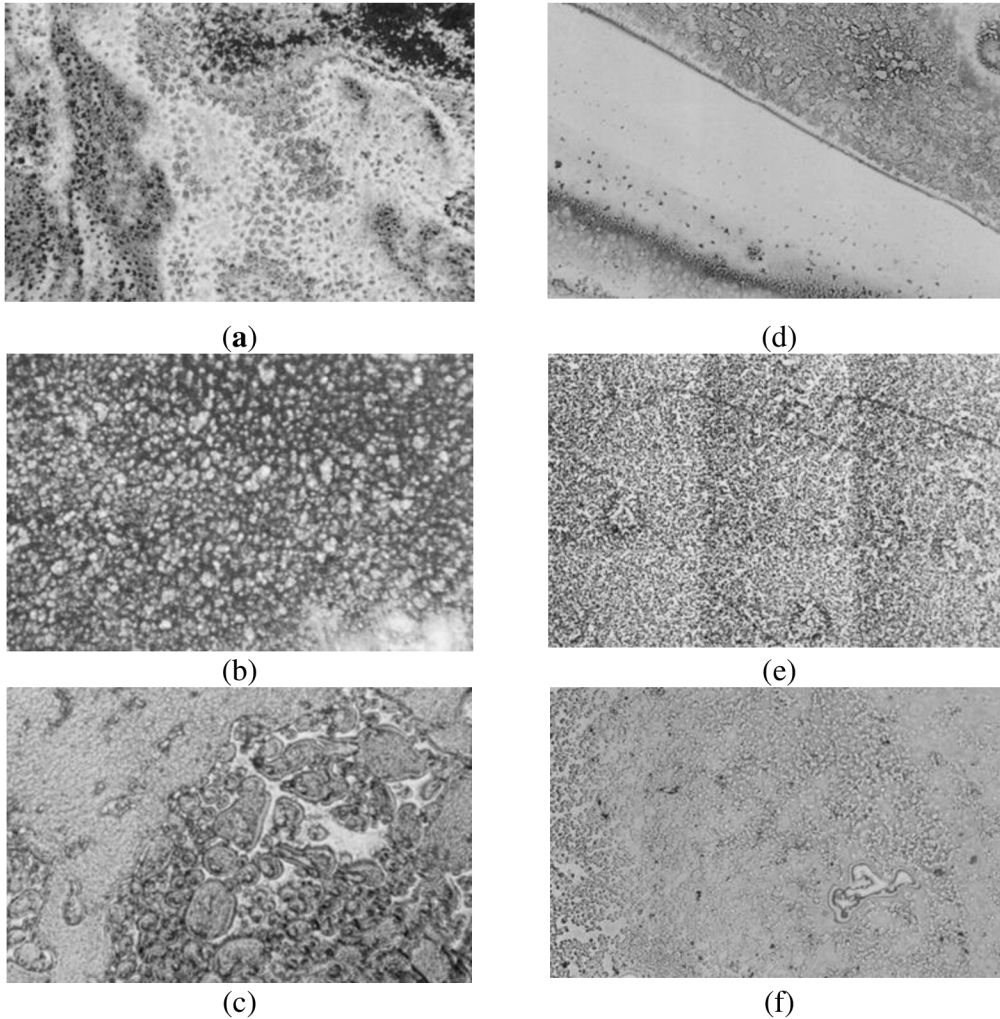
11

Figure 8. Optical images of (a) SF1 on BIOLOX®delta (b) SF2 on BIOLOX®delta (c) SF3 on BIOLOX®delta (d) SF1 on BIOLOX®forte (e) SF2 on BIOLOX®forte (f) SF3 on BIOLOX®forte. The horizontal size of panels is 5µm for (a), (b) and (c) and 20 µm for (d), (e)and (f); panels all blended across several fields of view of the microscope.

Figure 8 shows the ceramic balls surface with model SFs after the tribological test. SF1 produced on both BIOLOX®delta and BIOLOX®forte balls 8(a) and 8(d), respectively, flows of the liquid across the ball surface. But on BIOLOX®delta ball, the liquid was found almost on all surface, while on BIOLOX®forte ball, part of the surface remained almost without fluid as shown in figure 8(d). For SF2 on BIOLOX®delta and BIOLOX®forte ball surface 8(b) and 8(e), respectively, the model fluid spread on the whole surface of the balls more evenly compared to SF1. For SF3 on BIOLOX®delta ball surface 8(c), the film showed significant variation in concentration, while on the BIOLOX®forte ball surface 8(f) the same fluid was spread more consistently.
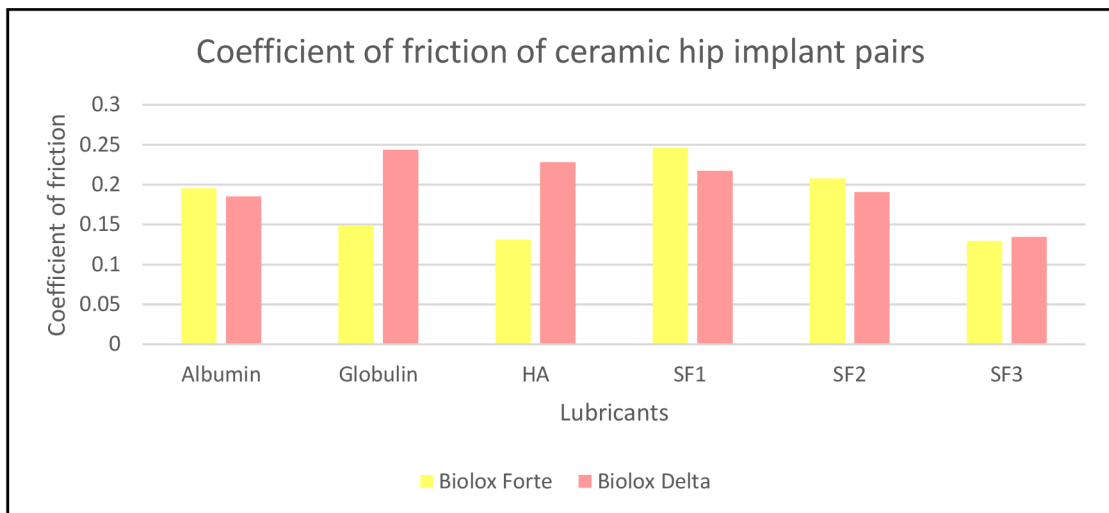
12

Figure 9. Coefficient of friction for BIOLOX®delta and BIOLOX®forte Ceramic contact pairs respectively for albumin, γ-globulin, HA and SF1, SF2 and SF3 model SFs.

Coefficient of friction was measured for both BIOLOX®delta and BIOLOX®forte ceramic ball and cup contact pairs with albumin, γ-globulin, HA and all three types of model fluids SF1, SF2 and SF3. For albumin, BIOLOX®delta provides value 0.1853 and BIOLOX®forte provides 0.1954, which are very close. On the other hand, γ-globulin results in coefficient of friction with higher variation between BIOLOX®delta and BIOLOX®forte surfaces, 0.2436 and 0.1488, respectively. Similarly, the value for HA with BIOLOX®forte ball, 0.1312, is much lower than the value 0.2282 with BIOLOX®delta. For the model fluids, values of coefficient of friction for BIOLOX®delta and BIOLOX®forte balls are much closer. For SF1 and SF2, value for BIOLOX®forte is higher than for BIOLOX®delta, just as with albumin. BIOLOX®forte shows value 0.2466 and 0.2077 for SF1 and SF2, respectively, while BIOLOX®delta shows 0.217 and 0.1908 for SF1 and SF2, respectively. For SF3 with BIOLOX®delta contact pair, a bit higher value 0.1347 is shown than the for SF3 with BIOLOX®forte, 0.1297.

4. Discussion

Due to the compositional variability of the SF, the characteristics of formed films are dependent on the amount of present proteins and other constituents. The main objective of this research is to trace the chemical conditions present within the joint replacement, while measurement of frictional coefficient may also reveal some reality.

The marker bands of tetragonal zirconia are found [9] at 265 cm^{-1}, 313 cm^{-1}, 459 cm^{-1} and 648 cm^{-1}. Therefore, these bands are visible as basic skeleton of zirconia toughened alumina components, including the BIOLOX®delta. In contrast, the 380 cm^{-1} band is attributed to the monoclinic polymorph, while band at 419 cm^{-1} is described by Taddei et al. [12] as belonging to alumina. The latter, observed here for BIOLOX®delta ball without any tribological test at 417 cm^{-1}, shifted to 420 cm^{-1} after test with both albumin and γ-globulin, which is agrrement with value 419 cm^{-1}, given by Taddei et al. Concerning optical images, the protein fluids do not show any significant changes on the BIOLOX®delta ball surface. In the microscopic view of the BIOLOX®delta surface for

13

both albumin and γ-globulin, a thin film was observed, with probably no chemical adsorption to the BIOLOX®delta surface.

The BIOLOX®forte surface exhibited before test a prominent peak at 418 cm^{-1} due to presence of alumina, this peak is also visible after tribological tests with both albumin and γ-globulin, without change of position. Other peaks recognizable for BIOLOX®forte components are found at 751 cm^{-1}, 645 cm^{-1}, 578 cm^{-1} and 380 cm^{-1} with only slight differences throughout all measurements. An exceptional peak at 1453 cm^{-1} is observed on BIOLOX®forte surface after test with albumin, providing information on CH$_2$/CH$_3$ deformation in the protein. Also, a peak at 475 cm^{-1} is visible on the BIOLOX®forte surface with albumin and γ-globulin, which is due to C-C skeletal deformation [12, 38, 39]. Both peaks are probably markers of albumin and γ-globulin chemisorption on the surface of the BIOLOX®forte ball.

The HA fluid shows several peaks before test. There is a double peak near 1366 cm-1 and 1416 cm-1, which is due to C-H bending [40] and due to C-N stretching and C-H deformation, respectively. Additionaly, there is a peak at 1090 cm^{-1} due to C-OH bending and acetyl group [40, 41]. The prominent peak at 992 cm^{-1} is due to ring breathing vibration [42] (p. 482). The 879 cm^{-1} peak is also reported in literature [40] for HA.

HA collected after the tribological test with BIOLOX®delta is showing change of the chemical structure, especially near 1000 cm^{-1}: the ring-bretahing mode at 993 cm^{-1} is altered and the C-OH bending peak shifts to 1098 cm^{-1}. In addition, the peak at 879 cm^{-1} is lost completely. In contrast, the main features of HA fluid remain mostly unchanged after test with BIOLOX®forte. The most significant change is the shift of C-N stretching peak from 1416 cm^{-1} to 1409 cm^{-1} and dissapearance of the 879 cm^{-1} band.

For the spectra of BIOLOX®delta surface after test with HA, only tetragonal zirconia peaks at 265 cm^{-1} and 646 cm^{-1} remain well resolved. The other tetragonal zirconia peaks as well the alumina peak at 417 cm^{-1} are masked by strong after-test luminescence.

Concerning the surface of BIOLOX®forte after testing with HA, luminescence was also observed, but in lesser extent and the peaks characteristic for the clean surface remain mostly unchaged, including the prominent 418 cm^{-1} alumina peak.

More importantly, a peak on the after test surface appeared at 475 cm^{-1} due to C-C skeletal deformation. This peak was also visible on the BIOLOX®forte surface after testing with albumin and γ-globulin. Further, well resolved peaks at 1457 cm^{-1}, 1520 cm^{-1} and 1761 cm^{-1} appear after test with HA on the BIOLOX®forte surface, which cannot be identified with the clean surface peaks at 1355 cm^{-1} and 1511 cm^{-1}. The peak at 1457 cm^{-1} gives information about CH$_2$/CH$_3$ deformation [42 (p. 480), 43], while the 1761 cm^{-1} peak could be due to the C=O stretch [42] (p. 479). The peak at 1520 cm^{-1} and an additional peak at 316 cm^{-1} cannot be precisely defined.

In summary, it can be assumed that chemical reaction is taking place between the ceramic balls and HA. For BIOLOX®forte, strong peak due to C-C skeletal deformation is found at 475 cm^{-1} after the test, this peak is also found for proteins on the same surface. Also, four other peaks at 316 cm^{-1}, 1457 cm^{-1}, 1520 cm^{-1} and 1761 cm^{-1} are probably due to chemical adsorption of HA on the ball. For the BIOLOX®delta ball surface, some marker bands of tetragonal zirconia disappeared

and strong luminescence was observed after the experiment with HA. As the two ceramic balls exhibit a differently patterned film in the microscopic picture for HA, it can be presumed that HA is adsorbing chemically on both balls, but different chemical structure is created by HA for the BIOLOX®forte and the BIOLOX®delta surfaces.

The model fluid SF1 has shown the smallest changes due to test with the ceramic balls. The prominent peak near 1651 cm^{-1} before test is due to water, however, its shift to 1656 cm^{-1} with BIOLOX®forte ball and to 1654 cm^{-1} with BIOLOX®delta ball suggests contribution of the α helix Amide I range (1645-1660 cm^{-1}), which could be explained by bonding of albumin [44] (p. 217). Concerning other peaks, the 1449 cm^{-1} peak is an expression of CH_2/CH_3 deformation [42 (p. 480), 43] and 1336 cm^{-1} peak comes from CH_2-CH_3 wagging [42 (p. 10), 43]. Two further peaks exhibited by all SF1 liquid spectra at 1003 cm^{-1} and 945 cm^{-1} are due to ring breathing [45] and C-C skeletal stretching α helix [45], respectively. The broad spectral feature shown in all SF1 spectra near 450 cm^{-1} could be due to C-C skeletal deformation [42] (p. 11).

The spectra of SF2 liquid shows similar properties concerning the α-helix Amide I range, but there are also more visible changes. The SF2 CH_2/CH_3 deformation shifts from 1451 cm^{-1} before test to 1448 cm^{-1} after test with BIOLOX®delta and to 1453 cm^{-1} after test with BIOLOX®forte. The SF2 before-test 1336 cm^{-1} peak due to CH_2-CH_3 wagging shifts to 1338 cm^{-1} after test with BIOLOX®delta ball and cup pair. Also, two small peaks near 750 cm^{-1} and 850 cm^{-1} can be resolved in all SF2 fluid spectra. The peak near 850 cm^{-1} could be due to symmetric C-N-C stretch in secondary amines, while the peak near 750 cm^{-1} could be due to C-C, C-O skeletal deformation [45]. In addition, this peak shifts from its before test value of 754 cm^{-1} to 755 cm^{-1} after test with BIOLOX®forte and to 761 cm^{-1} after test with BIOLOX®delta ball.

In the spectra of SF3 liquid, the before-test water peak at 1656 cm^{-1} shifts after the test with both types of ceramic balls more significantly to 1654 cm^{-1} after test with BIOLOX®delta ball and cup. Since this peak lies in the range of α-helix Amide I band, the observed shifts may be due to changes in albumin, present in the SF3. The CH_2/CH_3 deformation peak is present at 1456 cm^{-1} in the before -test liquid and, similarly to SF2, it shifts more prominently (to 1449 cm^{-1}) after test with BIOLOX®delta. The before-test values of the CH_2-CH_3 wagging peak at 1340 cm^{-1} and the ring-breathing peak at 1004 cm^{-1} remain mostly unaffected by the tests. On the other hand, the SF3 C-C skeletal stretching of α helix shifts from 943 cm^{-1} before testing to 941 cm^{-1} and 945 cm^{-1} after test with BIOLOX®delta and BIOLOX®forte ball and cup pairs, respectively. Also, the C-C skeletal stretch shifts from 852 cm^{-1} without test to 858 cm^{-1} after test with BIOLOX®delta and to 851 cm^{-1} after test with BIOLOX®forte. The broad feature near 450 cm^{-1} in all SF3 fluid spectra is probably due to C-C skeletal deformation [42] (p. 11).

The three types of model SFs conducted in the tribological tests with BIOLOX®delta and BIOLOX®forte hip implant balls mimicked the condition of a healthy joint (SF1), a total joint replacement (SF2) and an osteoarthritic joint (SF3). The distinctly smallest changes in the fluid were shown after tests by SF1, which had the lowest protein content in our study. One can thus conlude that elevated protein content is a significant factor for interaction with the ceramic balls of both types.

Concernig the ball surfaces, BIOLOX®delta showed smaller differences after tests for SFs. Thus, for the tribological test of model SFs with BIOLOX®delta, it can be assumed that there is little

reaction between proteins and the ball surface. This is in accordance with Parkes et al. [11], who state that phase transformation of the BIOLOX®delta femoral head was not triggered by wear simulated implants. On the other hand, the elevated after-test reaction of the BIOLOX®forte surface was confirmed also with individual SF protein constituents and HA.

In particular, after testing with BIOLOX®delta ball, all three model fluids on the ball surface presented characteristic spectra found also on the clean BIOLOX®delta ball, only with slight peak shifts. However, after testing with SF2 and SF3, differences were found also on the BIOLOX®delta ball surface. Althoug before-test peak at 459 cm^{-1} does not shift significantly after test with SF1, there is an apparent shift to 476 cm^{-1} after the test for both SF2 and SF3. In addition, the before-test peak at 380 cm^{-1} shifts to 381 cm^{-1} after test with SF2 and to 383 cm^{-1} after test with SF3.

More pronounced changes after tests with SFs were provided by the BIOLOX®forte balls. Most significant is the appearance of new bands near 1350 cm^{-1}, 1460 cm^{-1} and 1670 cm^{-1} after the tests with SF2 and SF3, confirming again the higher activity of these two fluid types. The 1460 cm^{-1} band lies in the region of CH$_2$/CH$_3$ deformation [42 (p. 480), 43], a peak in this range was also found on the BIOLOX®forte surface while reacting with HA. The peak near 1670 cm^{-1} may give Amide I evidence of the β-sheet structure. The peak near 1350 cm^{-1} is likely due to CH$_2$-CH$_3$ wagging.

Concerning microscopic images of model SFs, the SF1, mimicking a healthy joint, produced uneven films on both ceramic balls. In addition, some parts of the BIOLOX®forte surface are clear without any visible film. On the contrary, the SF2, mimicking a total joint replacement, produced uniform distribution of fluid components on the ceramic ball surfaces. Finally, the SF3, mimicking an osteoarthritic joint, displayed inconsistent accumulation of fluid on the balls surface in the microscopic picture. Concerning film thickness, for ceramic implants a slightly increasing tendency of adsorbing layer was shown by the model fluids. Finally, a thin layer of the film was observed [8].

The coefficient of frictions was measured for all the tribological tests conducted with BIOLOX®forte and BIOLOX®delta ball and cup contact pairs. For both pairs, albumin, γ-globulin, HA and all three model SFs were used as lubricants. With BIOLOX®delta contact pair the coefficient of friction was found higher in case of γ-globulin, HA and a bit higher in case of osteoarthritic model SF compared to BIOLOX®forte contact pair. However, the BIOLOX®forte contact pair exhibited a higher coefficient of friction in the case of albumin, model SF of healthy joint and model SF of total joint replacement. Literature shows that the friction coefficients are influenced more by the combination of materials specifically in case of ceramic-on-ceramic implants, than by the diameter of a femoral head [46].

Therefore, the coefficient of friction of both ceramic contact pairs with all these lubricants could not be correlated with chemical reaction occuring within the ceramic contact pairs with model SFs and its components.

5. Conclusions

This research aims to obtain evidence on the occurring biochemical reaction to perceive a relevant explanation of the synovial liquid film formation on ceramic balls within the joint replacement. Due to the compositional variability of the SF, the attributes of formed films are dependent on the

extent of present proteins and other constituents. The experiments were conducted within a ball-on-cup configuration in a hip joint simulator with the balls and cups made from two types of ceramics: alumina ceramic BIOLOX®forte and zirconia toughened alumina ceramic BIOLOX®delta. SF constituents such as albumin, γ-globulin, HA and three model SF fluids were considered as lubricants in the experimental set up. The results revealed from Raman analysis and frictional coefficient measurement are summarized as below:

- the BIOLOX®delta ball does not significantly react with albumin and γ-globulin. These two proteins are not adsorbed chemically on the BIOLOX®delta ball surface in physiological concentration, when used separately. On the other hand, on the BIOLOX®forte ball surface, after-test albumin and γ-globulin individual chemisorption is evidenced by Raman spectroscopy in their physiological concentration.

- HA is adsorbed chemically on both types of ceramic balls, while changing its chemical structure after the tribological test with BIOLOX®delta and BIOLOX®forte in a different way. The ceramic ball surfaces spectra also show variations after tests with HA. A patterned film formation is observed on ceramic ball surfaces with HA.

- All three model fluid types did not exhibit considerable changes in Raman spectra after the tests with ceramic balls. In particular healthy joint SF shows the least difference. Thus, elevated protein content can be assumed as a significant factor for interaction with the ceramic balls of both types.

- The BIOLOX®delta ball surface showed small differences after the test with model fluids; it can be assumed that there is little reaction between SF components and zirconia toughened alumina ball surface. In contrast, reaction of osteoarthritic joint and total joint replacement model SFs on the BIOLOX®forte surface was confirmed after the tests, and similar reactions occured with individual SF protein constituents and HA. Most likely, HA and/or γ-globulin are attached chemically on the BIOLOX®forte surface for osteoarthritis joint fluid and total joint replacement fluid. In contrast, model SF of healthy joint did not chemically attach to BIOLOX®forte surface.

- The coefficient of friction for BIOLOX®delta contact pair was found higher in the case of γ-globulin, HA and a bit higher in the case of osteoarthritic model SF than for BIOLOX®forte contact pair. However, BIOLOX®forte contact pair exhibited a higher coefficient of friction in case of albumin and model SFs of healthy joint and of total joint replacement than BIOLOX®delta ball and cup pair.

- Both ceramic contact pairs' coefficients of friction with all these lubricants could not be correlated with chemical reaction occuring within the ceramic contact pairs with model SFs and its components separately.

Therefore, it is revealed that zirconia toughened alumina is not much active in tribo-chemical reactions concerning formation of protein films in the synovial joint. In comparison, alumina implants react to form protein tribo-film. Nevertheless, BIOLOX®delta shows chemical reactivity

with HA as a separate lubricant. From chemical perspective, zirconia toughened alumina seems to surpass alumina as material for artificial hip implants.

References

1. Čípek P, Vrbka M, Rebenda D, Nečas D, Křupka I. Biotribology of Synovial Cartilage: A New Method for Visualization of Lubricating Film and Simultaneous Measurement of the Friction Coefficient. *Materials* **2020,** 13(9), 2075.

2. Kerns JG, Gikas PD, Buckley K, Shepperd A, Birch HL, McCarthy I, Miles J, Briggs TW, Keen R, Parker AW, Matousek P. Evidence from Raman spectroscopy of a putative link between inherent bone matrix chemistry and degenerative joint disease. *Arthritis & Rheumatology* **2014**, 66(5), 1237-1246.

3. Navarro M, Michiardi A, Castano O, Planell JA. Biomaterials in orthopaedics. *Journal of the royal society interface* **2008**, 5(27), 1137-1158.

4. Holzwarth U, Cotogno G. Total hip arthroplasty. Brussels: European Commission. **2012**.

5. Gallo J, Goodman SB, Konttinen YT, Raska M. Particle disease: biologic mechanisms of periprosthetic osteolysis in total hip arthroplasty. *Innate immunity* **2013,** 19(2), 213-224.

6. Bedard NA, Callaghan JJ, Stefl MD, Liu SS. Systematic review of literature of cemented femoral components: what is the durability at minimum 20 years followup?. *Clinical Orthopaedics and Related Research®* **2015**, 473(2), 563-571.

7. Affatato S, Modena E, Toni A, Taddei P. Retrieval analysis of three generations of Biolox® femoral heads: Spectroscopic and SEM characterization. *Journal of the mechanical behavior of biomedical materials* **2012,** 13, 118-128.

8. Nečas D, Vrbka M, Rebenda D, Gallo J, Galandáková A, Wolfová L, Křupka I, Hartl M. In situ observation of lubricant film formation in THR considering real conformity: The effect of model synovial fluid composition. *Tribology International* **2018**, 117, 206-216.

9. Taddei P, Modena E, Traina F, Affatato S. Raman and fluorescence investigations on retrieved Biolox® delta femoral heads. *Journal of Raman Spectroscopy* **2012**, 43(12), 1868-1876.

10. Gregori G, Burger W, Sergo V. Piezo-spectroscopic analysis of the residual stresses in zirconia-toughened alumina ceramics: the influence of the tetragonal-to-monoclinic transformation. *Materials Science and Engineering: A* **1999**, 271(1-2), 401-406.

18

11. Parkes M, Sayer K, Goldhofer M, Cann P, Walter WL, Jeffers J. Zirconia phase transformation in retrieved, wear simulated, and artificially aged ceramic femoral heads. *Journal of Orthopaedic Research* **2017,** 35(12), 2781-2789.

12. Taddei P, Pavoni E, Affatato S. Raman and Photoemission Spectroscopic Analyses of Explanted Biolox® Delta Femoral Heads Showing Metal Transfer. *Materials* **2017**, 10(7), 744.

13. Tateiwa T, Marin E, Rondinella A, Ciniglio M, Zhu W, Affatato S, Pezzotti G, Bock RM, McEntire BJ, Bal BS, Yamamoto K. Burst Strength of BIOLOX® delta Femoral Heads and Its Dependence on Low-Temperature Environmental Degradation. *Materials* **2020**, 13(2), 350.

14. Bennike T, Ayturk U, Haslauer CM, Froehlich JW, Proffen BL, Barnaby O, Birkelund S, Murray MM, Warman ML, Stensballe A, Steen H. A normative study of the synovial fluid proteome from healthy porcine knee joints. *Journal of Proteome research* **2014**, 13(10), 4377-4387.

15. Blewis ME, Nugent-Derfus GE, Schmidt TA, Schumacher BL, Sah RL. A model of synovial fluid lubricant composition in normal and injured joints. *Eur Cell Mater* **2007**, 13(1), 26-39.

16. Nakashima K, Sawae Y, Murakami T. Effect of conformational changes and differences of proteins on frictional properties of poly (vinyl alcohol) hydrogel. *Tribology International* **2007**, 40(10-12), 1423-1427.

17. Ghosh P, Guidolin D. Potential mechanism of action of intra-articular hyaluronan therapy in osteoarthritis: are the effects molecular weight dependent?. In Seminars in arthritis and rheumatism 2002, 32 (1), 10-37. WB Saunders.

18. Jegina S, Salaka L, Kukle S, Livkisa D, Gravitis J. A preliminary study on sodium hyaluronate loaded polyvinyl alcohol nanofiber webs obtained via roller electrospinning. *In IOP Conference Series: Materials Science and Engineering* **2019** (Vol. 500, No. 1, p. 012024) IOP Publishing.

19. Rydell N, Balazs EA. Effect of intra-articular injection of hyaluronic acid on the clinical symptoms of osteoarthritis and on granulation tissue formation. *Clinical Orthopaedics and Related Research (1976-2007)* **1971**, 80, 25-32.

20. Kogan G, Šoltés L, Stern R, Gemeiner P. Hyaluronic acid: a natural biopolymer with a broad range of biomedical and industrial applications. *Biotechnology letters* **2007**, 29(1), 17-25.

21. Rebenda D, Vrbka M, Čípek P, Toropitsyn E, Nečas D, Pravda M, Hartl M. On the Dependence of Rheology of Hyaluronic Acid Solutions and Frictional Behavior of Articular Cartilage. *Materials* **2020**, 13(11), 2659.

22. Ghosh S, Choudhury D, Das NS, Pingguan-Murphy B. Tribological role of synovial fluid compositions on artificial joints—a systematic review of the last 10 years. *Lubrication Science* **2014**, 26(6), 387-410.

23. Walker PS, Sikorski J, Dowson D, Longfield MD, Wright V, Buckley T. Behaviour of synovial fluid on surfaces of articular cartilage. A scanning electron microscope study. *Annals of the rheumatic diseases* **1969**, 28(1), 1.

24. Galandáková A, Ulrichová J, Langová K, Hanáková A, Vrbka M, Hartl M, Gallo J. Characteristics of synovial fluid required for optimization of lubrication fluid for biotribological experiments. *Journal of Biomedical Materials Research Part B: Applied Biomaterials* **2017**, 105(6), 1422-1431.

25. Hills BA, Crawford RW. Normal and prosthetic synovial joints are lubricated by surface-active phospholipid: a hypothesis. *The Journal of arthroplasty* **2003**, 18(4), 499-505.

26. Depciuch J, Sowa-Kućma M, Nowak G, Dudek D, Siwek M, Styczeń K, Parlińska-Wojtan M. Phospholipid-protein balance in affective disorders: Analysis of human blood serum using Raman and FTIR spectroscopy. A pilot study. *Journal of pharmaceutical and biomedical analysis* **2016**, 131, 287-296.

27. Park JB, Duong CT, Chang HG, Sharma AR, Thompson MS, Park S, Kwak BC, Kim TY, Lee SS, Park S. Role of hyaluronic acid and phospholipid in the lubrication of a cobalt–chromium head for total hip arthroplasty. *Biointerphases* **2014**, 9(3), 031007.

28. Nečas D, Vrbka M, Gallo J, Křupka I, Hartl M. On the observation of lubrication mechanisms within hip joint replacements. Part II: Hard-on-hard bearing pairs. *Journal of the mechanical behavior of biomedical materials* **2019**, 89, 249-259.

29. Dowson D. Lubrication and wear of joints. *Physiotherapy* **1973**, 59(4), 104.

30. Furmann D, Nečas D, Rebenda D, Čípek P, Vrbka M, Křupka I, Hartl M. The Effect of Synovial Fluid Composition, Speed and Load on Frictional Behaviour of Articular Cartilage. *Materials* **2020**, 13(6), 1334.

31. Brandt JM, Brière LK, Marr J, MacDonald SJ, Bourne RB, Medley JB. Biochemical comparisons of osteoarthritic human synovial fluid with calf sera used in knee simulator wear testing. *Journal of Biomedical Materials Research Part A* **2010,** 94(3), 961-971.

32. Stevenson H, Parkes M, Austin L, Jaggard M, Akhbari P, Vaghela U, Williams HR, Gupte C, Cann P. The development of a small-scale wear test for CoCrMo specimens with human synovial fluid. *Biotribology* **2018**, 14, 1-10.

33. Han XX, Zhao B, Ozaki Y. Surface-enhanced Raman scattering for protein detection. *Analytical and bioanalytical chemistry* **2009**, 394(7), 1719-1727.

34. Rufaqua R, Vrbka M, Choudhury D, Hemzal D, Křupka I, Hartl M. A systematic review on correlation between biochemical and mechanical processes of lubricant film formation in joint replacement of the last 10 years. *Lubrication Science* **2019**, 31(3), 85-101.

35. Vrbka M, Nečas D, Hartl M, Křupka I, Urban F, Gallo J. Visualization of lubricating films between artificial head and cup with respect to real geometry. *Biotribology* **2015**, 1, 61-65.

36. Nečas D, Vrbka M, Urban F, Gallo J, Křupka I, Hartl M. In situ observation of lubricant film formation in THR considering real conformity: The effect of diameter, clearance and material. *Journal of the Mechanical Behavior of Biomedical Materials* **2017**, 69, 66-74.

37. Nečas D, Usami H, Niimi T, Sawae Y, Křupka I, Hartl M. Running-in friction of hip joint replacements can be significantly reduced: The effect of surface-textured acetabular cup. *Friction*, 1-6.

38. Vuurman MA, Wachs IE. In situ Raman spectroscopy of alumina-supported metal oxide catalysts. *The Journal of Physical Chemistry* **1992**, 96(12), 5008-5016.

39. Liu Y, Cheng B, Wang KK, Ling GP, Cai J, Song CL, Han GR. Study of Raman spectra for γ-Al2O3 models by using first-principles method. *Solid state communications* **2014**, 178, 16-22.

40. Essendoubi M, Gobinet C, Reynaud R, Angiboust JF, Manfait M, Piot O. Human skin penetration of hyaluronic acid of different molecular weights as probed by Raman spectroscopy. *Skin Research and Technology* **2016**, 22(1), 55-62.

41. Kotzianová A, Řebíček J, Pokorný M, Hrbáč J, Velebný V. Raman spectroscopy analysis of biodegradable electrospun nanofibers prepared from polymer blends. *Monatshefte für Chemie-Chemical Monthly* **2016**, 147(5), 919-923.

42. Lin-Vien D, Colthup NB, Fateley WG, Grasselli JG. *The handbook of infrared and Raman characteristic frequencies of organic molecules*. Elsevier, 1991.

43. Esmonde-White KA, Mandair GS, Raaii F, Jacobson JA, Miller BS, Urquhart AG, Roessler BJ, Morris MD. Raman spectroscopy of synovial fluid as a tool for diagnosing osteoarthritis. *Journal of biomedical optics* **2009**, 14(3), 034013.

44. Diem M. *Modern vibrational spectroscopy and micro-spectroscopy: theory, instrumentation and biomedical applications*. John Wiley & Sons, 2015.

45. Chourpa I, Ducel V, Richard J, Dubois P, Boury F. Conformational modifications of α gliadin and globulin proteins upon complex coacervates formation with gum arabic as studied by Raman microspectroscopy. *Biomacromolecules* **2006**, 7(9), 2616-2623.

46. Vrbka M, Nečas D, Bartošík J, Hartl M, Křupka I, Galandáková A, Gallo J. Determination of a friction coefficient for THA bearing couples. *Acta chirurgiae orthopaedicae et traumatologiae Cechoslovaca* **2015**, 82(5), 341-347.

7   CONCLUSIONS

SF film formation on implant material of the hip prosthesis is a complex procedure. For the clear understanding of the process of film formation, chemical adsorption of the lubricant film within the joint replacement is to be manifested. Apparently, individual fluid components and compositional variability of SF lubricants due to different stages of joint are reacting with implant materials in diversified manner. Lubrication mechanism, including tribo-chemical reactivity of the material of the prosthesis are vital factors to improve the service life of the joint replacement.

In the present dissertation, chemical composition and chemical structure of the SF films are apprehended while differentiating the variability of the SF lubricants. However, four main constituents of SF albumin, γ-globulin, HA and phospholipids were considered here as lubricants while limiting the effect of other components present in SF in trace amount to entail simplification of the methodology. Furthermore, between the contact pairs, only the heads of implant materials were analysed to realize the film formations, neglecting the Raman measurement of the cups. Nevertheless, inclusive of these impediments, we able to determine chemical reactivity of each of the component of SF separately and within a mixture with metal and ceramic implant head. Besides, it was possible to indicate the structural changes of lubricants due to tribological activity. Additionally, the frictional behaviour of the contact pairs, including the lubricants were investigated to express the correlation between friction and chemical adsorption.

Into the bargain, this modern approach would allow to comprehend chemical analysis of joint replacement and clarify the perception of lubrication mechanism chemistry, even if introducing new materials for joint implants. There is a massive room for improvement to expand the area of joint replacement with spectroscopy and accumulate knowledge on mechanochemical research on biotribology.

Article A

A systematic review was executed to proclaim the necessity of the rectification of chemistry within the joint replacement environment. Some original results were included to validate the methodology of in vitro chemical analysis in joint replacement. It has been disseminated that vibrational fingerprint of the Raman spectrum is proficient at describing the biochemical behaviour of the implant materials in hip joint replacement.

The chemical structural changes of the lubricants could be visualized distinctly by this powerful technique, from the analysis of SF components before and after tribological test in the hip joint simulator. Therefore, explained that by the surface analysis of implant material, it is practicable to define the chemical bond formation and breaking due to film formation by SF lubricants.

Afterwards, expressing the results of chemical analysis of BSA, albumin and γ-globulin after tribological effect on Co–Cr–Mo implant head presumed the occurrence of heterogeneous catalysis process, where Co–Cr–Mo is acting as a contact catalyst to emphasis denaturation of protein molecules. Further, this conception leads to evaluate the spectroscopical analysis of different constitutional combinations of SF within a specific range of physiological concentration. It is exposed that the assessment of different SF lubricants with various implant material may enlighten lubrication chemistry and mechanism SF film formation within artificial prosthesis explicitly.

Article B

As a consequence, Co–Cr–Mo and UHMWPE contact pair with HA and three different model SF analysis resumed comprising frictional behaviour of the pair with these lubricants. Evidence of Chemisorption on the Co–Cr–Mo surface were found for HA and all three models fluid imitating physiologic, total joint replacement and osteoarthritic SF. Traces of albumin were revealed on the metal surface from the combination of SF components. Diseased and operated joint fluids seem to be more chemically reactive regarding film formation. No remarkable correlations were observed with frictional coefficient and chemisorption for this contact pairs with specific lubricants.

Article C

In a similar fashion, we extend our research with ceramic contact pairs with a variety of lubricants, including two types of proteins (albumin and γ-globulin), HA and model SF treatment as previous. Two different types of ceramic balls and cups sets were used, made from alumina ceramic called BIOLOX®forte and zirconia toughened alumina ceramic named BIOLOX®delta. Chemical analysis of lubricant film and frictional behaviour of contact pairs due to tribological activity were investigated accordingly. No significant chemical reactivity were observed for BIOLOX®delta, excluding HA, when this lubricant was used individually.

In contrast, chemical adsorption of albumin, γ-globulin, HA and model SF of the diseased and operated joint were confirmed on the surface of BIOLOX®forte implant head by Raman fingerprints. Presumably, γ-globulin and/or HA are adsorbed chemically on the BIOLOX®forte surface from OA joint fluid and total joint replacement fluid. Analogously as the previous article, specific correlation ship with chemisorption process and frictional coefficient of ceramic contact pairs could not be identified.

The principal ascertainments of the thesis are summarized in the following points:

- Among three types of contact pairs, BIOLOX®delta implant material seems to be mostly chemically inert with individual SF components and all model SF types. On the contrary, Co–Cr–Mo head shows maximum reactivity in case of chemisorption and tribo-film formation of SF components separately and in combinations of the components.

- When albumin, γ-globulin and HA were used as individual lubricants, albumin and γ-globulin changed their chemical structures due to tribological effect in case of Co–Cr–Mo with UHMWPE and BIOLOX®forte contact pairs and HA alters its chemical structure with both ceramic contact pairs. Although the combined mixture did not exhibit remarkable chemical structural modifications with any of the contact pairs after tribological activity.

- SF model imitating OA joint fluid and total joint replacement fluid are more intended to be chemically adsorbed on Co–Cr–Mo and BIOLOX®forte surface than the lubricant simulating healthy synovial joint fluid, despite the fact of chemical inertness of BIOLOX®delta as described in above point. Elevated concentrations of proteins could be the prime reason for this phenomenaon.

- Eventually, consistencies were not maintained for the coefficient of friction values and chemisorption occurrence by the different contact pairs with various lubricants. Thus, it can be assumed that frictional behaviour is not an influencing factor of the chemisorption process of SF lubricant on the implant materials surfaces.

The notion of scientific questions and hypotheses can be interpreted by our obtained conviction summarized in the concluding remarks:

H1: On the surface of implant material, protein content is a significant factor for chemical interaction and involving chemisorbed film formation rather than HA and phospholipids.

In case of individual lubricants usage, both proteins albumin, γ-globulin adsorbed chemically on Co–Cr–Mo and BIOLOX®forte and HA adsorbed chemically on all three implant surface. While using model SF lubricants, on Co–Cr–Mo surface albumin presence is evident from all three model SFs and on BIOLOX®forte surface γ-globulin and/or HA chemisorption has taken place, from OA joint fluid and total joint replacement fluid. These two types of model fluid have elevated concentrations of proteins, while expressed more reactivity with Co–Cr–Mo and BIOLOX®forte material surface. Furthermore, adsorption of phospholipids was not observed from Raman spectra. **(Hypothesis H1 was confirmed).**

H2: Metal hip implant materials are more chemically reactive with SF components to form tribo-film on the surface and could act as heterogeneous catalyst to form lubricant film within joint replace. In comparison, ceramic implant materials are less chemically reactive to sustain chemisorption process with SF fluid contents.

Co–Cr–Mo actively induced chemisorption with all types of lubricants, including individual SF components and in combination. Whereas zirconia toughened alumina ceramic exhibits chemical inertness in most of the cases and pure alumina shows reactivity for individual SF components and model fluids of diseased and operated joint. Although it could be assumed Co–Cr–Mo surface played a role of heterogeneous catalyst when albumin, γ-globulin were used as separate lubricants, as these two protein molecules changed their chemical structures after tribological effect, but rest of the lubricants remained unchanged even after tribological tests. Therefore, it could be supposed that catalysis procedure was not initiated for other lubricants. **(Hypothesis H2 was partially confirmed).**

H3: With the elevation of chemical reaction occurring within a certain arrangement of implant materials and the lubricants, the friction coefficient of friction of the contact pairs is probably increased.

No linear relationship was observed for the coefficient of friction values and chemisorption occurrence by a certain arrangement of implant materials and the lubricants. However, frictional behaviour could not be presumed as an indicator of the chemisorption process of SF lubricant on the implant materials surfaces. **(Hypothesis H3 was falsified).**

8   LIST OF PUBLICATIONS

8.1   Papers published and submitted in journal

Rufaqua R, Vrbka M, Choudhury D, Hemzal D, Křupka I, Hartl M. A systematic review on correlation between biochemical and mechanical processes of lubricant film formation in joint replacement of the last 10 years. Lubrication Science. 2019 ;31(3):85-101.

Rufaqua R, Vrbka M, Hemzal D, Choudhury D, Rebenda D, Křupka I, Hartl M. Raman analysis of chemisorbed tribo-film for metal-on-polyethylene hip joint prostheses. (Submitted to the Journal Biosurface and Biotribology).

Rufaqua R, Vrbka M, Hemzal D, Choudhury D, Rebenda D, Křupka I, Hartl M. Analysis of chemisorbed tribo-film for ceramic-on-ceramic hip joint prostheses by Raman spectroscopy. (Submitted to the Journal of Functional Biomaterials).

8.2   Conference abstracts

Rufaqua, R., Vrbka, M., Choudhury, D., Hemzal, D., Křupka, I., and Hartl, M. The biochemical process of lubricant film formation in joint replacement. 24TH International Conference, Engineering Mechanics 2018, Svratka, Czech Republic.

Rufaqua, R., Vrbka, M., Choudhury, D., Hemzal, D., Rebenda, D., Křupka, I., and Hartl, M. Raman spectroscopic analysis of the biochemical reaction of hyaluronic acid in joint replacement. 74TH STLE Meeting and Exhibition 2019, Nashville, Tennessee USA.

9 LITERATURE

1. Navarro M, Michiardi A, Castano O, Planell JA. Biomaterials in orthopaedics. Journal of the royal society interface. 2008; 5 (27):1137-1158.

2. Glyn-Jones S, Palmer AJ, Agricola R, Price AJ, Vincent TL, Weinans H, Carr AJ. Osteoarthritis. The Lancet. 2015; 386(9991):376-387.

3. Čípek P, Vrbka M, Rebenda D, Nečas D, Křupka I. Biotribology of Synovial Cartilage: A New Method for Visualization of Lubricating Film and Simultaneous Measurement of the Friction Coefficient. Materials. 2020; 13(9):2075.

4. Kerns JG, Gikas PD, Buckley K, Shepperd A, Birch HL, McCarthy I, Miles J, Briggs TW, Keen R, Parker AW, Matousek P. Evidence from Raman spectroscopy of a putative link between inherent bone matrix chemistry and degenerative joint disease. Arthritis & Rheumatology. 2014; 66(5):1237-1246.

5. Holzwarth U, Cotogno G. Total hip arthroplasty. Brussels: European Commission. 2012.

6. Gallo J, Goodman SB, Konttinen YT, Raska M. Particle disease: biologic mechanisms of periprosthetic osteolysis in total hip arthroplasty. Innate immunity. 2013; 19(2):213-224.

7. Bedard NA, Callaghan JJ, Stefl MD, Liu SS. Systematic review of literature of cemented femoral components: what is the durability at minimum 20 years followup?. Clinical Orthopaedics and Related Research®. 2015; 473(2):563-571.

8. Nečas D, Sawae Y, Fujisawa T, Nakashima K, Morita T, Yamaguchi T, Vrbka M, Křupka I, Hartl M. The influence of proteins and speed on friction and adsorption of metal/UHMWPE contact pair. Biotribology. 2017; 11:51-59.

9. Stevenson H, Parkes M, Austin L, Jaggard M, Akhbari P, Vaghela U, Williams HR, Gupte C, Cann P. The development of a small-scale wear test for CoCrMo specimens with human synovial fluid. Biotribology. 2018; 14:1-0.

10. Nečas D, Vrbka M, Gallo J, Křupka I, Hartl M. On the observation of lubrication mechanisms within hip joint replacements. Part II: Hard-on-hard bearing pairs. Journal of the mechanical behavior of biomedical materials. 2019; 89:249-259.

11. Nečas D, Vrbka M, Rebenda D, Gallo J, Galandáková A, Wolfová L, Křupka I, Hartl M. In situ observation of lubricant film formation in THR considering real conformity: The effect of model synovial fluid composition. Tribology International. 2018; 117:206-216.

12. Nečas D, Vrbka M, Urban F, Gallo J, Křupka I, Hartl M. In situ observation of lubricant film formation in THR considering real conformity: The effect of diameter, clearance and material. Journal of the Mechanical Behavior of Biomedical Materials. 2017; 69:66-74.

13. Nečas D, Vrbka M, Křupka I, Hartl M. The effect of kinematic conditions and synovial fluid composition on the frictional behaviour of materials for artificial joints. Materials. 2018; 11(5):767.

14. Brandt JM, Brière LK, Marr J, MacDonald SJ, Bourne RB, Medley JB. Biochemical comparisons of osteoarthritic human synovial fluid with calf sera used in knee simulator wear testing. Journal of Biomedical Materials Research Part A. 2010; 94(3):961-971.

15. Greene GW, Banquy X, Lee DW, Lowrey DD, Yu J, Israelachvili JN. Adaptive mechanically controlled lubrication mechanism found in articular joints. Proceedings of the National Academy of Sciences. 2011; 108(13):5255-5259.

16. Zhang Z, Barman S, Christopher GF. The role of protein content on the steady and oscillatory shear rheology of model synovial fluids. Soft matter. 2014; 10(32):5965-5973.

17. Galandáková A, Ulrichová J, Langová K, Hanáková A, Vrbka M, Hartl M, Gallo J. Characteristics of synovial fluid required for optimization of lubrication fluid for biotribological experiments. Journal of Biomedical Materials Research Part B: Applied Biomaterials. 2017; 105(6):1422-1431.

18. Park JB, Duong CT, Chang HG, Sharma AR, Thompson MS, Park S, Kwak BC, Kim TY, Lee SS, Park S. Role of hyaluronic acid and phospholipid in the lubrication of a cobalt–chromium head for total hip arthroplasty. Biointerphases. 2014; 9(3):031007.

19. Blewis ME, Nugent-Derfus GE, Schmidt TA, Schumacher BL, Sah RL. A model of synovial fluid lubricant composition in normal and injured joints. Eur Cell Mater. 2007; 13(1):26-39.

20. Esmonde-White KA, Mandair GS, Raaii F, Jacobson JA, Miller BS, Urquhart AG, Roessler BJ, Morris MD. Raman spectroscopy of synovial fluid as a tool for diagnosing osteoarthritis. Journal of biomedical optics. 2009; 14(3):034013.

21. Hills BA, Crawford RW. Normal and prosthetic synovial joints are lubricated by surface-active phospholipid: a hypothesis. The Journal of arthroplasty. 2003; 18(4):499-505.

22. Mazzucco D, Scott R, Spector M. Composition of joint fluid in patients undergoing total knee replacement and revision arthroplasty: correlation with flow properties. Biomaterials. 2004; 25(18):4433-4445.

23. Nečas D, Vrbka M, Urban F, Křupka I, Hartl M. The effect of lubricant constituents on lubrication mechanisms in hip joint replacements. Journal of the mechanical behavior of biomedical materials. 2016; 55:295-307.

24. Fan J, Myant C, Underwood R, Cann P. Synovial fluid lubrication of artificial joints: protein film formation and composition. Faraday discussions. 2012; 156(1):69-85.

25. Bennike T, Ayturk U, Haslauer CM, Froehlich JW, Proffen BL, Barnaby O, Birkelund S, Murray MM, Warman ML, Stensballe A, Steen H. A normative study of the synovial fluid proteome from healthy porcine knee joints. Journal of Proteome research. 2014; 13(10):4377-4387.

26. Sophia Fox AJ, Bedi A, Rodeo SA. The basic science of articular cartilage: structure, composition, and function. Sports health. 2009; 1(6):461-468.

27. Walker PS, Sikorski J, Dowson D, Longfield MD, Wright V, Buckley T. Behaviour of synovial fluid on surfaces of articular cartilage. A scanning electron microscope study. Annals of the rheumatic diseases. 1969; 28(1):1.

28. Depciuch J, Sowa-Kućma M, Nowak G, Dudek D, Siwek M, Styczeń K, Parlińska-Wojtan M. Phospholipid-protein balance in affective disorders: Analysis of human blood serum using Raman and FTIR spectroscopy. A pilot study. Journal of pharmaceutical and biomedical analysis. 2016; 131:287-296.

29. Nakashima K, Sawae Y, Murakami T. Effect of conformational changes and differences of proteins on frictional properties of poly (vinyl alcohol) hydrogel. Tribology International. 2007; 40(10-12):1423-1427.

30. Ghosh S, Choudhury D, Das NS, Pingguan-Murphy B. Tribological role of synovial fluid compositions on artificial joints—a systematic review of the last 10 years. Lubrication Science. 2014; 26(6):387-410.

31. Kitano T, Ateshian GA, Mow VC, Kadoya Y, Yamano Y. Constituents and pH changes in protein rich hyaluronan solution affect the biotribological properties of artificial articular joints. Journal of biomechanics. 2001; 34(8):1031-1037.

32. Vrbka M, Křupka I, Hartl M, Návrat T, Gallo J, Galandáková A. In situ measurements of thin films in bovine serum lubricated contacts using optical interferometry. Proceedings of the Institution of Mechanical Engineers, Part H: Journal of Engineering in Medicine. 2014; 228(2):149-158.

33. Parkes M, Myant C, Cann PM, Wong JS. Synovial fluid lubrication: The effect of protein interactions on adsorbed and lubricating films. Biotribology. 2015; 1:51-60.

34. Parkes M, Myant C, Cann PM, Wong JS. The effect of buffer solution choice on protein adsorption and lubrication. Tribology International. 2014; 72:108-117.

35. Milošev I, Strehblow HH. The composition of the surface passive film formed on CoCrMo alloy in simulated physiological solution. Electrochimica Acta. 2003; 48(19):2767-2774.

36. Vidal CV, Muñoz AI. Study of the adsorption process of bovine serum albumin on passivated surfaces of CoCrMo biomedical alloy. Electrochimica Acta. 2010; 55(28):8445-8452.

37. Yan Y, Neville A, Dowson D. Biotribocorrosion of CoCrMo orthopaedic implant materials—assessing the formation and effect of the biofilm. Tribology international. 2007; 40(10-12):1492-1499.

38. Choudhury D, Ghosh S, Ali F, Vrbka M, Hartl M, Krupka I. The Influence of Surface Modification on Friction and Lubrication Mechanism Under a Bovine Serum–Lubricated Condition. Tribology Transactions. 2016; 59(2):316-322.

39. Wu BJ, Deng QY, Leng YX, Wang CM, Huang N. Characterization of adsorption and lubrication of synovial fluid proteins and HA on DLC joint bearings surface. Surface and Coatings Technology. 2017; 320:320-332.

40. Punt IM, Visser VM, van Rhijn LW, Kurtz SM, Antonis J, Schurink GW, van Ooij A. Complications and reoperations of the SB Charite lumbar disc prosthesis: experience in 75 patients. European Spine Journal. 2008; 17(1):36-43.

41. Sun D, Wharton JA, Wood RJ, Ma L, Rainforth WM. Microabrasion–corrosion of cast CoCrMo alloy in simulated body fluids. Tribology International. 2009; 42(1):99-110.

42. Contu F, Elsener B, Böhni H. Characterization of implant materials in fetal bovine serum and sodium sulfate by electrochemical impedance spectroscopy. II. Coarsely sandblasted samples. Journal of Biomedical Materials Research Part A. 2003; 67(1):246-254.

43. Cawley J, Metcalf JE, Jones AH, Band TJ, Skupien DS. A tribological study of cobalt chromium molybdenum alloys used in metal-on-metal resurfacing hip arthroplasty. Wear. 2003; 255(7-12):999-1006.

44. Nakashima K, Sawae Y, Murakami T, Mischler S. Behavior of adsorbed albumin film on CoCrMo alloy under in-situ observation. Tribology Online. 2015; 10(2):183-189.

45. Duong CT, Lee JH, Cho Y, Nam JS, Kim HN, Lee SS, Park S. Effect of protein concentrations of bovine serum albumin and γ-globulin on the frictional response of a cobalt-chromium femoral head. Journal of Materials Science: Materials in Medicine. 2012; 23(5):1323-1330.

46. Schmidt TA, Gastelum NS, Nguyen QT, Schumacher BL, Sah RL. Boundary lubrication of articular cartilage: role of synovial fluid constituents. Arthritis & Rheumatism. 2007; 56(3):882-891.

47. Pelton JT, McLean LR. Spectroscopic methods for analysis of protein secondary structure. Analytical biochemistry. 2000; 277(2):167-176.

48. Timchenko E, Timchenko P, Volova L, Dolgushkin D, Markova M, Yagofarova E. The synovial fluid analysis by using Raman Scattering spectroscopy in order to educe the synovial joint pathology. InJournal of Physics: Conference Series 2018 Jun 1 (Vol. 1038, No. 1, p. 012084). IOP Publishing.

49. Diem Max. Modern vibrational spectroscopy and micro-spectroscopy: Theory, instrumentation and biomedical applications. *John Wiley & Sons* 2015.

50. Han XX, Zhao B, Ozaki Y. Surface-enhanced Raman scattering for protein detection. Analytical and bioanalytical chemistry. 2009; 394(7):1719-1727.

51. Zou S, Weaver MJ. Surface-enhanced Raman scattering on uniform transition-metal films: toward a versatile adsorbate vibrational strategy for solid-nonvacuum interfaces?. Analytical chemistry. 1998; 70(11):2387-2395.

52. Shanmukh S, Jones L, Driskell J, Zhao Y, Dluhy R, Tripp RA. Rapid and sensitive detection of respiratory virus molecular signatures using a silver nanorod array SERS substrate. Nano letters. 2006; 6(11):2630-2636.

53. Reymond-Laruinaz S, Saviot L, Potin V, de Lucas MD. Protein–nanoparticle interaction in bioconjugated silver nanoparticles: a transmission electron microscopy and surface enhanced Raman spectroscopy study. Applied Surface Science. 2016; 389:17-24.

54. Zhu W, Marin E, Sugano N, Pezzotti G. Tensor-resolved raman spectroscopic analysis of wear-induced residual stress fields in long-term alumina hip-joint retrievals. Journal of the mechanical behavior of biomedical materials. 2017; 66:201-210.

55. Visentin M, Stea S, Squarzoni S, Antonietti B, Reggiani M, Toni A. A new method for isolation of polyethylene wear debris from tissue and synovial fluid. Biomaterials. 2004; 25(24):5531-7.

56. Pezzotti G. Raman spectroscopy of biomedical polyethylenes. Acta biomaterialia. 2017; 55:28-99.

57. Choudhury D, Ranuša M, Fleming RA, Vrbka M, Křupka I, Teeter MG, Goss J, Zou M. Mechanical wear and oxidative degradation analysis of retrieved ultra high molecular weight polyethylene acetabular cups. Journal of the mechanical behavior of biomedical materials. 2018; 79:314-323.

58. Taddei P, Pavoni E, Affatato S. Comparative micro-Raman study on standard, cross-linked and vitamin E-blended polyethylene acetabular cups after long-term in vitro testing and ageing. Journal of Raman Spectroscopy. 2017; 48(8):1065-1074.

59. Stevenson H, Jaggard M, Akhbari P, Vaghela U, Gupte C, Cann P. The role of denatured synovial fluid proteins in the lubrication of artificial joints. Biotribology. 2019; 17:49-63.

60. Kerwell S, Baer D, Martin E, Liao Y, Wimmer MA, Shull K, Mathew MT. Electrochemically induced film formation on CoCrMo alloy for hip implant application. Journal of Bio-and Tribo-Corrosion. 2017; 3(1):1-8.

61. Wimmer MA, Laurent MP, Mathew MT, Nagelli C, Liao Y, Marks LD, Jacobs JJ, Fischer A. The effect of contact load on CoCrMo wear and the formation and retention of tribofilms. Wear. 2015; 332:643-649.

62. Taddei P, Modena E, Traina F, Affatato S. Raman and fluorescence investigations on retrieved Biolox® delta femoral heads. Journal of Raman Spectroscopy. 2012; 43(12):1868-1876.

63. Taddei P, Pavoni E, Affatato S. Raman and Photoemission Spectroscopic Analyses of Explanted Biolox® Delta Femoral Heads Showing Metal Transfer. Materials. 2017; 10(7):744.

64. Dowson D. Lubrication and wear of joints. Physiotherapy. 1973; 59(4):104-6.

65. Affatato S, Modena E, Toni A, Taddei P. Retrieval analysis of three generations of Biolox® femoral heads: Spectroscopic and SEM characterisation. journal of the mechanical behavior of biomedical materials. 2012; 13:118-28.

66. Vrbka M, Nečas D, Hartl M, Křupka I, Urban F, Gallo J. Visualization of lubricating films between artificial head and cup with respect to real geometry. Biotribology. 2015; 1:61-65.

67. Nečas D, Usami H, Niimi T, Sawae Y, Křupka I, Hartl M. Running-in friction of hip joint replacements can be significantly reduced: The effect of surface-textured acetabular cup. Friction. 2020; 22:1-6

68. Choudhury D, Urban F, Vrbka M, Hartl M, Krupka I. A novel tribological study on DLC-coated micro-dimpled orthopedics implant interface. Journal of the mechanical behavior of biomedical materials. 2015; 45:121-31.

69. Vašková H. A powerful tool for material identification: Raman spectroscopy. Int. J. Math. Model. Methods Appl. Sci. 2011; 5:1205-1212.

70. Lin-Vien D, Colthup NB, Fateley WG, Grasselli JG. The handbook of infrared and Raman characteristic frequencies of organic molecules. Elsevier; 1991.

71. Furmann D, Nečas D, Rebenda D, Čípek P, Vrbka M, Křupka I, Hartl M. The effect of synovial fluid composition, speed and load on frictional behaviour of articular cartilage. Materials. 2020; 13(6):1334.

72. Alkrad JA, Mrestani Y, Stroehl D, Wartewig S, Neubert R. Characterization of enzymatically digested hyaluronic acid using NMR, Raman, IR, and UV–Vis spectroscopies. Journal of pharmaceutical and biomedical analysis. 2003; 31(3):545-550.

73. Hughes, D. O. Catalysis in Practice. *Chemsa* 1982; 8: 114-116.

74. Thompson DT. Some basic research in coordination chemistry and catalysis, related to applications for industry. Coordination chemistry reviews. 1996; 154:179-192.

75. Sachtler WM, Boer ND. Chemisorption as a prerequisite to heterogeneous catalysis. The Journal of Physical Chemistry. 1960; 64(10):1579-1580.

76. Barth JV. Fresh perspectives for surface coordination chemistry. Surface Science. 2009; 603(10-12):1533-1541.

10 LIST OF FIGURES AND TABLE

11 LIST OF SYMBOLS AND ABBREVIATIONS

SF   Synovial fluid

OA   Osteoarthritis

UHMWPE   Ultra-high molecular weight polyethylene

HSF   Human synovial fluid

SAPL   Surface-active phospholipids

PRG4   Proteoglycan 4

LUB   Glycoprotein lubricin

TKA   Total knee arthroplasty

BGG   Bovine γ-globulin

BSA   Bovine serum albumin

Co-Cr-Mo   Cobalt chromium molybdenum

BS   Bovine serum

OCP   Open circuit potential

DLC   Diamond-like carbon

HGG   Human γ-globulin

PBS   Phosphate buffer solution

DPPC   Dipalmitoylphosphatidylcholine

AFM   Atomic force microscopy

PE   Polyethylene

SERS   Surface-enhanced Raman scattering

XLPE   Highly cross-linked polyethylene

ThT   Thioflavin T

Vm   Monoclinic volume fraction